5-2006

Molecular and Physiological Basis for Hair Loss in *Near Naked Hairless* and *Oak Ridge Rhino-like* Mouse Models: Tracking the Role of the *Hairless* Gene

Yutao Liu
University of Tennessee - Knoxville

To the Graduate Council:

I am submitting herewith a dissertation written by Yutao Liu entitled "Molecular and Physiological Basis for Hair Loss in *Near Naked Hairless* and *Oak Ridge Rhino-like* Mouse Models: Tracking the Role of the *Hairless* Gene." I have examined the final electronic copy of this dissertation for form and content and recommend that it be accepted in partial fulfillment of the requirements for the degree of Doctor of Philosophy, with a major in Life Sciences.

Brynn H. Voy, Major Professor

We have read this dissertation and recommend its acceptance:

Naima Moustaid-Moussa, Yisong Wang, Rogert Hettich

Accepted for the Council:

Carolyn R. Hodges

Vice Provost and Dean of the Graduate School

(Original signatures are on file with official student records.)

To the Graduate Council:

I am submitting herewith a dissertation written by Yutao Liu entitled "Molecular and Physiological Basis for Hair Loss in *Near Naked Hairless* and *Oak Ridge Rhino-like* Mouse Models: Tracking the Role of the *Hairless* Gene." I have examined the final electronic copy of this dissertation for form and content and recommend that it be accepted in partial fulfillment of the requirements for the degree of Doctor of Philosophy, with a major in Life Sciences.

Brynn H Voy
Major Professor

We have read this dissertation
and recommend its acceptance:

Naima Moustaid-Moussa

Yisong Wang

Robert Hettich

Acceptance for the Council:

Anne Mayhew
Vice Chancellor and Dean of
Graduate Studies

(Original Signatures are on file with official student records)

Molecular and Physiological Basis for Hair Loss in *Near Naked Hairless* and *Oak Ridge Rhino-like* Mouse Models: Tracking the Role of the *Hairless* Gene

A Dissertation

Presented for the

Doctor of Philosophy

Degree

The University of Tennessee, Knoxville

Yutao Liu

May 2006

Dedication

This dissertation is dedicated to my wife, Fangfang Chen, my daughter, Sabrina Liu, my parents and parents-in-law, and my brother, for always supporting me, encouraging me, and inspiring me to make progress to reach my goals.

Acknowledgements

I would like to thank my wife, my daughter, my parents and parents-in-law, and the rest of the family, for their great support and encouragement throughout my study.

I wish to thank all those who helped me to finish my PhD degree in life sciences. I would like to thank my major advisor, Dr. Brynn H Voy, for the great guidance and mentoring. It was a great honor to have my dissertation research done in her lab. I would also like to thank Dr. Naima Moustaid-Moussa, Dr. Yisong Wang, and Dr. Robert Hettich, for serving my committee. I would also like to thank Dr. Yisong Wang for the help with the protein work with *hairless*. I would like to thank Dr. John Sundberg in Jackson Laboratory for the great help on the pathology with both mutant mice. I would like to thank Dr. Arnold Saxton in UT for help with part of microarray data analysis. I would like to thank Dr. Edward Michaud to provide the mutant mice for my dissertation research. I would also like to thank Mrs. Suchita Das in Dr. Brynn Voy's lab with all the great helps every day throughout my research. Without the help from Mr. Don Carpenter, Robert Olszewski, Lisa Branstetters, Ginger Shaw, K.T. Cain, and other animal care personnel, I will not be able to do the dissertation research at all. I would like to thank Mr. Xiaochen Lu in Lawrence Livermore National Laboratory for the support with *in situ* hybridization. I would also like to thank Dr. Peter Hoyt, Dr. Mitchel Doktycz and Dr. Dorothea Thompson in Oak Ridge National Laboratory for help in using the microarray scanner, which is critical for my research. I felt very grateful to all the members in Dr. Brynn Voy's lab for their endless technical and scientific help as well as their friendship. I would like to thank all the people in the group of Mammalian Genetics and Genomics for endless support. I would like to acknowledge UT-ORNL graduate school of Genome Science and Technology, Life Sciences Division at ORNL, and United States Department of Energy for the financial support during the research.

Abstract

Hairless mice have been widely used in basic research and clinical trials. Two new mouse mutants with hair loss arose spontaneously in the breeding colony of Oak Ridge National Laboratory. The first homozygotes mutant, called *near naked hairless* (Hr^{n}), never develops a normal coat, while heterozygotes display a sparse coat and become completely nude as they age. The Hr^{n}/Hr^{n} mutant mice are significantly smaller in body size and have very short, curly, and few vibrissae. Histological analysis revealed premature keratinization in the precortical region of hair follicles, formation of mineralized dermal cysts, and loss of hair follicles. Adult heterozygotes display pili multigemini (i.e. more than one hair from one piliary canal) after the first hair cycle, suggesting abnormal regulation of hair shaft formation by the mutation. A mutation was not identified in the coding region of *Hr* nor in candidate genes around *Hr*, suggesting a possible regulatory mutation of *Hr*. Microarray analysis was used to survey the gene expression profile and to identify the molecular mechanisms altered by the Hr^{n} mutation. Several pathways including Wnt/β-catenin, TGF-β, and apoptosis are significantly altered in Hr^{n} mutants, indicating the involvement of Hr^{n} in these pathways. Hr^{n} mutant mice are also suggested to be a research model for human MUHH (Marie Unna Hereditary Hypotrichosis).

The second mouse mutant, called *rhino-like* (Hr^{rhR}), displays progressive and random hair loss and wrinkling skin, leading to a rhinocerotic appearance. Histological analysis revealed the formation of utricles at as early as 10 days of age, the formation of dermal cysts, and the destruction of hair follicles. Since the phenotype in the homozygous mutants is very close to that in Hr^{rh} mutant mice, the genomic DNA of *Hr* gene was directly sequenced. A nonsense mutation was identified in the exon 12, leading to significantly reduced *Hr* expression, probably due to nonsense-mediated decay. The allele was named as rhino in Oak Ridge with the symbol Hr^{rhR} (R for Oak Ridge). Microarray analysis of skin from mice at 7, 10, and 35 days was applied to identify the downstream events of the Hr^{rhR} mutation. Several genes including *Krt1-10*, *Krt2-1*, *IL-17*, and *Itgb4*, were identified as the potential targets of Hr^{rhR}. Wnt/β-catenin, apoptosis, and ERK/MAPK signaling pathways were altered in Hr^{rhR}/Hr^{rhR} mutant mice, suggesting

a possible role of *Hr* to regulate these pathways. Microarray analysis also shows many immune-related genes with differential expression, indicating the possible involvement of *Hr* in immune response. Identification of this new *Hr* allele and its related research allows further understanding about the function of *Hr* and the mechanisms of alopecia, i.e. hair loss.

Table of Contents

List of Tables

Page

Page

List of Figures

Page

Page

Chapter 1 Introduction

The hair follicle represents a very complex biological system with growth and cycling throughout the whole life. Hair follicle is widely used as a model to study epithelial-mesenchymal interactions during animal and human development. Hair follicles are also used as a source of pluripotent stem cells from adult skin. Hair loss in mice can be used to model many different human diseases with hair loss. Mouse models can be treated as preclinical models to test new treatments for human alopecia, i.e. hair loss. In industry, hair follicle is also the scientific foundation for a multi-billion dollar industry. Therefore it is critical to study the mechanisms involved with hair growth and cycle in both mouse and human.

In this dissertation research, two mouse mutants, each with a hair loss phenotype, were used to study the mechanisms of hair loss. Both of the mutants arose spontaneously in Oak Ridge National Laboratory (ORNL) mouse colony. The first one, called *near naked hairless* (Hr^{n}), arose spontaneously in the 1980s. Homozygous Hr^{n}/Hr^{n} mice never grow a normal coat of hair and are virtually hairless. The phenotype of heterozygous mice is less severe. They develop a sparse coat early in life, but become completely nude with age. Homozygous mutants also exhibit reduced body growth, and the homozygous females have difficulties in caring for their offspring. Allelism testing with the known *hairless* mice (Hr^{hr}) (Stelzner, 1983) suggested that the mutation might be an allele of the *hairless* gene (*Hr*) with 95% confidence. However, no mutation was found by sequencing the entire *Hr* gene, including introns, exons, 3'UTR and 5'-UTR region. Although a mutation was not identified in the Hr^{n} mutants, the Hr^{n} mutant mice were characterized systematically by using histological study, scanning electron microscopy, immunohistochemistry, microarray analysis, sequencing, and other molecular biological techniques. A group of differentially expressed genes and related signal pathways were identified in the mutant mice through microarray analysis, which suggests the possible functions of the mutated gene. Hr^{n} mice are potential models for Marie Unna Hereditary Hypotrichosis (MUHH), a hair loss syndrome in humans for which the genetic cause is not yet known.

The second mutant is named as Rhino-like (registered as *Oak Ridge rhino allele* of *Hr* (Hr^{rhR}) in MGI (Mouse Genome Informatics)). It arose spontaneously downstream from a translocation experiment in ORNL, but the mutation is not due to a translocation in the genome. Homozygous mutant mice have a normal coat of hair until 2-3 weeks after birth, the time at which the first hair cycle initiates. Mutant mice fail to initiate the first hair cycle and begin to lose their hair. By 5-weeks of age the mice are hairless and their skin is wrinkled. The phenotype of this mutant is very similar to the known rhino (Hr^{rh}) mice. The mutation was identified in exon 12 of *Hr* as a nonsense mutation leading to a premature stop codon, by genomic sequencing. Formation of utricles was identified as the earliest phenotypic changes that started at day 10 after birth, through histological analysis. Microarray experiments were used to characterize the downstream events caused by the mutation with the mice at 7, 10, and 35 days after birth. Groups of differentially expressed genes were identified as well as their related signal pathways, which suggest possible roles of *Hr* protein in hair follicle cycling.

Altogether, the research related with these two mouse mutants will promote the understanding of hair growth and cycle. It will help to understand how the hair growth and cycles in mouse are regulated, and eventually help to cure the hair loss in human patient or remove hair from patients.

Chapter 2 The mammalian hair follicle and alterations that lead to hair loss

Reasons to study hair loss in mice

Hair follicles in mammalian skin produce hair shafts for many functions including decoration, thermoregulation, collecting sensory information, protection against trauma and insect penetration, social communication, and mimicry (Stenn and Paus, 2001). Hair loss, i.e. alopecia, is a chronic dermatological disorder. There are a variety of different causes for hair loss, including but not limited to hormones (Schmidt, 1994), chemotherapy (Rosman, 2004), radiotherapy (Rosman, 2004), genetic mutations (O'Shaughnessy and Christiano, 2004), stress (Brajac et al., 2003), smoking (Trueb, 2003), cancer (Pierard-Franchimont and Pierard, 2004) and systemic diseases (Spencer and Callen, 1987). Hair loss itself is neither life threatening nor very painful. However, the aesthetic effects can induce a strong stress and anxiety, especially for women patients with complete hair loss (Cash et al., 1993; Hadshiew et al., 2004; Hunt and McHale, 2005).

The hair follicle is unique with its cycling characteristic of regression and regeneration during the entire life span in mammals as it completely regenerates itself with each hair follicle cycle due to the presence of a stem cell population in the region known as the bulge (Christiano, 2004). It represents a stem cell-rich, prototypic neuroectodermal-mesodermal interaction system and a classical model for the study of epithelial-mesenchymal interactions during development (Rendl et al., 2005; Reynolds and Jahoda, 2004). Mouse hair loss mutants are potential models for human alopecia (Irvine and Christiano, 2001; O'Shaughnessy and Christiano, 2004; Porter, 2003), and they offer two distinct advantages for hair loss research: one is the synchronized cycles that occur during the first two hair cycles in mouse, while the other is the short time of mouse hair cycles, only 28 days compared to several years in human (Porter, 2003). Study of hair follicle cycle is also potentially important to promote further understanding of skin tumors, as many types of skin cancer are thought to originate from cells within the hair follicle (Paus et al., 1999a; Paus and Cotsarelis, 1999; Stenn and Paus, 2001). Altogether, research with hair follicle will be critical to further our understanding about development and growth control of keratinocytes and stem cells.

Structure of the hair follicle

The size and shape of hair follicles varies with their locations (Paus and Cotsarelis, 1999). However, they all have the same basic structure, shown in figure 2-1. The hair shaft is produced from the hair matrix as the end product of hair follicle proliferation and differentiation. Hair matrix contains rapidly proliferating keratinocytes and melanocytes. The hair shaft is divided into the hair cuticle on the outside, the cortex, and the medulla in the center. Hair shaft cuticle consists of overlapping cells that are arranged like shingles pointing outward and upward. Hair shaft cortex, the bulk of the hair shaft, is composed of hair-specific keratin filaments and keratin-associated proteins with melanin produced by melanocytes in the matrix region (Paus and Cotsarelis, 1999). Hair shaft medulla, the central part of the hair shaft, is composed of large, loosely connected keratinized cells with large intercellular air spaces. The hair shaft is surrounded by the inner and outer root sheath (IRS and ORS). The inner root sheath contains three concentric layers including Henle's layer, Huxley's layer, and the cuticles (Muller-Rover et al., 2001). The bulge is a portion of the outer root sheath, located at the region of the insertion of the arrector pili muscle. It contains epithelial stem cells responsible for regenerating the follicle during early anagen (Fuchs, 1998; Gho et al., 2004; Morris et al., 2004). The outer root sheath also contains melanocytes, Langerhan's cells (dendritic antigen-presenting cells), and Merkel cells, which are specialized neurosecretory cells. The dermal papilla at the base of hair follicles is a cluster of mesenchymal cells and is thought to control the number of matrix cells and thus the size of hair (Hardy, 1992; Paus and Cotsarelis, 1999). Hair follicles have a very complex immunologic profile that includes perifollicular macrophages, mast cells and other immunocytes.

Hair follicle morphogenesis

Normal development of hair follicles requires interactions between the epithelium and underlying mesenchyme *in utero*. Different types of hair follicles have different time-courses of induction during morphogenesis. In murine dorsal skin, hair follicle morphogenesis is induced at E14.5 and development is complete at postnatal day 6 to 8. The induction of vibrissae hair follicle morphogenesis starts at E12.5, earlier than dorsal skin hair follicles. Hair follicles for the secondary shorter and thinner hair develop from

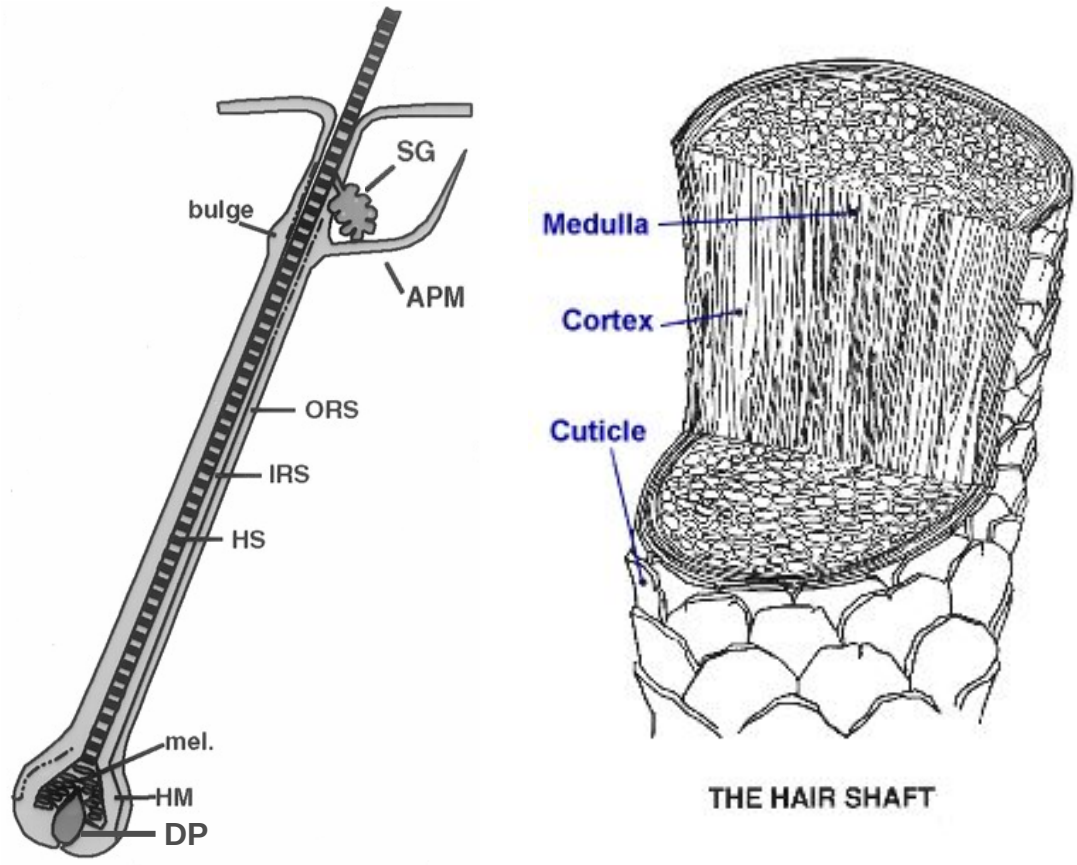

Figure 2-1 Schematic illustration of the structure of hair follicle (Botchkarev and Paus, 2003; Fuchs, 1998) and hair shafts (Adapted from www.regentpharmacy.co.uk).
Abbreviations: SG: sebaceous gland; APM: arrector pili muscle; ORS: outer root sheath; IRS: inner root sheath; HS: hair shaft; mel: melanocytes; HM: hair matrix; DP: dermal papilla.

E16.5 to postnatal day 0.5. There are eight consecutive stages in hair follicle morphogenesis as shown in figure 2-2 (Botchkarev and Paus, 2003).

In stage 1, hair germ or hair placode forms in the basal layer of epidermis. The source of the first dermal message to form a hair placode is not known. The keratinocytes in hair placodes are distinguished from other keratinocytes by the expression of growth factors (*Wnt-10b*, *Eda*, *BMP*-2), growth factor receptors (*Edar*, *TGFβRII*, *BMPR-1A*) and transcriptional regulators (*Lef1*, *β-catenin* and *Msx2*) (Botchkarev and Kishimoto, 2003; Schmidt-Ullrich and Paus, 2005). Accordingly, at least three signaling pathways including *Wnt/β-catenin/Lef-1*, *Eda/Edar*, and *TGFβ2/TGFβ-RII*, are involved in the positive regulation of hair placode formation (Fuchs, 1998). There are two signaling pathways inhibiting hair follicle induction, including *BMP-2/4* and *EGF* (epidermal growth factor) signaling (Botchkarev and Paus, 2003). The balance between these inhibitors and stimulators tightly controls the initiation stage of hair follicle development.

Hair placode grows down into the dermis and forms hair peg in stage 2 and 3. The keratinocytes in hair peg highly express sonic hedgehog (*Shh*) and its receptor *Ptc1*, platelet-derived growth factor A (*PDGF-A*), *neurotrophins*, *TGFβ-RII*, and neural-cell adhesion molecule (*N-CAM*) (Rogers, 2004). The mesenchymal cells express *Wnt-5a* and downstream effectors *Lef1*, *Ptc1*, *Gli1*, *PDGF-Rα*, *Noggin*, and alkaline phosphatase (Botchkarev and Kishimoto, 2003; Fuchs, 1998). All these molecules are essential to promote the morphogenesis of dermal papilla (Botchkarev and Kishimoto, 2003).

In stage 4, the dermal papilla is formed and is incorporated into the epithelial hair bulb. The keratinocytes in hair bulb proliferate and differentiate into the inner root sheath and hair shaft cells (Paus and Cotsarelis, 1999). At stage 5, sebocytes are visible in the distal parts of the hair follicle and melanin granules and hair shaft are above the dermal papilla (Schmidt-Ullrich and Paus, 2005). The hair shaft reaches the level of sebaceous gland and the hair canal becomes visible in skin during stage 6-7. In stage 8, the hair follicle elongates to the maximal length and hair bulb is visible; sebaceous gland and arrector pili muscle are present in the dermis and the hair shaft finally emerges through

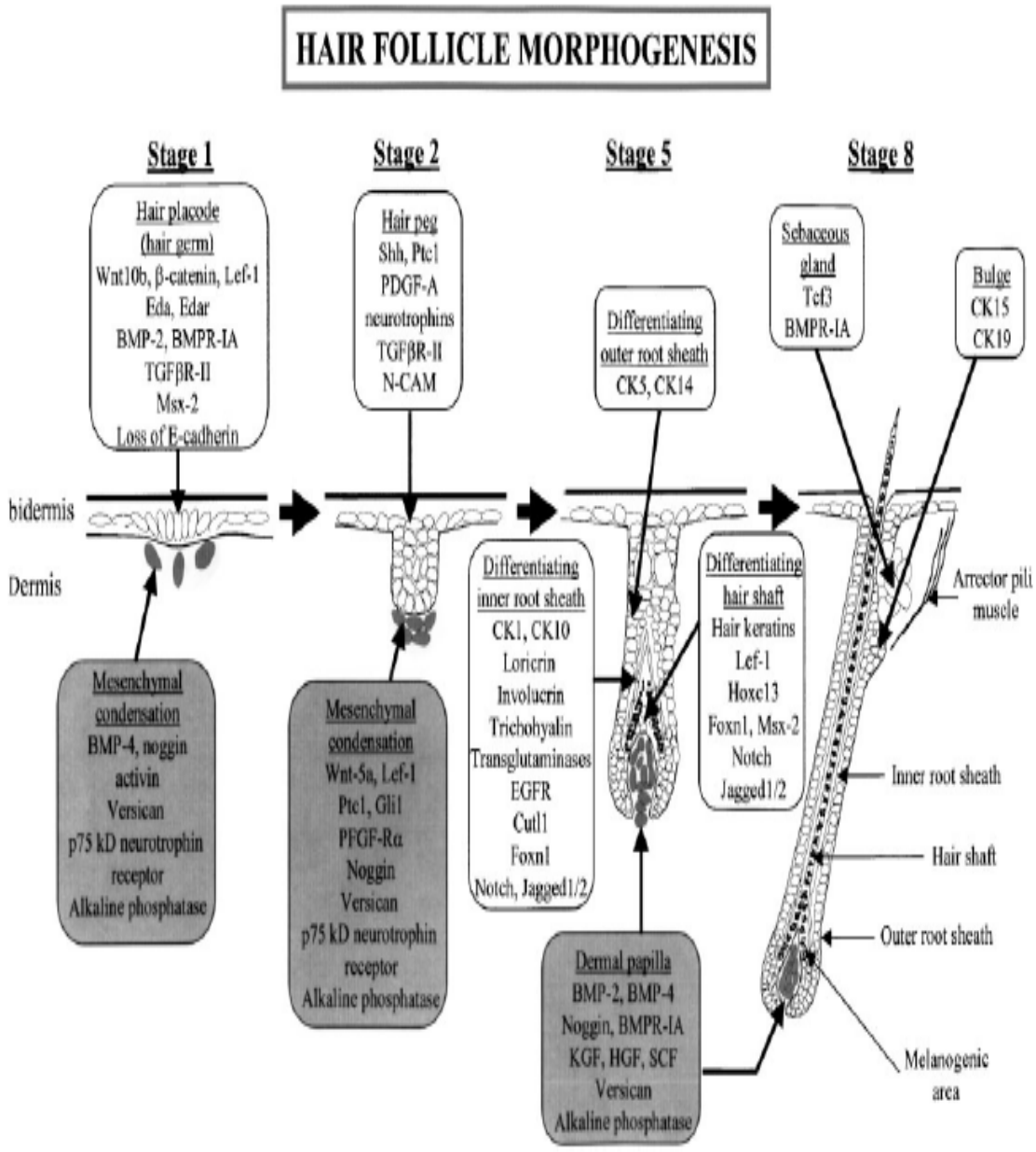

Figure 2-2 Schematic diagram of hair follicle morphogenesis and its molecular regulation (adapted from (Botchkarev and Paus, 2003))

the epidermis (Rogers, 2004; Schmidt-Ullrich and Paus, 2005). It is found that *Foxn1*, *Cutl1*, *EGF* receptor or its ligand *TGF-β*, keratin 1-10 and keratin 2-1, trichohyalin, and the components of the cornified envelope including transglutaminases, loricrin, and involucrin affect the differentiation of inner root sheath (Botchkarev and Paus, 2003; Fuchs, 1998). Hair shaft differentiation is controlled by multiple signaling pathways including *Wnt*/*β-catenin*/*Lef-1*, *Hoxc13*, *BMP/Msx-2/Foxn1*, *Notch*, and *desmoglein* 4 (*Dsg4*) (Botchkarev and Paus, 2003; Fuchs, 1998). Interestingly, BMP signaling is involved in controlling the expression and function of *Lef1*, *Hoxc13*, and *Foxn1* transcription factors in differentiating hair shaft precursor cells.

Hair follicle cycling

Hair follicles show periodic changes in their activity during hair cycles. The most unique feature of a hair follicle is its ability to regress and regrow in a regulated manner throughout life. The length of the hair cycle, i.e. the period between catagens in two continuous hair cycles, varies widely across species. In human it is about 10 years, while in mice it is about 28 days. Many species, like humans, exhibit asynchronous cycles, in which adjacent hair follicles can be in completely different stages of the hair follicle cycle. In mice, at least in the first few cycles, follicles are synchronized and proceed in a head to tail manner. Hair follicle cycle includes three stages: intensive growth and hair production in anagen, apoptosis-driven regression in catagen, and resting stage in telogen (Stenn and Paus, 2001) as shown in figure 2-3. Hair follicle cycling represents repetitive tissue regeneration and involution. The first hair cycle in mice begins with hair follicle development and anagen prenatally and ends with the first catagen, about 14 days after birth. Catagen is induced by regulated apoptosis, leading to retraction of the epithelial strand and its disconnection from the dermal papilla. In telogen, the hair fiber becomes loosened and falls out. A new cycle initiates, the follicle regrows, and the next anagen proceeds. The cycling of hair follicles begins with catagen instead of anagen shortly after the hair follicle morphogenesis with the first coat. Therefore, the chronology of hair follicle cycling is from catagen to telogen, to anagen, and back to catagen. The hair follicle alters its normal cycling behavior in response to damage, such as by chemotherapy so that hair follicle cycling continues later (Paus and Foitzik, 2004).

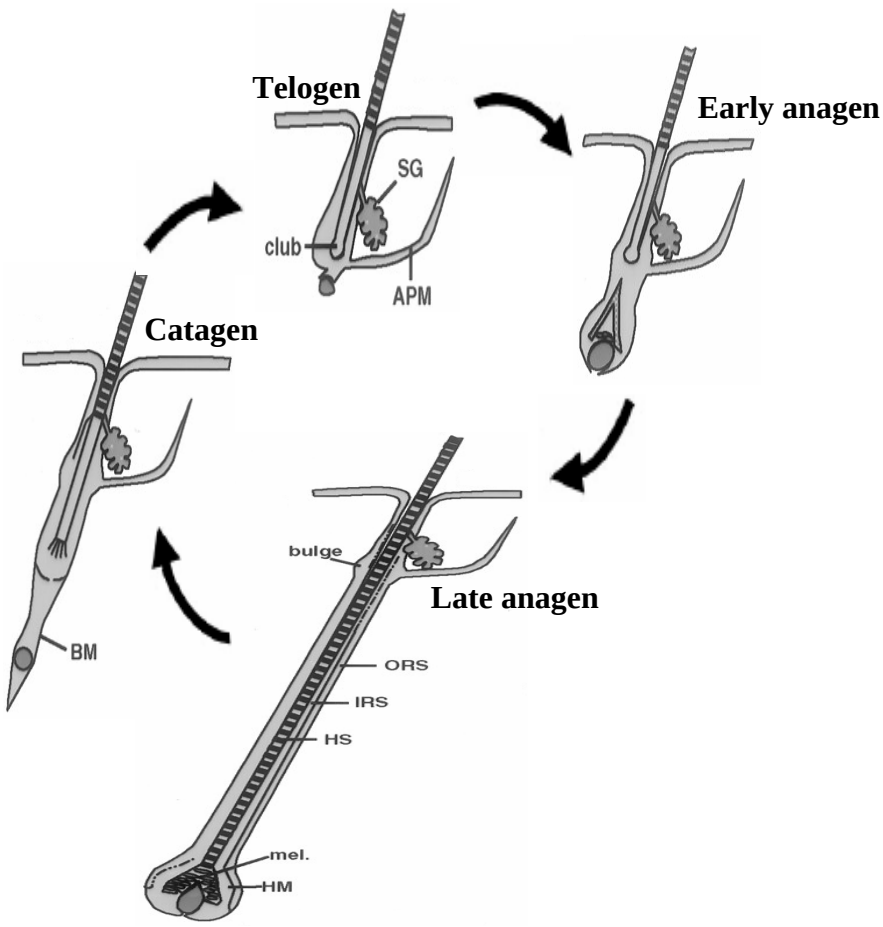

Figure 2-3 Schematic illustration of the hair follicle cycle.

Pigmented hair shafts are actively produced and the follicle reaches it maximal length and volume during anagen. All new hair shaft production and pigmentation is ceased as the club hair is formed during catagen. The club hair rest loosely in the hair canal and is actively shed during telogen (Paus and Foitzik, 2004).

It is known that a large number of cytokines, growth factors, transcription factors, enzymes, and adhesion molecules, including members of the epidermal, fibroblast, and transforming growth factor families, are implicated in the hair growth cycle (Reviewed in (Nakamura et al., 2001; Paus and Foitzik, 2004)). For instance, insulin-like growth factor 1, fibroblast growth factor 5 and 7, play very important roles in hair follicle development and cycling, especially in the anagen stage (Paus, 1998; Paus and Cotsarelis, 1999; Paus and Foitzik, 2004; Paus et al., 1999b). The genes that are important in the hair follicle cycle are summarized in table 2-1.

General mechanisms of hair growth disorders

Hair follicle morphogenesis and hair cycle are the scientific foundations of the vast majority of human patients with hair growth disorders. For the genes involved in hair follicle morphogenesis or the hair cycle, mutations in these genes leading to reduced expression or overexpression could destroy the balance required for hair follicle morphogenesis and hair follicle cycles, thus leading to disorders of hair growth, including hair loss. *Telogen effluvium* is an extremely common form of alopecia, i.e. hair loss with excessive shedding of hair. Normally, most of the hair follicles are in the anagen stage while a rather small portion of hair follicles are in telogen. A larger portion of hair follicles stays in telogen leading to hair shedding when telogen effluvium occurs. The causes for *telogen effluvium* include pregnancy, medications including minoxidil, change of exposure to sunlight, psychological stress, and high fever (Cotsarelis and Millar, 2001). The hair follicles in telogen effluvium are still intact and able to generate new hairs later. *Androgenetic alopecia* is due to the progressive shortening of successive anagen cycles and is commonly manifested as telogen effluvium. The hair loss in male is patterned as frontal recession and thinning at the vertex and that in female is as loss of hair over the crown with sparsing of the frontal hair line. *Androgenetic alopecia* results in a decrease in hair follicle size as well as a decrease in the duration of anagen and an increase in the

Table 2-1. The genes involved in mammalian hair cycles

Interfaces	List of genes involved in the process
Anagen-catagen transition	*FGF-5, FGFR1, TGFβ-1 and 2, Neurotrophins (BDNF, NT-3, NT-4) and their receptors (TrkB, TrkC), SCF, VEGF, HGF, IGF-1, KGF, Endothelin-1 (ET-1), IL-1α/β, IGF-BP3/4/5, vitamin D receptor, prolactin, RXRα, glucocorticoid receptors, neuropeptide substance P, BMP-2, follistatin, PTHrp, calcitriols, retinoids, estrogens, activin, GDNF, INF-γ*
Cell death and survival during catagen	*TNF receptor, Fas/CD95, p75 kD neurotrophin receptor, Caspase-1, 3, 4, 7, P53, Bax, Bcl-2, Bcl-X_L, desmoglein-3 and cathepsin L*
Telogen-anagen transition	*BMP-4, BMPR-IA, noggin, STAT3, FGF7, WNTs, desmoglein-3, cathepsin L, neuropeptide substance P, estrogen receptor, Ssh, HGF, IGF-1, TGF-α, KGF, ACTH, SP, β-catenin, desmoglein 1/3, Msx2*

Abbreviations: *FGF*: fibroblast growth factor; *TGF*: transforming growth factor; *BDNF*: brain-derived neurotrophin factor; *NT*: neurotrophins; *SCF*: stem cell factor: *VEGF*: vascular endothelial growth factor; *HGF*: hepatocyte growth factor; *IGF*: Insulin-like growth factor; *KGF*: Keratinocyte growth factor; *IGF-BP*: Insulin-like growth factor binding protein; *RXR*: retinoid X receptor; *BMP*: bone morphogenic protein; *PTHrp*: parathyroid-related peptide; *GDNF*: glial cell line-derived neurotrophic factor; *IL*: interleukin; *TNF*: Tumor necrosis factor; *STAT*: Signal Transducer and Activators of Transcription; *ACTH*: adrenocorticotrophin; *INF*: interferon; *SP*: substance P.

percentage of hair follicles in telogen (Cotsarelis and Millar, 2001). Testosterone is required for androgenetic alopecia to develop in men, but not determined in women.

Hypertrichosis is excessive hair growth beyond that considered normal according to age, race, sex, and skin region. *Hirsutism* is excessive hair growth in androgen-dependent areas in women. Both hypertrichosis and hirsutism result from a prolonged anagen with an abnormal enlargement of hair follicles. Small vellus hairs turn into large, terminal hairs. In mice, a mutation in *FGF5* causes the striking angora mouse phenotype with 50% longer hair growth due to 50% longer anagen phase and delay of the catagen phase. Overexpression of either *Bcl-*X_L or *Bcl-2* in the outer root sheath decreases the duration of anagen and causes alopecia. It has been known that a large number of different genes contribute to the switches for the transformations from one hair cycle stage to the next as shown in table 2-1. There are still a lot of unknowns about hair follicle cycle. There are no exact numbers on the times that a given hair follicle subtype in a given location could cycle during life time of a mammalian organism. The autonomy and spontaneity of hair follicle, the non-linkage to known perennial, seasonal, circadian or diurnal rhythms, disparate length of individual hair cycle phases, the micro- and macro-environment around hair follicles during hair cycles, are formidable challenge for dermatological research with hair follicle even if cycling of a single hair follicle is very-well known. However, many molecular players in hair cycle control have been identified in murine hair follicle cycle, including *Wnt* family members, *TGFβ/BMP* family members and their antagonists, the *Shh-patched-Gli* pathway, *notch* signaling, *HGF*, neurotrophins, and *FGFs* (reviewed in (Paus and Foitzik, 2004). Mutations in these genes contribute to abnormal hair growth and hair follicle cycling. *Hairless* is one of the key catagen controllers (Panteleyev et al., 1999) and mutations in *hairless* cause alopecia in both mouse and human (Panteleyev et al., 1998b). Below, two genes closely related with hair shaft differentiation and hair growth are described in detail.

Foxn1

Foxn1 gene, formerly called *Whn* and *Hfh11*, is the second gene to be defined to affect hair growth after *Hr*. Mutations in this gene, which are autosomal recessive, cause the "nude" phenotype first reported in 1966 by Flanagan SP in Edinburgh, UK (Flanagan,

1966). It was noticed that nude mice have normal hair follicle at birth, but that by 6 days of age the hair shaft starts to twist and coil with the follicular infundibulum, failing to penetrate the epidermis (Flanagan, 1966). Nude mice also suffer from agenesis of the thymus and are severely immunocompromised (Pantelouris, 1968; Pantelouris and Hair, 1970). This suggests the pleiotropic effects of Foxn1 in different tissues (Flanagan, 1966). *Foxn1* gene encodes a highly conserved transcription factor of the winged helix domain family containing a C-terminal transcriptional activation domain and a DNA binding domain (Mecklenburg et al., 2005). Loss of function of either one is thought to cause the lack of fur development and thymic agenesis. The mutation of *Foxn1* in nude mice is caused by a single base pair deletion in exon 3, which leads to a frameshift and a premature stop codon and a protein lacking the DNA binding domain (Nehls et al., 1994). There are totally six spontaneously arisen mutations in *Foxn1* gene as well as two targeted mutations (Blake et al., 2003). Both the skin and the thymic phenotype of nude mice were able to be rescued by an engineered 110kb transgene containing *Foxn1*, but not by a cosmid-derived 26kb transgene containing Foxn1 (Cunliffe et al., 2002). Mutations in *Foxn1* gene have been described in rats and in humans (Frank et al., 1999; Fuchs, 1998; Nehls et al., 1994)

Nude mice are actually not hairless at all. They have a normal number of hair follicles and normally cycling hair follicles despite the marked defects within the hair shafts (Mecklenburg et al., 2005). However, the keratinization in the hair follicles is severely impaired. A decreased sulfur concentration in nude mice was found in hair fibers (Kopf-Maier et al., 1990; Mecklenburg et al., 2005). The IRS cuticle and the cuticle of the hair shaft are fragmented into globular amorphous structures (Kopf-Maier et al., 1990) due to the lack of keratin *mHa3*. The cortex of hair shaft is composed by abnormal globular aggregates (Kopf-Maier et al., 1990). The epidermis shows only few and thin bundles of tonofilaments in the basal, spinous and granular layers and bizarrely formed and irregularly arranged lamellae of corneocytes in the stratum corneum (Kopf-Maier et al., 1990). The medulla of hair shaft in nude mice is less septulated than in heterozygous or wild type animals probably due to the reduced expression of desmocollin-2 (Johns et al., 2005). The nails of nude mice are severely malformed showing an onychodystrophy

associated with a basophilic stippling of the dorsal nail plate and a significantly reduced sulfur concentration (Flanagan, 1966; Mecklenburg et al., 2005).

Foxn1 is not expressed in the formation of the hair bud, but in the pre-cortical matrix of developing hair follicles as well as in the hair matrix keratinocytes, precortical hair matrix cells, trichocytes of the hair cortex, and the outer root sheath keratinocytes in cycling hair follicles (Mecklenburg et al., 2005). Foxn1 is very important for maintaining the balance between keratinocyte growth and differentiation in differentiating keratinocytes. Overexpression of *Foxn1* under the control of involucrin promoter in differentiating keratinocytes inhibited markers of late differentiation including profilaggrin, involucrin, and loricrin while the keratinocytes from nude mice express higher levels of profilaggrin and loricrin than those from wild type mice after stimulation with calcium (Mecklenburg et al., 2005). *Foxn1* is suggested to be involved in the control of the expression of certain keratins, such as *mHa1*, *mHa3*, and *mHa4*, which are downregulated in nude mice and upregulated with over-expression of *Foxn1* in HeLa cells (Mecklenburg et al., 2005; Schlake et al., 2000; Schorpp et al., 2000). *Foxn1* is also suggested to be a negative regulator of protein kinase C (PKC) activity, which is known to regulate keratinocyte proliferation and differentiation, and to inhibit hair growth (Harmon et al., 1995; Harmon et al., 1997; Xiong and Harmon, 1997). *Foxn1* might stimulate the expression of protein kinase B (*Akt* kinase) triggering the completion of the differentiation and formation of the granular and cornified epidermal layer despite of the lack of knowledge with the nude mice (Janes et al., 2004). The regulation of *Foxn1* is inhibited by the activation of MAP kinases and promoted by the overexpression of *Wnt4* or *Wnt5b* (Mecklenburg et al., 2005) or under the stimulation of bone morphogenic protein receptor 1a (*BMPr1a*) (Ma et al., 2003).

Hoxc13

Hoxc13 is the first hox gene shown to play a universal role in hair follicle development as both *Hoxc13*-deficient and over-expressing mice exhibit severe hair growth and patterning defects (Godwin and Capecchi, 1998; Tkatchenko et al., 2001). *Hoxc13* is expressed in the vibrissae and hair follicles, mainly in the matrix of the hair

bulb and the precortical region of the hair shaft as well as in the filiform papillae of the tongue (Awgulewitsch, 2003; Godwin and Capecchi, 1998).

Hoxc13 mutant mice lack vibrissae, all pelage hair types, peri-anal hairs, eyelashes due to the brittleness of the hair fibers although the mice develop morphologically normal hair follicles (Godwin and Capecchi, 1998). Most homozygotes die between postnatal day 7 and 14 with progressive weight loss and weakness relative to the littermates (Godwin and Capecchi, 1998). The lack of external hair in *Hoxc13* mutant mice suggests that *Hoxc13* plays important roles in hair shaft differentiation by either regulating the expression of hair specific keratin or controlling the differentiation of precursor cells in hair follicle, which are supported by the following evidence.

The GC13 mice, which overexpress murine *Hoxc13* in differentiating keratinocytes of hair follicles, showed short tails, taut skin, kinky whiskers, and smaller stuture, progressive alopecia with age with epidermal thickening and follicular enlargement due to thickened outer root sheath and keratinaceous materials filled cysts (Tkatchenko et al., 2001). The expression of a cluster of keratin-associated proteins complex 16 (*krtap16*) was downregulated due to in GC13 mice, suggesting the possible role of *Hoxc13* in the regulation of keratin expression.

It was also found that *Hoxc13* was involved in the regulation of human hair keratin gene expression via binding to the recognition motif TT(A/T)ATNPuPu (Jave-Suarez et al., 2002). The reduced expression of bone morphogenic protein 4 (*BMP-4*) in hair follicles, which had the similar expression pattern with *Hoxc13* in hair follicles, caused down-regulation of *Hoxc13* and impaired hair shaft differentiation and distal expansion of proliferating keratinocytes normally restricted in the proximal matrix region (Kulessa et al., 2000). It suggests that *Hoxc13* might be involved in the control of precursor cell differentiation in hair follicles. *Hoxc13* might help to maintain the balance of hair keratin expression and of the controls for keratinocytes differentiation through a negative autoregulatory feedback control of *Hoxc13* expression level (Awgulewitsch, 2003; Tkatchenko et al., 2001).

Hairless and hair loss

History of *hairless* mice

In the search of genes responsible for hair loss, *hairless* (*Hr*) gene was the first one found to cause alopecia. The *hairless* mouse was first captured in an aviary in 1924 in North London, UK (Brooke, 1926). It was pink with smooth skin. The first description of rhino mice was reported by Gaskoin in 1856 (Gaskoin, 1856) as "rhinoceros" with hair loss and wrinkled skin. Later, it was shown that rhino and *hairless* are alleles of the same gene, *Hr* (Howard, 1940). *Rhino* alleles (Hr^{rh}) have a more severe phenotype than alleles designated as *hairless* (Hr^{hr}). It should also be noted that the skin from different *Hr* alleles differ in subtle details, which may be due to strain differences or the mutations themselves (Panteleyev et al., 1998c; Sundberg, 1994). The *hairless* (Hr^{hr}) mice, widely used in dermatological research today, arose spontaneously in 1939 at McGill University in Montreal, Canada (Sundberg, 1994).

Both *hairless* (Hr^{hr}/Hr^{hr}) and *rhino* (Hr^{rh}/Hr^{rh}) mutants are born with normal hair coat but lose their hair around the age of 3 - 4 weeks, and are more sensitive to UV and chemical carcinogens (Panteleyev et al., 1998b). Both have been extensively used for many cutaneous studies due to the absence of hair, including ultraviolet and chemical induced carcinogenesis, topical application of compounds, wound healing, and microcirculation (Sundberg, 1994). Homologs of murine *hairless* have been identified in human, rat, monkey, sheep, and pig (Ahmad et al., 1998a; Ahmad et al., 2002; Fernandez et al., 2003; Finocchiaro et al., 2003; Thompson, 1996).

Features of *Hr* gene

There are 19 exons in both human and murine *Hr* (Ahmad et al., 1998a; Cachon-Gonzalez et al., 1994; Cichon et al., 1998). *Hr* is mainly expressed in brain and the epidermis and hair follicle in the skin, with lower expression in cartilage, developing tooth, inner ear, retina, testis, colon, stomach, pituitary gland, small intestine, appendix, liver, kidney, pancreas, spleen, and thymus (Ahmad et al., 1998a; Cachon-Gonzalez et al., 1999; Cichon et al., 1998). It was found that *Hr* in rat is expressed at high levels in cerebellum shortly after birth, reaching a peak between postnatal days 14 and 21 (Potter et al., 2001). It was first cloned in rat as part of a screen for thyroid hormone-responsive

genes in the brain (Thompson and Bottcher, 1997). Three different isoforms of *Hr* have been described in human: isoform 1 (full length), and isoform 2 (short without exon 17) (Cichon et al., 1998), and isoform 3, which is not experimentally confirmed (Strausberg et al., 2002). Isoform 2 is exclusively expressed at high levels in the human skin (Cichon et al., 1998). No alternative transcripts have been reported in murine *Hr* thus far.

Hairless protein (HR) is highly conserved in human, mouse, and rat (Cichon et al., 1998) with approximately 85% identity between human and rodent HR (Panteleyev et al., 1998b). The *hairless* protein (HR) in human, rat, and monkey have similar length to murine HR (Ahmad et al., 2002). The identified sheep HR is similar to the fragment of 1-715 amino acids in murine HR (Finocchiaro et al., 2003). The identified pig *HR* is similar to the fragment of 818-1153 amino acids in murine HR (Fernandez et al., 2003). All of them share at least 70% similarity in protein sequence. Interestingly, no homologs of HR have been identified outside of mammals.

HR contains a single zinc finger domain, which is a conserved 4-cysteine motif ($C\text{-}X_2\text{-}C\text{-}X_{18}\text{-}C\text{-}X_2\text{-}C$) and is predicted to bind with DNA (Cachon-Gonzalez et al., 1994). It shares structural homology to the GATA family and to *TSGA*, a protein mainly expressed in rat testis (Cachon-Gonzalez et al., 1994). The homologs of murine *hairless* in sheep and monkey also contain the putative zinc finger domain by multiple sequence alignment (Ahmad et al., 2002; Finocchiaro et al., 2003). Although most GATA family members contain two zinc finger domains, it is indicated that a single zinc finger domain found in GATA family members is sufficient for DNA binding (Pedone et al., 1997). In addition to the putative zinc finger domain, HR is translocated into the nucleus via a novel bipartite nuclear localization signal (NLS) of the form KRA(X13)PKR (amino acid 412-430), and is associated with components of the nuclear matrix, which may play roles in DNA organization, replication, gene transcription, RNA processing, potentially intra-nuclear signaling for the regulation of gene transcription (Djabali et al., 2001; Djabali and Christiano, 2004). Mutation of the third cysteine residue in the conserved zinc finger domain to a glycine residue in human (C622G) is shown to be associated with APL (Aita et al., 2000). However, a residue change between the second and the third cysteines

(R620Q) does not cause APL or AUC in human (Hillmer et al., 2001; Hillmer et al., 2002). It suggests that the putative zinc finger domain is critical for the function of HR. It has been shown that HR has three LXXLL motifs within two separate α-helical regions (Djabali et al., 2001). This LXXLL motif is conserved in many transcriptional coactivators, including TRIPs (Thyroid hormone Receptor Interacting Proteins) (Voegel et al., 1998) and DRIPs (vitamin D Receptor Interacting Proteins) (Rachez and Freedman, 2000), and is required for interaction with nuclear receptors.

Interestingly, HR has been shown to directly and specifically interact with thyroid hormone receptor (TR) and histone deacetylases (HDACs) in rat brain (Potter et al., 2001; Potter et al., 2002) and with vitamin D receptors (VDR) *in vitro* (Hsieh et al., 2003). HR expression is directly regulated by thyroid hormone through TR, and then HR will bind with TR and facilitate the transcriptional repression by unliganded *TR* through the interaction with HDACs (Histone Deacetylases) (Potter et al., 2001; Thompson, 1996; Thompson and Bottcher, 1997). A thyroid hormone responsive element was identified in the rat *Hr* promoter (Thompson, 1996). However, the *Hr* promoter was transactivated by T3 in neuroblastoma cells but not in keratinocytes (Engelhard and Christiano, 2004), suggesting that HR interacts with TR signaling in brain but not skin. The interaction of HR and TR is further found not to be involved in the pathogenesis of atrichia with popular lesions in human (Djabali et al., 2004).

VDR is a nuclear receptor that functions as a ligand-activated transcription factor (Haussler et al., 1998). Co-expression of HR with VDR inhibits VDR-mediated transactivation (Hsieh et al., 2003). VDR knockout mice (Li et al., 1997) also develop alopecia in skin, and are a phenocopy of Hr^{hr}/Hr^{hr} mutants (Miller et al., 2001). Targeted expression of VDR in the skin promotes initiation of the postnatal hair follicle cycle and rescues the alopecia in VDR null mice (Kong et al., 2002a). Both HR (Djabali et al., 2001) and VDR (Haussler et al., 1998) are translocated into the nucleus via bipartite nuclear localization signals. Expression of both HR and VDR are localized to normal murine epidermis and hair follicles (Gurlek et al., 2002), and are also differentially regulated during different hair cycle stages (Panteleyev et al., 2000; Reichrath et al., 1994). Mutations in human *Hr* cause atrichia with papular lesions, while mutations in

human VDR cause vitamin D-dependent rickets type IIA (*VDDRIIA*; OMIM 277440) along with atrichia with papular lesions in patients. A detailed clinical and histological comparison was done between these two genetically distinct forms of atrichia with papules (Zlotogorski et al., 2003). The similarity between these two distinct forms of APL suggests a functional relationship between HR and VDR. It was found recently that induction of vitamin D responsive genes including involucrin, transglutaminase, 24-hydroxylase, was potentiated by inhibition of HR expression in the presence of vitamin D3, and vice versa (Xie et al., 2005). This suggests that HR functions as a co-repressor of VDR to block vitamin D3 action on keratinocytes.

HR also contains a domain called Jumonji C (jmjC) (amino acids 999-1133) (Letunic et al., 2002). Human homozygous missense mutations in this domain (D1012N and V1056M) (Klein et al., 2002; Zlotogorski et al., 2002a) cause AUC or APL, suggesting that this domain is critical for the normal function of HR in hair follicle cycles. One of the interaction domains of HR with thyroid hormone receptor (TR) is amino acids 1024-1040 (Potter et al., 2001), which is part of the JmjC domain. The exact function of this domain still remains unknown. There are over 370 proteins containing the jmjC domain, ranging from *Saccharomyces cerevisiae*, C. elegans, Drosophila, and Arabidopsis, to mouse and human (Letunic et al., 2002). Most of these proteins are hypothetical or putative proteins, which may represent a large family of proteins with unknown functions. It is also found that many transcription factors contain jmjC domains suggesting the possible single functional unit within the folded proteins (Balciunas and Ronne, 2000). The jmjC domain is a part of the cupin metalloenzyme superfamily and is described as "probable enzymes, but of unknown functions, that regulate chromatin reorganization processes" (Letunic et al., 2002). The function of jmjC domain was recently linked to the modulation of heterochromatization in fission yeast by showing that *Epe1*, a nuclear protein with jmjC domain, counteracts transcriptional silencing by negatively affecting heterochromatin stability (Ayoub et al., 2003). In addition, the jmjC domain is essential for the normal function of *Epe1* in yeast (Ayoub et al., 2003). This suggests that HR might act through chromosome remodeling to regulate the expression of downstream genes.

Mutations in mice and phenotypes

A large variety of mutations of *Hr* have been identified in mouse and human, all of which display autosomal recessive inheritance. Many different *Hr* alleles have been cloned in mice and are summarized in table 2-2. There are two general classes of phenotypes that result from the mutations in murine *hairless*. The less severe mutants are designated as *hairless*, while the more severe mutants are known as rhino. The phenotype of Hr^{ba} is intermediate between *hairless* and *rhino*(Garber, 1952). The mutations Hr^{ba}, $Hr^{rh\text{-}2J}$, $Hr^{rh\text{-}9J}$ are now extinct (Panteleyev et al., 1998b). *Hr* was originally cloned in HRS/J mice as an insertion of a polytrophic provirus in the intron 6, which results in the aberrant splicing of *Hr* transcript therefore significantly reduced expression as low as 5-10% of that in +/+ mice (Cachon-Gonzalez et al., 1994; Jones et al., 1993). Most of the mutations identified in rhino mice are nonsense mutations in different exons of *hairless* (Brancaz et al., 2004; Panteleyev et al., 1998b; Zhang et al., 2005), leading to nonsense-mediated decay of *Hr* transcripts (Maquat, 2005; Panteleyev et al., 1998b). The phenotype of different *rhino* alleles varies in terms of the severity of the wrinkling, possibly due to the genetic backgrounds. The skin phenotype in both Hr^{hr} and Hr^{rh} mutants has been linked to massive and premature apoptosis that leaves the dermal papilla stranded and unable to reinitiate induction of the epithelial strand into follicle formation (Panteleyev et al., 1998b). Utricles and dermal cysts filled with keratins form in the skin of rhino mutant mice and expand with age. The dermis becomes filled with cysts, causing the severe skin wrinkling (Mann, 1971; Panteleyev et al., 1998b; Sundberg, 1994; Sundberg and Boggess, 1998). All confirmed alleles of *Hr* are autosomal recessive and most of them have been genetically characterized. The near naked (Hr^{n}) is a semi-dominant allele at the *Hr* locus (Stelzner, 1983). The homozygous Hr^{n}/Hr^{n} mice never grow their hair. Homozygotes are recognizable at 5 days of age with their thin, slick skin and short, curly vibrissae. Heterozygous adults undergo repeated hair loss and regrowth in contrast to heterozygous hairless and rhino mice with normal hair and permanent fur coat. The vibrissae of $Hr^{n}/+$ mice are very short, their skin is very thin, and wrinkles extensively with age. Both sexes are fertile, but females are poor mothers for breeding. The expression of all the alleles of murine *Hr* except Hr^{n} is downregulated at

Table 2-2 Genetic mutations and phenotypes in murine *hairless* gene

Alleles	Mutation	Location	Phenotype	Inheritance	Reference
Hr^{hr}	MLV insertion	Intron 6	Hairless	Recessive	(Stoye et al., 1988)
Hr^{rh}	R597X	Exon 6	Rhino	Recessive	(Cachon-Gonzalez et al., 1999; Howard, 1940)
$Hr^{rh\text{-}J}$	E534del	Exon 5	Rhino	Recessive	(Cachon-Gonzalez et al., 1999)
$Hr^{rh\text{-}7J}$	W292X	Exon3	Rhino	Recessive	(Sundberg, 1994)
$Hr^{rh\text{-}8J}$	K512X	Exon 4	Rhino	Recessive	(Ahmad et al., 1998d)
Hr^{rhChr}	R467X	Exon 4	Rhino	Recessive	(Ahmad et al., 1998c)
Hr^{rhY}	13 bp insertion	Exon 16	Rhino	Recessive	(Panteleyev et al., 1998a)
Hr^{rhbmh}	296 bp deletion	Exon 19 & 3'-UTR	Rhino-Bald	Recessive	(Brancaz et al., 2004)
Hr^{rhsl}	W911X	Exon 12	Rhino	Recessive	(Zhang et al., 2005)
Hr^{rhR}	R814X	Exon12	Rhino	Recessive	Liu unpublished
Hr^{ba}	N/A	N/A	Bald	Recessive	(Garber, 1952)
$Hr^{rh\text{-}2J}$	N/A	N/A	Rhino	Recessive	(Bailey and Bunker, 1973)
$Hr^{rh\text{-}9J}$	N/A	N/A	Rhino	Recessive	(Sundberg and Boggess, 1998)
Hr^{N}	N/A	N/A	Near naked	Semi-Dominant	(Stelzner, 1983)
$Hr^{Tg5053Mm}$	Transgene insertion	Intron 5 – Exon 8	Rhino	Recessive	(Jones et al., 1993)
Hr^{tm1Cct}	Transgene	Exon 8-10	Rhino	Recessive	(Zarach et al., 2004)

N/A: not available

least 10-fold in homozygous mutant mice compared to the wild type regardless of age (Cachon-Gonzalez et al., 1994; Cachon-Gonzalez et al., 1999; Panteleyev et al., 1998b; Panteleyev et al., 1998c).

Both Hr^{hr}/Hr^{hr} and Hr^{rh}/Hr^{rh} mutants have very low levels of *Hr* expression and start to lose their hair around 2-3 weeks age due to the disruption of the integrity of key functional tissue units in the hair follicle (Panteleyev et al., 2000). This suggests that normal levels of *Hr* protein are important for hair follicle to initiate the first hair cycle (Panteleyev et al., 1998c) and that *Hr* may be involved in the control of the first hair follicle cycling (Panteleyev et al., 2000). More specifically, the absence of *Hr* in hairless mice may cause dysregulation of normal, catagen-associated apoptosis and an impairment of cell adhesion (Panteleyev et al., 2000).

Hr mutant mice are also found to be dramatically more susceptible to dioxin than the wild type mice (Sundberg, 1994). The aryl hydrocarbon receptor (AhR), a ligand-activated transcription factor, is shown to mediate most of the toxic effects of dioxin (Whitlock, 1990). This suggests that *Hr* may be protective against aryl hydrocarbon (Ah) receptor-mediated dioxin toxicity in mouse skin (Knutson and Poland, 1982). Ornithine decarboxylase (ODC) is an important enzyme in the polyamine biosynthetic pathway, which plays an essential role in epithelial tumorogenesis (Weeks et al., 1982). Overexpression of ODC in the epidermis of transgenic mice causes a phenotype similar to hairless mutant mice (Soler et al., 1996). The transgenic mice have a normal first hair cycle, but lose the hair around 2-3 weeks old (Soler et al., 1996). The overexpression of ODC in the transgenic mice is first detected at day 12 (Soler et al 1996). Interestingly, it is found that dioxin is able to modulate ODC activity in skin of ODC transgenic mice (Raunio and Pelkonen, 1983) while hairless mutant mice are more susceptible to dioxin in the skin. This suggests that ODC plays an important role in hair follicle cycling and that there might be a direct interaction between HR and AhR.

It is also found that there might be *Hr* mutation-associated impairment of mammary gland function (Panteleyev et al., 1998b) since HR is expressed in mammary gland. However, the details still remain unknown. *Hr* mutants also show some neurological phenotypes, such as altered neuronal morphology, inner ear defects, and

abnormal retinal cytoarchitecture (Cachon-Gonzalez et al., 1999; Garcia-Atares et al., 1998). *Hr* mutants demonstrate a tendency toward skin ulceration upon minor epidermal trauma, suggesting a potential role for HR in the regulation of wound healing (Sundberg, 1994). All together these findings indicate that HR is pleiotropic and plays wide roles in development.

Mutations in human and related diseases

It is shown that mutations of *Hr* homolog in human are related with two autosomal recessive diseases, including congenital alopecia universalis (AUC, OMIM 203655) and atrichia with popular lesions (APL, OMIM 209500). Atrichia with popular lesions (APL, OMIM 209500) in human patients is the counterpart of the Hr^{hr}/Hr^{hr} in mice. The features of APL include papillary lesions over most of the body and almost complete absence of hair. Patients are born with hair that falls out shortly after birth and is not replaced. Malformations of the hair follicles are shown in histological studies. In addition to hair loss, other symptoms including concomitant mental retardation (Aita et al., 2000; del Castillo et al., 1974) and retardation of bone age (Kruse et al., 1999) are also reported in some cases.

The mutation in human *Hr* was first identified as causing APL by Christiano's group in 1998 (Ahmad et al., 1998a), although the missense mutation first reported was proved to be a single nucleotide polymorphism (Hillmer et al., 2002). A number of mutations in *Hr* responsible for causing APL have been found since 1998 (Ahmad et al., 1998a; Ashoor et al., 2005; Bergman et al., 2005; Djabali et al., 2004; Henn et al., 2002; Hillmer et al., 2001; Indelman et al., 2003; John et al., 2005; Masse et al., 2005b; Paradisi et al., 2003; Paradisi et al., 2005; Sprecher et al., 1999a; Sprecher et al., 1998; Sprecher et al., 2000; Yang et al., 2005; Zlotogorski et al., 2003; Zlotogorski et al., 2002a). There are four different types of mutations, including nonsense mutations, missense mutations, deletions/insertions, and splice site mutations, in human *Hr* that cause APL (Ashoor et al., 2005) as shown in table 2-3. In addition, the APL phenotype has been shown to result from compound heterozygosity in *Hr* (Ashoor et al., 2005). Interestingly, two originally reported mutations were shown to be just polymorphisms by examining a larger

Table 2-3 Genetic mutations and phenotypes of human *hairless* gene.

Mutation	Location	OMIM	Reference
Nonsense mutations			
R33X	Exon 2	APL	(Zlotogorski et al., 2002a)
R154X	Exon 2	APL	(Ashoor et al., 2005)
Q260X	Exon 3	APL	(Masse et al., 2005a)
Q478X	Exon 4	APL	(Sprecher et al., 1999b)
Q515X	Exon 4	APL	(Ashoor et al., 2005)
R613X	Exon 6	APL	(Ahmad et al., 1999a)
W699X	Exon 8	APL	(Masse et al., 2005a)
Q1176X	Exon 19	APL	(Henn et al., 2002)
Missense mutations			
E583V	Exon 5	APL	(Paradisi et al., 2003)
C622G	Exon 6	APL	(Aita et al., 2000)
N970S	Exon 14	APL	(Kruse et al., 1999)
D1012N	Exon 15	ALUNC	(Djabali et al., 2004)
T1022A	Exon 15	APL	(Ahmad et al., 1998a)
V1056M	Exon 16	APL	(Zlotogorski et al., 2002b)
V1136D	Exon 18	ALUNC	(Cichon et al., 1998)
Deletions/insertions			
177del11	Exon 2	APL	(Zlotogorski et al., 2003)
189-199del	Exon 2	APL	(Indelman et al., 2003)
1256delC; 1261del21	Exon 3	ALUNC	(Ahmad et al., 1999d)
2001delCCAG	Exon 7	APL	(Kruse et al., 1999)
2147delC	Exon 9	APL	(Zlotogorski et al., 1998)
2847-2delAG	Exon 14	APL	(Henn et al., 2002)
3434delC	Exon 18	APL	(Sprecher et al., 1999a)
Splice site mutations			
1557-1 G to T	Intron 4	APL	(Paller et al., 2003)
IVS8+2 T to G	Intron 8	APL	(Paradisi et al., 2005)
2776+1 G to A	Intron 12	APL	(Cichon et al., 1998)
2776+2 insT	Intron 12	APL	(Paller et al., 2003)
2847-3 C to G	Intron 13	APL	(Paller et al., 2003)

APL: atrichia with papular lesions; ALUNC: alopecia universalis congenital;

X: nonsense mutation; del: deletion; ins: insertion

population (Ahmad et al., 1998a; Ahmad et al., 1998b; Hillmer et al., 2001; Hillmer et al., 2002). Totally 17 different *Hr* genetic variants in human have been reported (Hillmer et al., 2002; Zhang et al., 2005), including nine amino acid substitutions, one amino acid deletion, four silent changes, and three variants in exon-flanking intronic sequences.

About this dissertation

The objective of this dissertation is to study the molecular and physiological mechanisms underlying hair loss in two mouse models: *near naked hairless* (Hr^{n}) and *Oak Ridge rhino-like* (Hr^{rhR}) mutant mice. Several major approaches were applied in the dissertation, including microarray analysis, histological analysis, and electron microscopy, to systematically characterize these two mutants. There are two different primary platforms of microarray: cDNA or long oligo arrays (also referred to as spotted or two-color arrays) and Affymetrix arrays, which consist of short oligos synthesized in situ (also known as single-color arrays). The Affymetrix platform has much greater probe density and can be used to profile expression across the entire genome. Two-color arrays are printed with either long oligonucleotides (~65mers) or cDNA, and are used to detect the relative expression changes. Oligonucleotide microarrays representing either 15,000 or 21,000 mouse genes are used in this dissertation. Histological analysis is a basic tool used in dermatological research and is widely used in this dissertation to detect morphological changes in hair follicles of skin due to the mutations. Scanning electron microscope is used to examine in fine detail the external defects in hair structure of the mutant mice.

This dissertation begins with the introduction of our research in chapter 1, followed by chapter 2, the background and significance of our research in the effort to search mutations underlying hair loss in mice models. In chapter 2, the basic information about hair follicle development and cycles is discussed, followed by a summary of the recent research with *hairless* gene (*Hr*). Chapter 3 summarizes all the materials and techniques used in this dissertation. Chapter 4 presents the effort in search for the genetic mutation in Hr^{n} mice, while chapter 5 shows the early molecular and physiological alterations in Hr^{n} mice. Chapter 6 displays the genetic basis for Hr^{rhR} mutation and the effort in search of the initial downstream event due to the mutation. Conclusion and

future works for elucidating the roles of HR are presented in Chapter 7 with a hypothesis about the possible roles of HR in both Hr^{n} and Hr^{rhR} mutants.

Chapter 3 Experimental methods and materials used in this study

Animals and tissue collection

Hr^{n} mice (Stelzner, 1983) were maintained in the ORNL mouse facility on a congenic BalbC/Rl background by crossing *Hr*^{n}/+ males (identified phenotypically) with wild type BalbC/Rl females (Stelzner, 1983). Because intercross matings of *Hr*^{n}/+ animals on the BalbC/Rl genetic background failed to reliably yield homozygous offspring, *Hr*^{n}/*Hr*^{n} animals were produced by first outcrossing *Hr*^{n}/+ males to FVB/N females and then intercrossing F1 *Hr*^{n}/+ mice to produce the three genotypes (+/+, *Hr*^{n}/+, and *Hr*^{n}/*Hr*^{n}). *Hr*^{n}/+ and *Hr*^{n}/*Hr*^{n} mice were identifiable by phenotype at approximately 6 days of age by the presence of sparse or absent pelage, respectively.

Hr^{rhR} mice arose several generations downstream of a translocation experiment. The male parent was a treated JH male and the female parent was an SB female. SB refers to the F1 hybrid made from SEC/E x C57BL/E. The mutant was outcrossed to BLH F1's for stock maintenance. BLH refers to C3Hf x C57BL10a. It was maintained in the ORNL mouse facility by mating *Hr*^{rhR}/*Hr*^{rhR} male with *Hr*^{rhR}/+ female with a mixed strain background. *Hr*^{rhR}/*Hr*^{rhR} mice are distinguishable as early as 2 weeks of age due to hair loss. *Hr*^{rhR}/+ mice were normal and do not have hair loss compared to +/+ mice.

At various ages, animals were euthanized by cervical dislocation, and dorsal skin was harvested from littermate animals of each genotype for RNA isolation and various histological analyses. Dorsal skin collected for RNA extraction was harvested into RNALater (Ambion, Texas), refrigerated at 4°C overnight, and then stored at -80°C until RNA extraction was performed. Skin harvested for histological analysis and immunohistochemistry was fixed in 10% neutral buffered formalin for 24-48 hours and then stored at room temperature in 70% ethanol. Liver and spleen samples used for genomic DNA isolation were collected into liquid nitrogen and stored at -80°C. Tails and ear snips used for genomic DNA isolation were collected into a 1.5 ml microtube and stored at -20°C.

PCR reactions and DNA sequencing of *Hr*

For *Hr*^{n} mutation, direct sequencing was performed with the PCR products amplified from both cDNA and genomic DNA templates. The full length *Hr* cDNA was

sequenced using cDNA templates prepared from skin RNA extracted from Hr^n/Hr^n animals on the BalbC/Rl / FVB/N mixed background and from C3H/HeJ and 101/Rl strains, the two potential strains on which the original Hr^n mutation arose. cDNA was synthesized in reverse transcription reactions using total skin RNA reverse transcription reactions were performed using SuperScript II reverse transcriptase, oligo d(T) primer, and 2 µg of DNase I-treated total RNA according to the manufacturer's protocol (Invitrogen.com). Primers to produce overlapping amplicons for both genomic DNA and cDNA templates were designed using the Primer3 database (Rozen and Skaletsky, 2000). Primers to amplify the entire *Hr* cDNA were designed according to the full-length mRNA sequence (GenBank accession number Z32675) originally reported by Cachon-Gonzalez, et al (1994). Melting temperature and $MgCl_2$ concentration were optimized for each primer pair, and products were verified by electrophoresis in 1% agarose gels to confirm amplicon size and check for nonspecific products. After optimization, PCR products were electrophoresed in 1% agarose gels and the specific bands were isolated and purified across columns (GFX PCR DNA and Gel Band Purification Kit, Amersham Biosciences). Purified amplicons were sequenced bidirectionally using BigDye Version 3.1 dye terminator kit (ABI, Foster City, CA) and analyzed on an ABI 3100 Genetic Analyzer. Genomic DNA from Hr^n/Hr^n mice was extracted from liver and spleen using a standard protocol (Bultman SJ, 1992). The entire *Hr* gene, including introns and exons, was sequenced from genomic DNA of Hr^n/Hr^n and +/+ animals, by sequencing the PCR products to cover the whole region. The primers for genomic DNA sequencing were listed in table 3-1. DNA corresponding to the genomic region between coordinates 62324459-62349944 on mouse chromosome 14 (based on UCSC May 2004 mouse draft genome), including the *Hr* gene and 8 kb upstream of the first exon, was sequenced.

For Hr^{rhR}, the sequencing was performed by sequencing the entire genomic region of *Hr*. Genomic DNA of Hr^{rhR} was extracted based on the method called HotSHOT (Truett et al., 2000). Briefly, tissue samples (ear punches, 0.2-cm tail snips) were collected into a 1.5 ml eppendorf microtube. The samples were lysed with 75 µl of alkaline lysis buffer (25mM NaOH, 0.2 mM Disodium EDTA, pH 12.0) at 95°C for 1 hour. After heating, samples were cooled to 4°C. Each sample was added with 75 µl

Table 3-1 List of primers used for *Hr* genomic sequencing (sequences from 5' to 3' end)

Primer Pairs	Sequence of Forward primers	Sequence of Reverse Primers	Size of Product
F2/R2	ATGGCGATCAGAGGTCCTG	CAAGCGAGGGAAAATTGAAC	872
F3/R3	CGACCCACCCTAGTCTGAAA	TTCAGGAAGCTGGGCATACT	871
F4/R4	ATGAGGGCAGGAGAGTGATG	AAACAGACCACGAGGACGAC	866
F5/R5	AAAGATGGGCATGAGAGTGC	GCCAGGTCTTTTTCAGCTTG	855
F6/R6	ATCACTGACCCGTGAGAACC	GTTCTCCCGCTTTCTGCTC	920
F7/R7	CAGGGGAATCCAGTGAAGAA	CGATGTACCCAAAAGGCTGT	912
F8/R8	AGCCTTTTGGGTACATCGTG	GAGTGCTGCTGGCTCTGACT	860
F9/R9	GCTCCAGGAGTCCAGACTTG	ACTAGGGGCTTCCCTCTCTG	910
F10/R10	GCAATGGTGTGAACTTCGTG	AGCCACCCTCTTAGGGACAT	953
F11/R11	TGTCCCTAAGAGGGTGGCTA	CCTCCTGTTTGCTTGGTCAT	910
F12/R12	TGATGACCAAGCAAACAGGA	TCAGCAAGCCACAAAACAAG	938
F13/R13	TTACATGCGCACAAGTTTCC	CTGCCAGGTGCCTGAGATAC	855
F14/R14	ACCTGGCAGGCACTTAACAT	GGAGAGGGAGAGAGGGAAAA	915
F15/R15	GCATTTTGACTTTCCCCAAT	ATTGTTTTGCTTGCCACCTC	924
F16/R16	GAGGTGGCAAGCAAAACAAT	AGTGTTGGGAAGGGAGAGGT	873
F17/R17	ACCTCTCCCTTCCCAACACT	TGAGACCCATCAGAGCTTCC	887
F18/R18	GGAAGCTCTGATGGGTCTCA	GGGAGCACATACAGGGACAT	757
F19/R19	CTGTGATGTCCCTGTATGTGCT	ACTCCCCTGCTAGACTCTCCTT	1016
F20/R20	GCTAGATCCAGGTGCAGAGG	TTTGGTGGTGGTGGTAGTCA	799
F21/R21	TGACTACCACCACCACCAAA	TCCCTTCAGCTAGGACCTCA	789
F22/R22	ATGGCTGAGGTCCTAGCTGA	ACCAGGTAAGCACCTGATGG	920
F23/R23	GAGAAGAGTGGGGTGTGAGC	CGGACCACACCGTCTAAGTT	950
F24/R24	ACTGGGGAACTTAGACGGTGT	TTCCGTAATCTCCACAGGTTG	804
F25/R25	AAAGAAGGCGAATGCAGAAA	TGTTCCATCACACCCAGCTA	758

neutralizing buffer (40 mM Tris-HCl, pH 5.0). Five to ten microliters of the final preparation are used per 50-µl PCR volume. The genomic region of *Hr* in mouse was sequenced with the primers designed to cover *Hr* DNA (listed in Table 3-1). The PCR reactions were performed to amplify all the fragments covering the *Hr* genomic DNA. The PCR products were then sequenced as described earlier.

The sequences from both Hr^{n} and Hr^{rhR} were analyzed by using a trial version of Chromas software provided by Technelysium Pty Ltd (Queensland, Australia) and compared to the public *Hr* sequence using two-sequence alignment in BLAST (NCBI). If a nucleotide change was seen in both sequences from forward and reverse primers of sequencing, the nucleotide change was considered as true. The sequences from either Hr^{n} or Hr^{rhR} were compared with those from wild type animals to identify any nucleotide change. If the change was also seen in either of the founder strains C3H/HeJ or 101/Rl, the change was considered as a SNP and not a true change. A base pair change in the exon 12 was identified as a nonsense mutation in Hr^{rhR} mutant mice. However, there was no base pair change found for Hr^{n} mutation in *Hr* gene.

Genotyping of Hr^{rhR} mice

After the mutation of *Hr* in exon 12 was identified, a pair of specific primers covering the DNA containing the mutation was used for genotyping of the mice. The sequence of the forward primer (GRHF) is 5′- CCAAGAACCTGAGGACCAGA-3′. The sequence of the reverse primer (GRHR) is 5′ GCCAGTGTTCCTGGAAGAGA -3′. PCR was performed using Platinum Taq DNA polymerase (Invitrogen, Carlsbad, CA) with standard protocols in an Eppendorf Mastercycler thermal cycler (Eppendorf, Westbury, NY). The PCR products were isolated through electrophoresis in a 1% agarose gel with 1X TAE buffer. The DNA was purified using GFX PCR DNA and Gel Band Purification kit (Amersham Biosciences Corp, Piscataway, NJ) and sequenced on both strands. The sequences were analyzed with Chromas software (Technelysium Pty Ltd, Queensland, Australia) and blasted to NCBI database directly.

Total RNA isolation

RNA was isolated from dorsal skin using the QIAGEN RNeasy mini RNA isolation system (Qiagen) according to a protocol modified for fibrous tissue supplied by

the manufacturer and including an optional DNase I treatment step to eliminate contaminating genomic DNA. RNA quality was assessed by visualization in denaturing agarose gel electrophoresis and spectrophotometrically by the 260 nm/280 nm ratio of absorbance. Samples were quantified spectrophotometrically based on the absorbance at 260 nm. Only RNA samples of high quality were used for further analysis.

Microarray construction, labeling, hybridization and data analysis

Two array platforms were used in these studies. Focused cDNA microarrays were designed and fabricated to represent genes of interest in skin and hair biology. Plasmid clones for selected cDNAs were purchased from Research Genetics and amplified and purified according to standard protocols (Sambrook et al., 1989). cDNA inserts contained in plasmid DNA were verified by bi-directional sequencing using universal M13 primers (TIGR). Sequences were analyzed using BLAST (NCBI). Clones with confirmed identity were amplified by PCR, lyophilized, resuspended in 3X SSC, and spotted in triplicate onto Corning UltraGAPS slides using an SDDC-2 arrayer (Virtek). After printing, slides were air-dried and the cDNAs irreversibly immobilized by UV-crosslinking. Spot quality was assessed by hybridization with fluorescently-labeled panomers according to manufacturer's protocols (Molecular Probes).

CompuGen Mouse Oligolibrary™ 2.0 representing about 21000 mouse genes was purchased from CompuGen (www.compugen.com). The oligonucleotides were printed on Corning Ultra Gap slides by the Center for Applied Genomics (Newark, NJ). After printing, slides were air-dried and the oligonucleotides were irreversibly immobilized by UV-crosslinking.

Total RNA (10 µg) from dorsal skin was fluorescently labeled with either cyanine-3 (Cy3) or cyanine 5 (Cy5) using an indirect dye incorporation protocol (TIGR). Briefly, RNA was reverse transcribed using 2.0 µg of anchored oligo(dT) (T_{20}-V-N) primer and SuperScript™ II reverse transcriptase in the presence of 5-(3-aminoallyl)-2'deoxyuridine-5'-triphosphate (AA-dUTP). The resulting cDNA was purified using QIAquick PCR columns (Qiagen) with a modification to eliminate Tris from the column washing buffers (TIGR) and the reaction efficacy confirmed by measuring cDNA yield spectrophotometrically. Purified, aminoallyl-labeled cDNA was coupled to either Cy3 or

Cy5 (Amersham) by incubation in the dark in a basic (pH 9.5) phosphate buffer. Unbound dyes were removed from cDNAs by column purification using QIAquick columns (Qiagen). Dye incorporation and labeled cDNA yield were measured by scanning spectrophotometry and calculated from the absorbance values at 260 nm (cDNA) and at either 550 nm (Cy3) or 650 nm (Cy5).

Each hybridization consisted of a pair of RNA samples from littermates. For Hr^{n}, either homozygous or heterozygous mice were compared to wild type; for Hr^{rhR}, Hr^{rhR}/Hr^{rhR} mice were compared to $Hr^{rhR}/+$ mice. For each pair of animals a dye swap was performed to control for dye-specific bias in labeling and to provide a replicate hybridization for each pair of samples. Cy3 and Cy5 labeled samples were combined in hybridization buffer (50% formamide, 5X SSC ad 0.1% SDS) containing 10 µg each mouse Cot-1 DNA and poly(dA) DNA (Invitrogen), applied to slides, coverslipped and hybridized to arrays overnight in a humidified chamber at 42°C according to established protocols (TIGR). After washing to remove nonspecifically bound probe, slides were scanned for Cy3 and Cy5 fluorescence using a ScanArray 4000 confocal laser scanner (Perkin Elmer), and fluorescent intensities were represented as TIFF images. Images were analyzed and median pixel fluorescence intensities collected using ImaGene (Biodiscovery). Data were normalized using Lowess after removing spots of poor quality or low expression and subtracting local background. Replicate values for each gene were combined and median expression values analyzed for differential expression using the Confidence Analyzer function available in GeneSight and a 95% confidence interval.

The differentially expressed genes from microarray analysis were uploaded to DAVID 2.1 (Database for Annotation, Visualization and Integrated Discovery, http://david.abcc.ncifcrf.gov/main.htm) for functional annotation including gene ontology (GO) analysis. The differentially expressed genes with their expression alterations were uploaded to Ingenuity (http://www.ingenuity.com/) for pathway and network analysis, suggesting potential signaling pathways altered due to the mutations.

Quantitative real time RT-PCR

cDNA was generated from 1-5 µg of total RNA using SuperScript II reverse transcriptase (Invitrogen, Carlsbad, CA) and oligo(dT) primer. All qRT-PCR reactions

were performed using a SmartCycler thermal cycler (Cepheid, Sunnyvale, CA), and software supplied by the manufacturer was used to identify threshold cycle (C_t) values. Expression levels of many genes were assayed using Assays-on-Demand^{TM} pre-designed gene-specific primer/TaqMan probe sets and TaqMan Universal Master Mix (Applied Biosystems), following the manufacturer's protocol. Expression levels of most of the genes were quantified using SYBR green I detection chemistry and custom primers designed using the Primer3 website (Rozen S, et al., 2000). Primers were designed to span at least two exons if possible and to produce amplicons 75-150 bp in size. SYBR green assays were done with Hotstart ExTaq DNA polymerase (TaKaRa Mirus Bio, Madison, WI) with the standard protocol supplied by TaKaRa. Annealing temperatures and $MgCl_2$ concentrations were optimized for each primer pair prior to quantitation, and products was verified by electrophoresis in ethidium bromide-stained 2% agarose gels. Each sample for both TaqMan and SYBR green detection systems was assayed in duplicate. A standard curve was generated for each primer pair using log dilutions (1:5) of a pool of skin cDNA samples.

Northern blot

Twenty micrograms of total RNA with a volume of 15 µl were mixed with 3 µl of 6X loading buffer (Formamide 720 µl, Formaldehyde 260 µl, 10X MOPS 160 µl, 80% Glycerol 100 µl, RNase-free water 80 µl). 10X MOPS buffer contains 200 mM MOPS, 50 mM EDTA, 21 mM NaOAC, and was adjusted to pH 7.0. Samples were denatured at 65°C for 10 minutes, chilled on ice, and loaded onto a RNA gel (1% agarose, 1X MOPS, 2.7% Formaldehyde, 0.5 ng/ml Ethidium Bromide). The running buffer is 1X TAE buffer (40 mM Tris, 1 mM EDTA, 20 mM acetic acid) containing 1X MOPS. The gel was electrophoresed at 4-5 Volts/cm for 5-6 hours. Gel was photographed under UV light. Positively charged nylon membrane (Roche Diagnostics GmbH, Mannheim, Germany) and transfer filter papers were equilibrated in 20X SSC buffer (3M NaCl, 0.3 M Na_3-citrate). The gel was then transferred to the nylon membrane overnight (Sambrook et al., 1989). The membrane was then crosslinked in Stratalinker.

The cDNA probes of *Hr* were generated from mouse skin total RNA by RT-PCR using two pair of primers covering different portions of *Hr*. One pair of primers is called

HrMF/HrMR to cover the exon 12 in *Hr* gene. Their sequences are HrMF: 5'-GATTCACATGGCCTTTGCTC-3'; HrMR: 5'- CCCCACAGGCTAAGTCTCAA-3'. The second pair of primers is called HrF5/HrR5 to cover the sequences of *Hr* mRNA from 1728-2567 base pairs in NM_021877. The sequences of these primers are Hr-F5: 5'-CAACGGATCCATATAGGAAGCAAGGCGGAG-3'; Hr-R5: 5'-CGCCGAATTCC-TCTTCTTTGATGTCCTTGGTC-3'. The blot was washed for 30 minutes in 1X SSC, 0.1% SDS (Sodium Dodecyl Sulfate) at 65°C. The blot was then incubated with hybridization buffer (0.1% SDS, 50% formamide, 5X SSC, 50 mM NaPO4, pH 6.8, 0.1% sodium Pyrophosphate, 5X Denhardt's solution, 50 μg/ml sheared herring sperm DNA) without the probe for at least 2 hours at 42°C. 5X Denhardt's solution contains 0.1% Ficoll (type 400), 0.1% polyvinylpyrrolidone, and 0.1% bovine serum albumin. The blotted membrane was then hybridized with [α-^{32}P]-CTP-labeled cDNA probe in hybridization buffer at 42°C overnight. The membrane was washed with fresh hybridization buffer for 30 minutes, 2X SSC containing 0.1% SDS for 30 minutes twice, 1X SSC containing 0.1% SDS for 30 minutes at room temperature. After the final wash with 0.2X SSC containing 0.1% SDS for 45 minutes at 55°C, the membrane was exposed to X-ray film with intensifying screens at -80°C.

Histological analysis

Hematoxylin and Eosin (HE) staining was done according to standard protocols (Prophet et al., 1992). Von Kossa staining was used to assess mineralization of dermal cysts. Sections were dewaxed, rinsed in alcohol and distilled water, and treated with 5% silver nitrate placed directly in front of a bright lamp for one hour. After rinsed in distilled water, the sections were rinsed in 5% sodium thiosulfate for 2 minutes and counterstained with nuclear fast red for 1 minute. Finally the sections were rinsed in distilled water, dehydrated, and mounted.

Actively replicating cells were selectively highlighted within tissue samples by immunostaining with an antibody to the Ki67 antigen. Five-micron sections were placed on charged slides and dehydrated. Endogenous peroxidases were neutralized with 0.03% hydrogen peroxide followed by a casein-based protein block (DakoCytomation) for nonspecific staining blocking. The sections were incubated with rabbit anti-human Ki-67

(NovaCastra Laboratories Ltd.) diluted 1:1500 for 60 minutes. Sections without primary antibody served as negative controls. The Dako Envision+ HRP/DAB System (DakoCytomation) was used to produce localized, visible staining. The slides were lightly counterstained with Mayer's hematoxylin, dehydrated and coverslipped.

Scanning electron microscopy

The samples were dehydrated in a graded ethanol series, then dried in CO_2 using a LADD Research critical point dryer. After drying the samples were mounted on sample supports using silver paint, and then lightly coated with gold in an SPI sputter coater. Samples were examined and photographed in a LEO 1525 scanning electron microscope (Zeiss, New York, USA) operating at 3KV.

***In situ* hybridization**

A standard protocol for paraffin embedding was used and sections were cut 6 micron in thickness using Lecia RM2135 microtome (Deerfield, IL). The transcribed region of mouse RefSeq NM_021877 was used for in vitro transcription reactions according to protocols supplied by the manufacture (Ambion, Texas). Antisense probe was labeled with a biotin RNA labeling mix (Roche, Germany). The in situ hybridization experiments were carried out according to a standard protocol with minimum modifications. The probe was detected by Tetramethyl-rhodamine Tyramide Signal Amplification System (PerkinElmer). DAPI was used for counter stain and then examined using Olympus BX61 microscope, and pictures were taken using a CC12 CCD camera (Melville, NY).

Hematology analysis

Mice from 9, 13, 15, and 35 days of age were anesthetized with isoflurane in a drop jar. Blood was collected from retro-orbital sinus with a microhematocrit blood tube filled with EDTA. The collected blood sample was released into a special tube in which the blood sample was loaded to Cell-Dyn 3500 automated hematology analyzer (Abbott Laboratories, Abbott Park, IL). The analyzer measures the complete blood count, different parameters of red blood cells and platelets.

Chapter 4 The *near naked hairless* (*Hr*^{n}) mutation disrupts hair formation but is not due to a mutation in the *hairless* gene

Part of the results presented in Chapter 4 and 5 are being combined into a single manuscript (with the same title as given to this chapter), which will be submitted to Physiological Genomics.

Introduction

The mammalian hair follicle is a unique structure due to its cyclical ability to regress and regrow throughout the life of the animal. The hair cycle consists of anagen, a growth stage, followed by orchestrated regression (catagen) and a resting phase (telogen) (Chase, 1954). Catagen is demarcated by cessation of proliferation and onset of apoptosis in the lower portion of the hair follicle, separating the hair bulb from the dermal papilla (Lindner et al., 1997). The lower follicle retracts toward the epithelial surface, where it remains quiescently in telogen until receiving a cue to proliferate, grow down towards the dermal papilla, and re-enter anagen (Stenn and Paus, 2001). The cascade of signals triggering onset of anagen are poorly defined (Stenn and Paus, 1999), but the delicate balance necessary to maintain normal cycling is evidenced by multiple mouse mutations that lead to hair loss by disrupting the hair cycle (Sundberg, 1994). Of these, the mostly well-characterized are mutations at the *hairless* (*Hr*) locus. Multiple allelic mutations have arisen in *Hr*, all of which manifest in mice as an inability to regrow a normal coat of hair after the initial catagen stage, resulting in a progressive loss of hair from head-to-tail beginning in the third week of life (Brooke, 1926; Howard, 1940). Mouse hairless mutants fall into two general categories, *hairless* (*Hr*^{hr}) and *rhino* (*Hr*^{rh}), based on phenotypic severity. Both classes of mutants display dermal cysts and wrinkling of the skin (Mann, 1971; Sundberg, 1994), but rhino mutants are characterized by progressively thickened and loosened skin that develops due to expansion of horn-filled cysts in the lower dermis (Sundberg et al., 1991). A fundamental role for *Hr* in the mammalian hair follicle is reflected in the fact that *Hr* mutations in sheep (Finocchiaro et al., 2003) and rhesus macaques (Ahmad et al., 2002) also cause a strikingly similar hair loss phenotype. Moreover, multiple mutations in the orthologous human gene underlie various forms of congenital atrichia, including those classified as atrichia with papular

lesions (APL; OMIM 290500) and alopecia universalis congenital (ALUNC; OMIM 203655) (Klein et al., 2002). While the molecular bases differ for *Hr* mutations characterized to date, all display recessive inheritance.

The underlying *Hr* gene was originally cloned in mouse by virtue of an endogenous murine leukemia provirus that inserted into intron 6, leading to defective *Hr* splicing and a significant reduction in *Hr* mRNA (~ 5% of wild type) in Hr^{hr}/Hr^{hr} animals (Cachon-Gonzalez et al., 1994; Stoye et al., 1988). The phenotypic severity of *Hr* mutations was recently linked to the level of mRNA and protein that remain, with the least severe allele Hr^{hr} (HRS/J) retaining some level of both mRNA and protein; $Hr^{rh\text{-}J}$, a rhino allele, expressing only a minor 3 kb *Hr* transcript; and a completely null allele ($Hr^{-/-}$) generated by gene targeting displaying no *Hr* expression and the most severe skin wrinkling (Zarach et al., 2004). *Hr* is highly conserved between mouse, rat and human, but orthologous genes in non-mammalian species have yet to be identified. It encodes a relatively novel protein of 127 kDa that includes a single zinc finger and a jumomji C domain (Cachon-Gonzalez et al., 1994), a metalloenzyme-like domain implicated in chromatin remodeling (Balciunas and Ronne, 2000). Its predicted role in control of gene expression is borne out by its demonstrated ability to function as a transcriptional corepressor by heterodimerization with the thyroid hormone receptor (*TR*) (Thompson and Bottcher, 1997), vitamin D receptor (*VDR*) (Hsieh et al., 2003) and retinoic acid-like orphan receptor α (*ROR-α*) (Moraitis et al., 2002), possibly mediated through association with histone deacetylases (Potter et al., 2002). *Hr* is expressed in multiple tissues, with highest levels in developing brain and skin (Cachon-Gonzalez et al., 1994). The skin phenotype in Hr^{hr} and Hr^{rh} mutants has been linked to massive and premature apoptosis that leaves the dermal papilla stranded and unable to reinitiate induction of the epithelial strand into follicle formation (Panteleyev et al., 1998b).

The only mutation allelic with *hairless* but not displaying recessive inheritance was first described by Stelzner in 1983 and designated near naked (Hr^{n}). The mutation arose spontaneously in the mouse colony at Oak Ridge National Laboratory, and allelism testing with Hr^{hr} suggested that the two mutations resided in the same or a closely linked locus (Stelzner, 1983) (figure 4-1). Hr^{n} differs from classical *Hr* mutations in that it

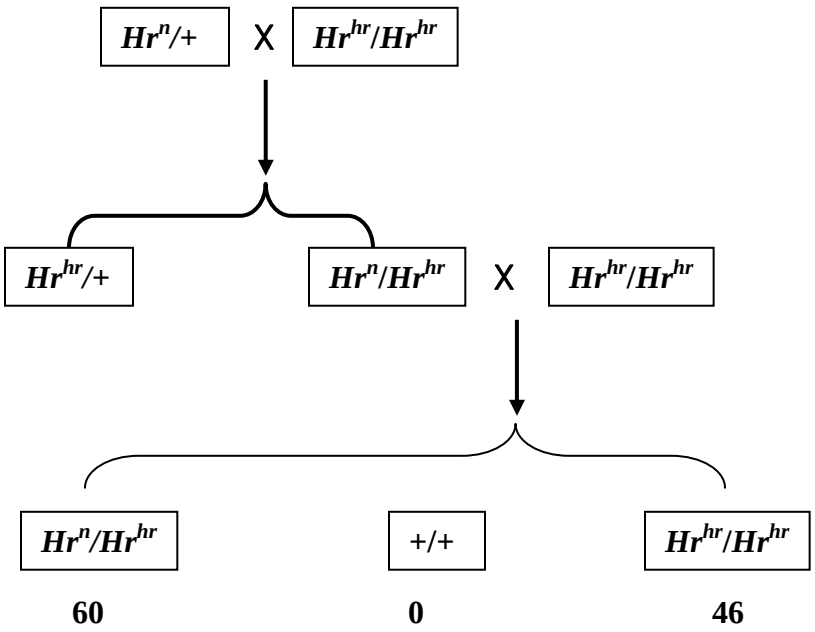

Figure 4-1 Schematic illustration of allelism test between $Hr^{n}/+$ and Hr^{hr}/Hr^{hr} (based on the report of (Stelzner, 1983).

exerts its effects in a semi-dominant rather than recessive manner. Heterozygous animals display a very sparse coat that undergoes some level of cyclic loss and regrowth, while Hr^n/Hr^n animals are virtually hairless. The etiology of the phenotype in Hr^n mutants also differs markedly from that of other *Hr* mutants in that mice never grow a normal coat of hair (Stelzner, 1983). We sought to identify the molecular basis for the Hr^n mutation and to define the alterations in skin and hair morphology that underlie hair loss. Because *Hr* encodes a transcriptional corepressor, we also investigated the changes in skin gene expression that result from the Hr^n mutation. We report here that despite original allelism tests suggesting that Hr^n is an allele of *Hr* (Stelzner, 1983), the phenotype of these animals is not due to a mutation in the *Hr* gene. Based on our collective results, we propose that the phenotype of Hr^n mice results from either an as yet unidentified regulatory mutation in *Hr*, or a mutation in a closely linked gene.

Results

Phenotype

Both $Hr^n/+$ and Hr^n/Hr^n are first distinguishable from their wild type littermates at approximately 5 days of age, when the hair coat begins to appear. Heterozygous animals display a sparse but uniform coat while homozygous animals exhibit a skin slick in appearance and are virtually devoid of hair. The sparseness of the coat in $Hr^n/+$ animals increases in severity as mice age and progress through successive hair cycles, with few hairs present in aged animals (figure 4-2). Vibrissae of Hr^n/Hr^n are extremely short and wavy, while those of $Hr^n/+$ are intermediate between Hr^n/Hr^n and +/+ in both length and texture (figure 4-3). The hairs in both $Hr^n/+$ and Hr^n/Hr^n are thinner compared to those in +/+ mice under the dissecting microscope with the same magnification (figure 4-3). There are no significant differences found between the mutants and the wild type animals in ear or foot or nails. The Hr^n mice also displayed impaired body growth. Both body weight and body length were significantly reduced in Hr^n/Hr^n mice beginning at 7 days of age. $Hr^n/+$ displayed a similar reduction in size that was significant at some but not all ages measured (figure 4-4).

HE stained sections of dorsal skin were examined in order to further define the morphological changes in hair follicles accompanying the gross hair loss defect in Hr^n

(A) 13-day old mice

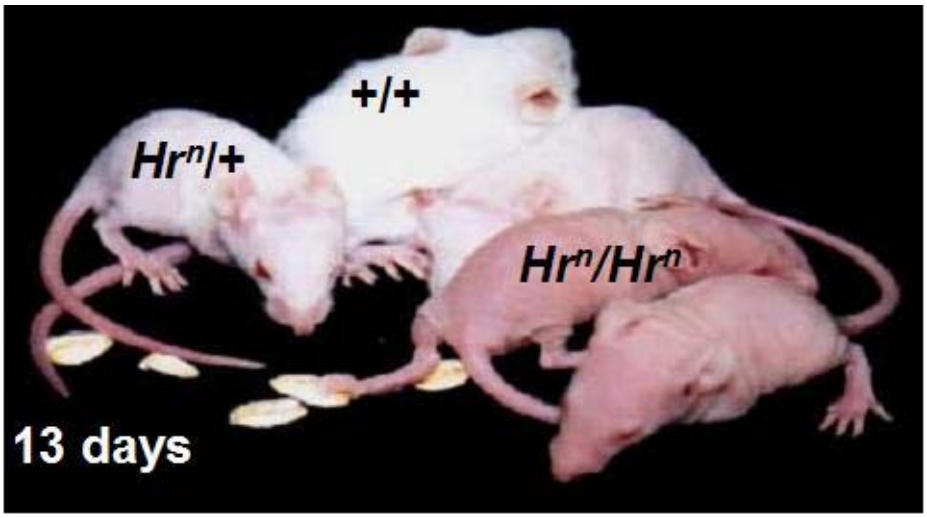

(B) adult mice

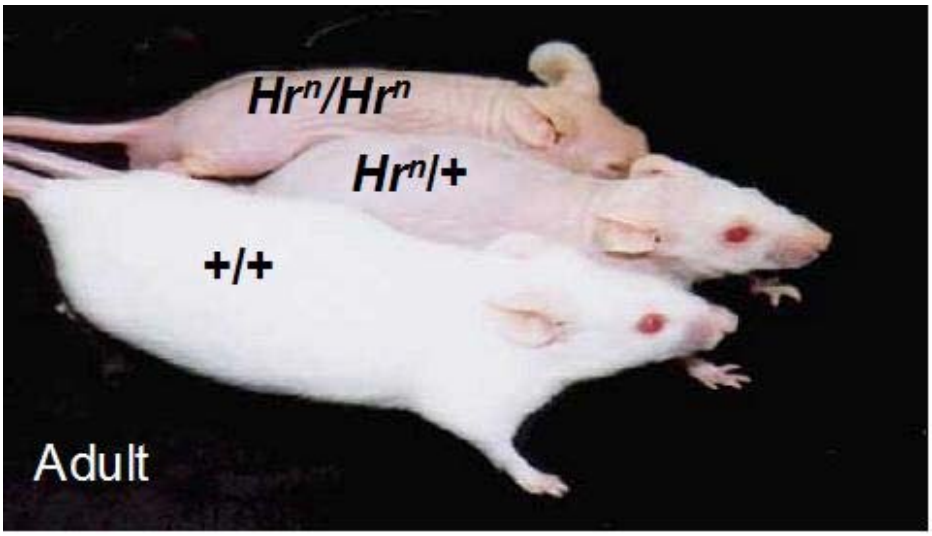

Figure 4-2 Phenotypes of Hr^n/Hr^n, $Hr^n/+$, and +/+ mice. (A) 13-day old mice; (B) 5-week old mice.

(A) 7-day

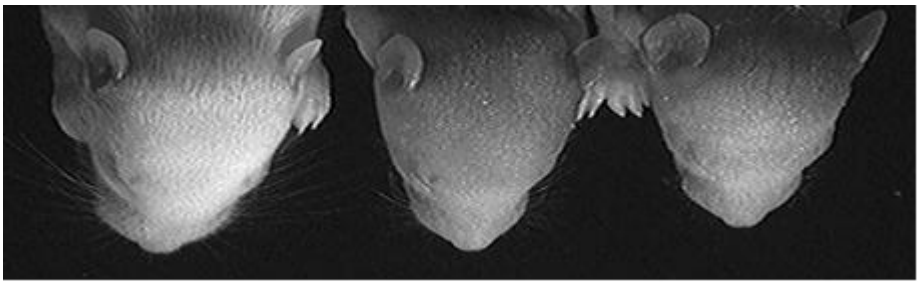

(B) 3-week +/+ $Hr^n/+$ Hr^n/Hr^n

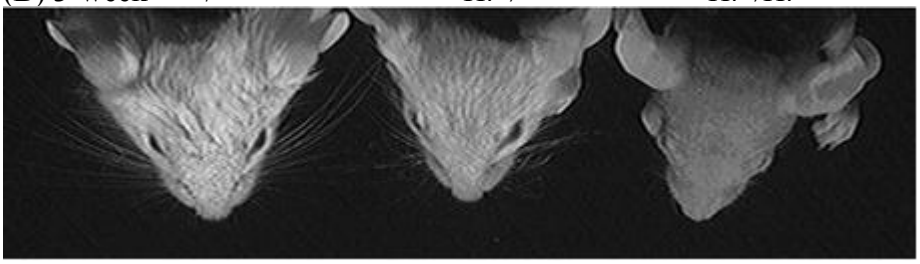

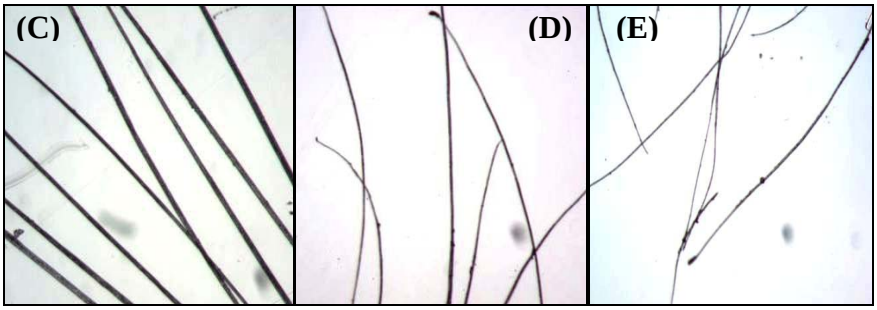

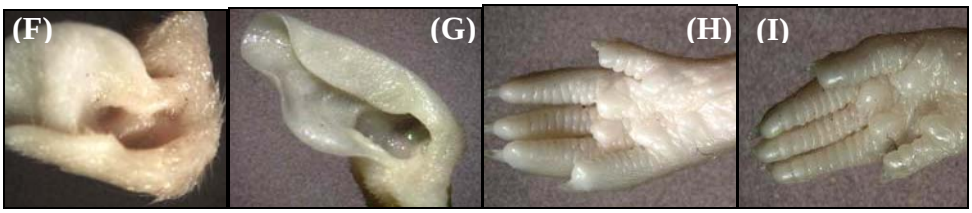

Figure 4-3 Comparison of phenotypes between +/+, $Hr^n/+$, and homozygous Hr^n/Hr^n mutant mice. (A) and (B): vibrissae of Hr^n/Hr^n, $Hr^n/+$, and +/+ mice at 7-day (A) and 3-week (B) old age; (C): hair from +/+; (D): hair from $Hr^n/+$ mutant mice; (E): hair from Hr^n/Hr^n mutant mice; (F): ear from +/+; (G): ear from Hr^n/Hr^n mutant mice; (H): foot from +/+ mice; (I): foot from Hr^n/Hr^n mutant mice.

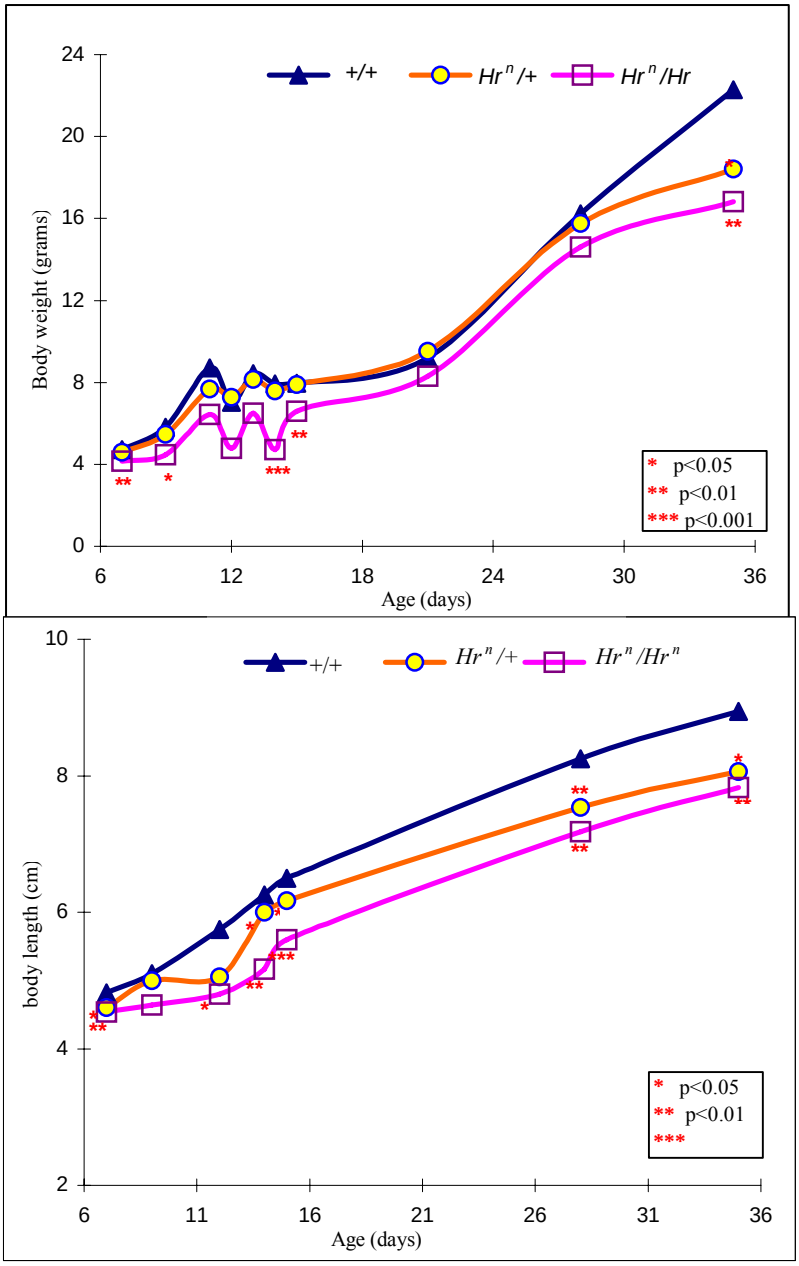

Figure 4-4 The growth curve of Hr^n/Hr^n, $Hr^n/+$, and +/+ mice based on body weight (top panel) and body length (bottom panel).

mutants. Morphological analysis began with mice at 7 days of age, the point at which the 3 genotypes (+/+, Hr^n/+ and Hr^n/Hr^n) are clearly phenotypically distinguishable from each other. Hair follicles were regularly distributed in skin and that their abundance and stage of follicle cycling were similar between the three genotypes. The dermal papilla and the bulb region of the follicles appeared normal in terms of shape and size. However, just distal to the bulb, striking changes in morphology were apparent. At the first age examined (7 days), follicles of Hr^n/Hr^n mice appeared to undergo premature degeneration of the hair shaft medulla and cortex (figure 4-5). In the majority of hair follicles, nucleated cells in the cortex and medulla were replaced with keratinized material. The degenerative changes occurred early in the follicle, well below the bulge in the region of the precortex. A mild degree of acanthosis and hyperkeratosis was also present. The outer root sheath appeared intact. As expected from the gross appearance, hair follicles from Hr^n/+ animals displayed a much more modest phenotype. Follicles in heterozygous animals were intermediate between those of wild type and Hr^n/Hr^n. Disorganization of the hair follicles progressed rapidly with age. By 9 or 11 days (figure 4-6 A-D) the cortex and medullary regions of the hair shaft in Hr^n/Hr^n mice consisted almost completely of keratin, with loss of nucleated cells in the precortex. By 13 or 15 days of age (figure 4-6 E-F) the cortex, medullary, and matrix regions of hair follicle are full of cornified materials. Filling with keratinized materials became more severe with age. By 4 weeks of age (figure 4-6 G), hair shafts region were filled with keratin. The lower portion of hair follicle including matrix and dermal papilla were also full of keratin. By 5 weeks, keratin-filled dermal cysts began to form from the follicle remnants (figure 4-6 H). Cysts were numerous at 6 months of age and were similar to those described in Hr^{hr} and Hr^{rh} mice (Data not shown). Staining with von Kossa indicated that some of the cysts contained mineralized deposits, consistent with those seen in other *Hr* mutants (figure 4-7).

These histopathological changes indicated significant structural changes in the medullary region and inner root sheath of the hair follicle. Scanning electron microscopy was then used to further examine the structural changes in Hr^n hair fibers and to determine if the cuticle was also disrupted. As expected, few hairs were present at the surface of Hr^n/Hr^n skin (figure 4-8). Those that did emerge displayed an abnormal form,

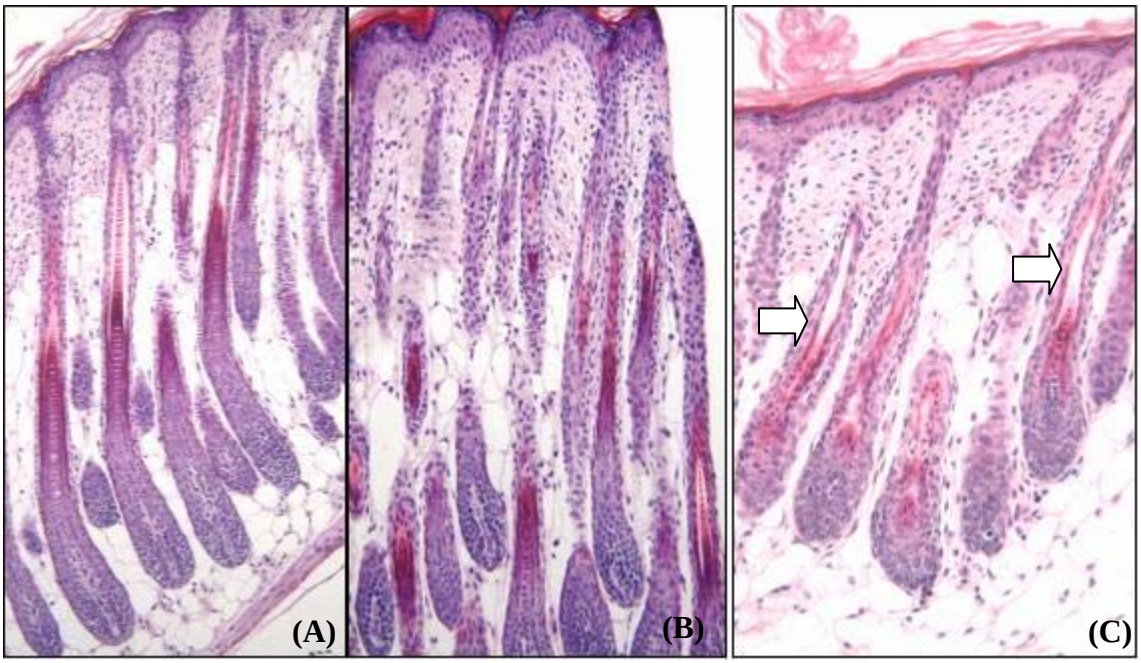

Figure 4-5 Histology of 7-day old mice (Hr^n/Hr^n, $Hr^n/+$, and +/+) with HE staining. (A) histology of 7-day +/+ mouse; (B) histology of 7-day $Hr^n/+$ mouse; (C) histology of 7-day Hr^n/Hr^n mouse.

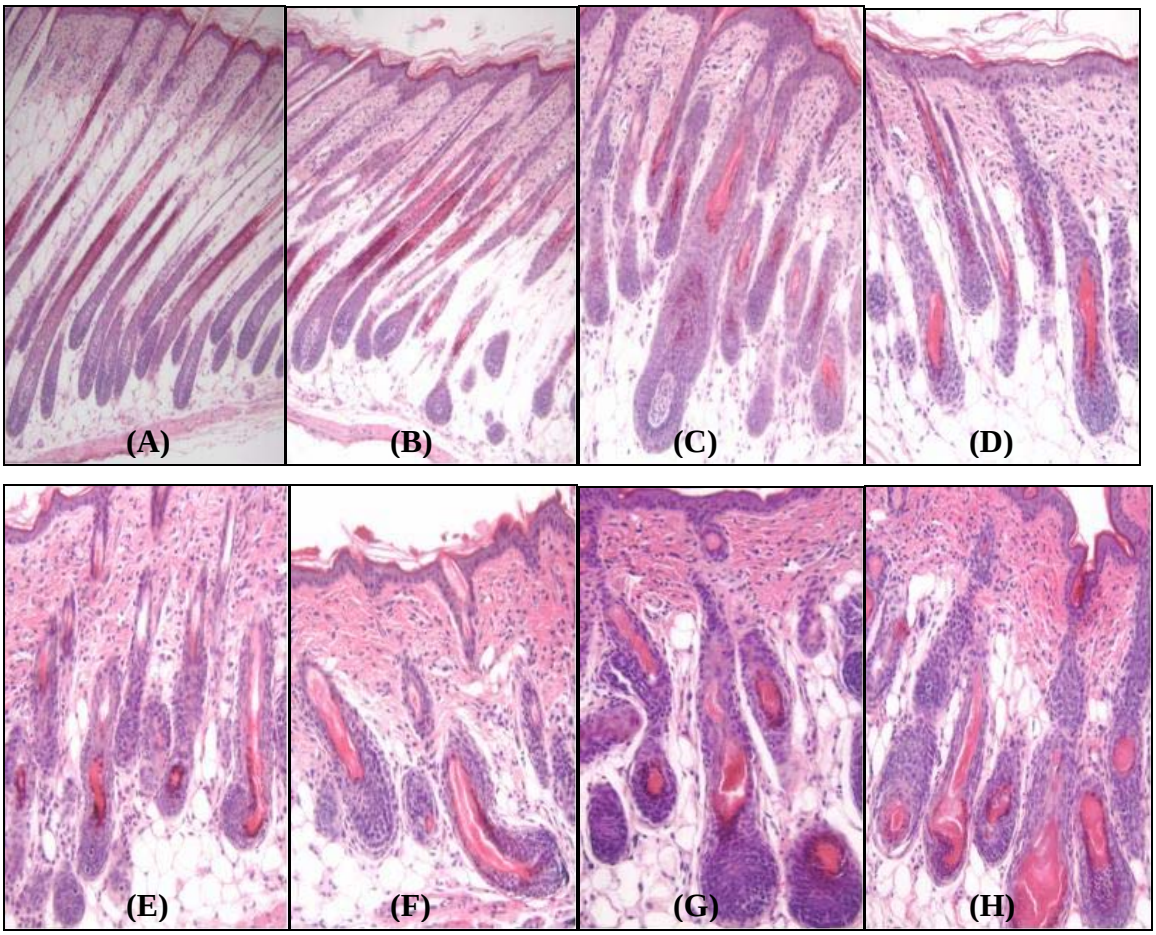

Figure 4-6 Histology of 9, 11, 13, 15, 28, and 35 -day old Hr^n/Hr^n, $Hr^n/+$, +/+ mice with HE staining. (A) histology of 9-day old +/+ mouse; (B) histology of 9-day old $Hr^n/+$ mouse; (C) histology of 9-day old Hr^n/Hr^n mouse; (D) Histology of 11-day Hr^n/Hr^n mice; (E) Histology of 13-day Hr^n/Hr^n mice; (F) Histology of 15-day Hr^n/Hr^n mice; (G) Histology of 28-day Hr^n/Hr^n mice; (H) Histology of 35-day Hr^n/Hr^n mice.

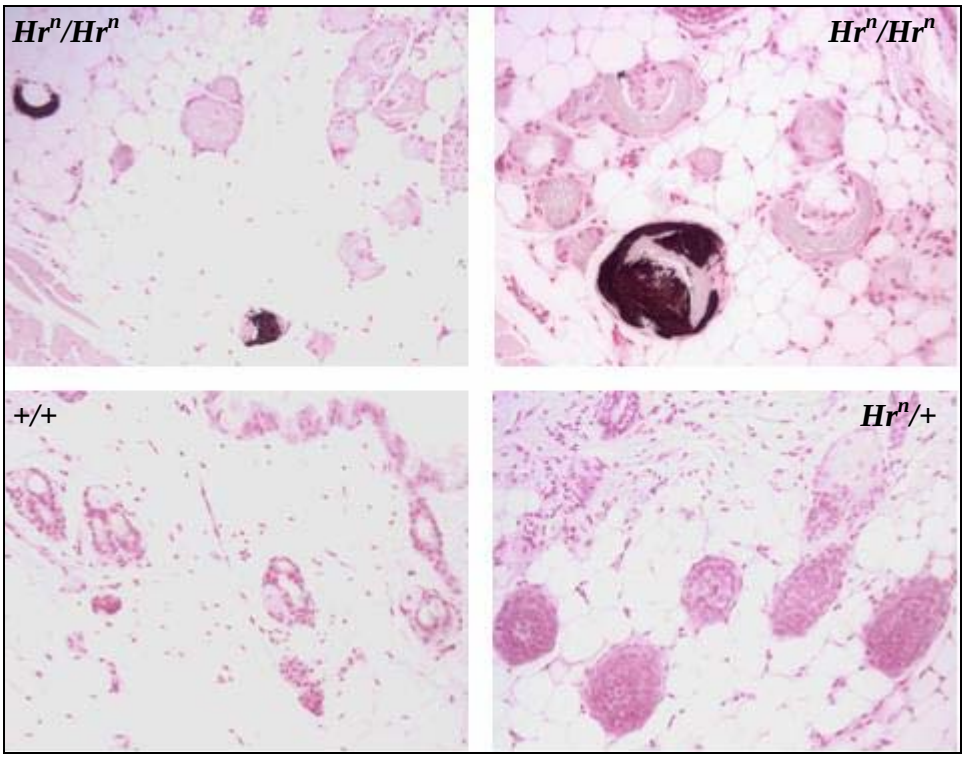

Figure 4-7 Von Kossa staining of Hr^n/Hr^n, $Hr^n/+$, +/+ mice skin. The dermal cysts in Hr^n/Hr^n are mineralized.

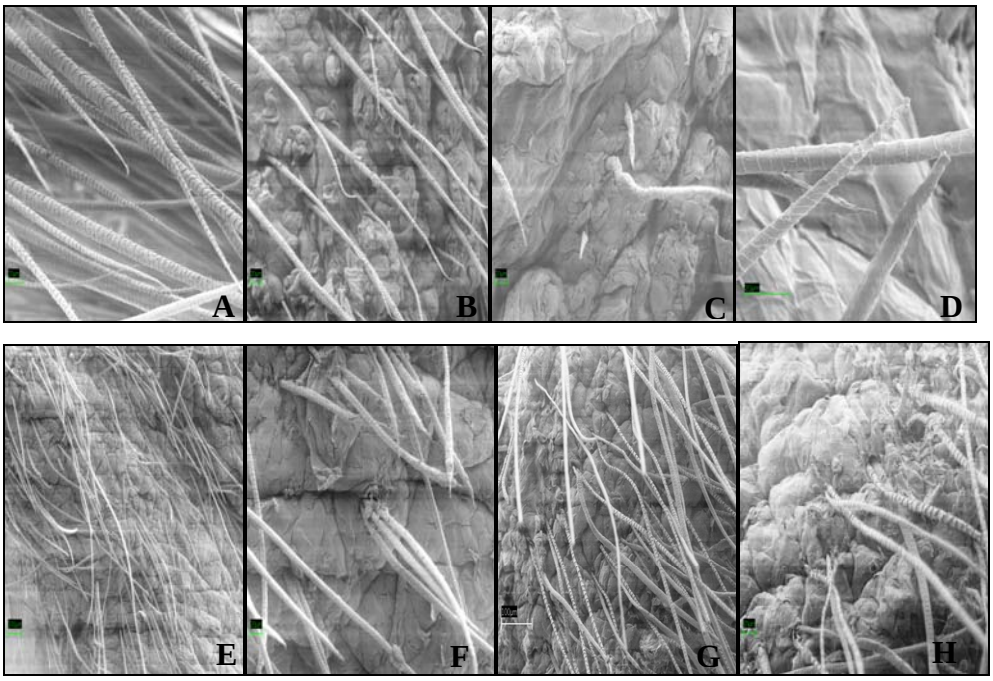

Figure 4-8 Hair structure from SEM (scanning electron microscope) with the hair from Hr^n/Hr^n, $Hr^n/+$, and +/+ mice at different ages. A, 8-day +/+ mice; B, 8-day $Hr^n/+$ mice; C, 8-day Hr^n/Hr^n mice; D, magnified view of hair shaft of 8-day Hr^n/Hr^n mice; E, 5-week $Hr^n/+$ mice; F, magnified view of hair shaft of 5-week $Hr^n/+$ mice; G, 5-month $Hr^n/+$ mice; H, magnified view of hair shaft of 5-month $Hr^n/+$ mice.

however, the cuticle appeared normal, with regular, overlapping scales. Hair fibers of both 8-day and 5 week-old Hr^n/+ mice exhibited an irregular contour, with variations in thickness spanning the entire length of the hair. Distal ends of the hair fibers were often curled, in contrast to the uniform shape observed in wild type mice. In addition to alterations in morphology, numerous follicles in 5-week and 5-month Hr^n/+ mice displayed pili multigemini with 2 or more hair fibers emerging from the same piliary canal on the surface of skin. Fibers emerging from the same canal did not appear to result from fiber splitting, as the cuticles were intact and the ends of the fibers relatively uniform. Re-examination of the H&E stained sections of 5-week Hr^n/+ mice found several examples of pili multigemini (figure 4-9). The additional fibers did not resemble club hairs that had not yet been lost during telogen; rather they were positioned at a depth in the follicle comparable to the primary hair fiber. In some cases, 2 follicles at the same level of the skin appeared to merge into a single hair canal.

The hair fibers observed in cross sections of both Hr^n/+ and Hr^n/Hr^n skin appeared to be prematurely keratinized from the earliest age examined (7 days), suggesting that keratinocyte differentiation was initiated prematurely in the developing fiber. To determine if the Hr^n mutation disrupted the normal transition from proliferation to differentiation in the precortex region, we stained skin sections from 7 day-old Hr^n/Hr^n and +/+ mice with the proliferation marker Ki67 (figure 4-10). Wild type displayed the expected gradual transition from proliferation to differentiation in matrix cells. Proliferation in Hr^n/Hr^n hair follicles, however, appeared to be reduced and the transition into differentiation was premature and abrupt. In this respect, hair fibers in Hrn mutants resemble those found in Lanceolate mice, in which the normal pattern of keratinocyte differentiation is altered by a mutation in the desmoglein 4 (Dsg4) gene that disrupts normal cellular adhesion (Kljuic et al., 2003).

Sequencing the *Hr* locus

The near naked allele arose spontaneously in the ORNL mouse colony and was not directly associated with mutagenesis experiments. Northern blots indicated that the *Hr* transcript was of similar size between Hr^n and wild type animals, indicating that the mutation was not due to a large deletion or insertion and did not cause production of a

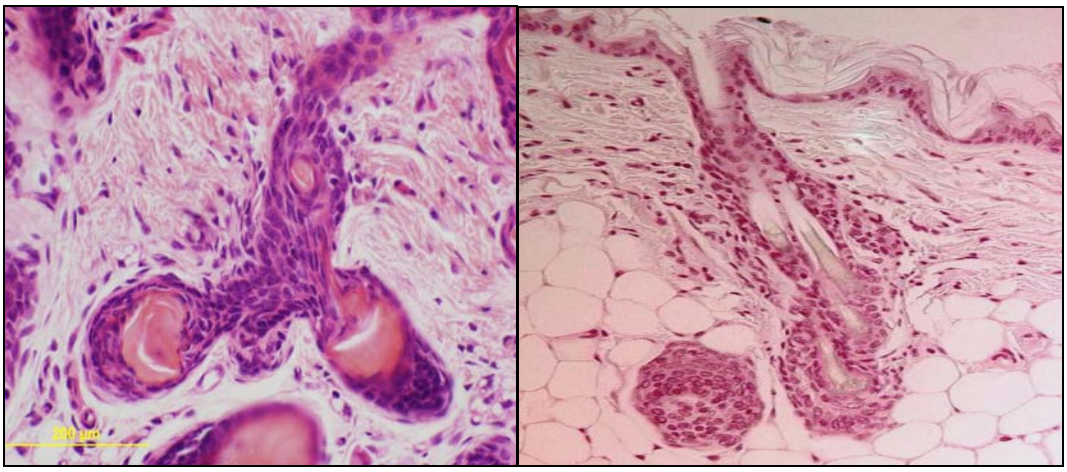

Figure 4-9 Histology of 5-week *Hr*^{n}/+ mice for pili multigemini.

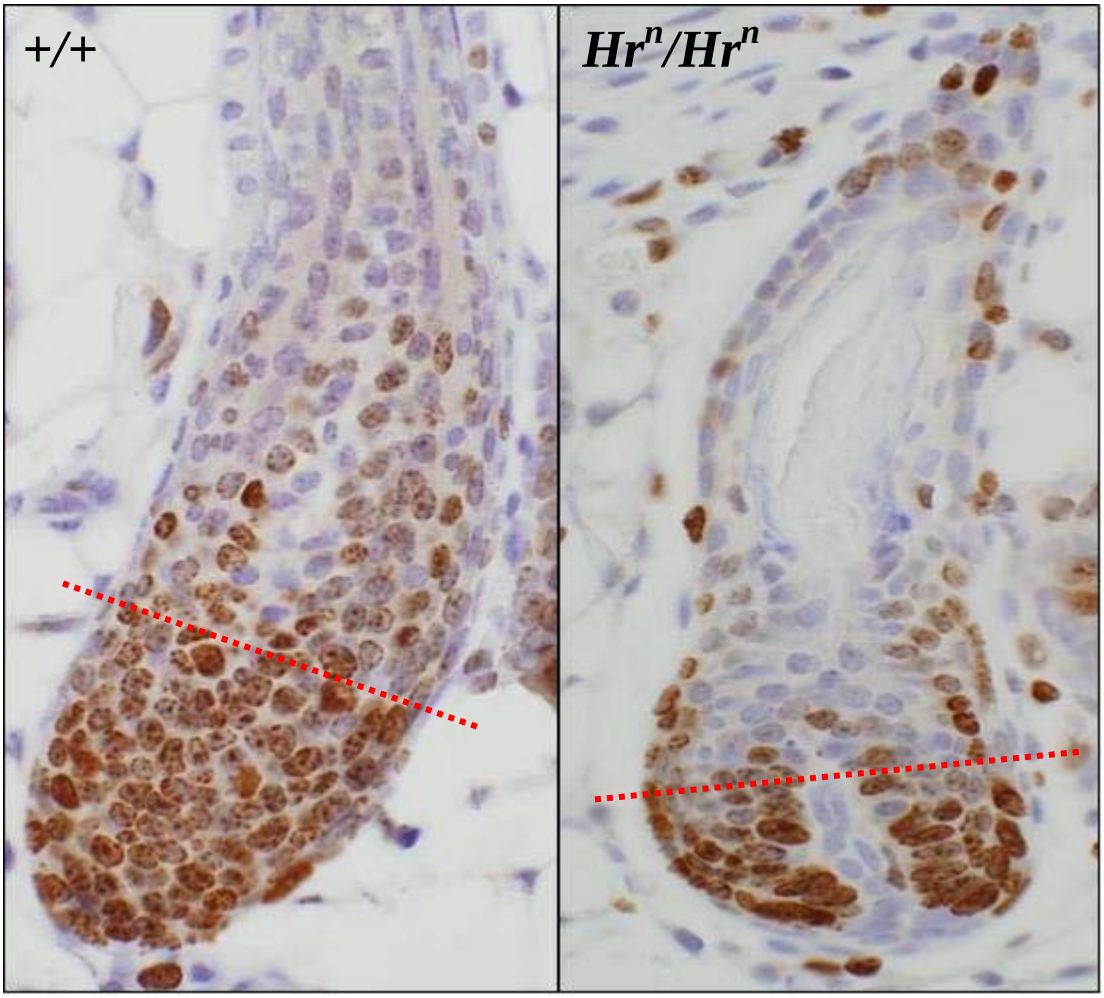

Figure 4-10 Ki-67 staining of hair follicle from +/+ and Hr^n/Hr^n mice

truncated transcript (data not shown). The entire *Hr* cDNA was sequenced from skin cDNA templates prepared from Hr^n/Hr^n mice (BalbC/Rl / FVB/N mixed genetic background) and from both C3H/HeJ and 101/Rl mice, the two potential parental strains in which the original mutation occurred, and comparing it to the published *Hr* sequence (GenBank accession number Z32675). The Hr^n sequence matched perfectly to the published *Hr* sequence, demonstrating that the Hr^n mutation does not lie in the *Hr* coding region. Based on these changes in *Hr* gene expression, we sequenced the entire *Hr* genomic region, including the introns, 8414 bp of the 3'-UTR, and 1483 bp upstream of the transcription start site from Hr^n/Hr^n animals and compared our sequence to the public sequence using BLAST analysis. The sequence from Hr^n/Hr^n perfectly matched that contained in the public database, indicating that the Hr^n mutation does not lie within the *Hr* gene and is not due to a regulatory mutation in the region immediately upstream of transcription.

Other genes in the region close to *Hr* gene on chromosome 14 were selected for sequencing the cDNA based on their possible roles in skin and no mutations was found on these genes. These genes include *Dok2*, *FGF17*, *Adam7*, *Adam28*, *RAI16*, *Gfra2*, *Pdlim2*, *TNFrsf10b*, *Loxl2*, BB150350 and BC036718. There are also two RIKEN cDNAs 1700020M16, and 4930506C02 differentially expressed with hair follicle cycles suggested by large-scale gene expression survey (Lin et al., 2004; Morris et al., 2004). These RIKEN cDNAs were sequenced by PCR and no mutation was found. MicroRNAs have recently been suggested to play important roles in different diseases including leukemia (Calin et al., 2002; Calin et al., 2005; Calin et al., 2004). There are two microRNAs close to the locus of *Hr* gene on mouse chromosome 14, microRNA 124a and 130. The pre-microRNAs of these two microRNAs were sequenced from genomic DNA and no mutation was identified. All of the sequencing primers were listed in table 4-1. This suggests that the mutation might be due to another unknown gene mutation of a regulatory mutation in *Hr*.

The *Hr* gene encodes a transcriptional regulator expressed in the developing hair follicle (Panteleyev et al., 2000), a site in which careful coordination of gene expression is necessary to produce and assemble the appropriate combinations of structural fibers

Table 4-1 Sequencing Primers genes and transcripts in the region close to *Hr* gene on mouse chromosome 14 (sequences from 5' to 3' end)

Genes	Primers	Sequences	Positions	Size
Lysyl oxidase-like 2 (*Loxl2*) (NM_033325.1)	LF1	AGCTTTTCTTCTGGGCAACC	53-834	782 bp
	LR1	AGACCACGTGGGAATTCTTG		
	LF2	TGTCACTGACTGCAAGCACA	575-1276	702 bp
	LR2	CCTGTGATGGCCTCTTTAGC		
	LF3	AGCTGTGGTCAGTTGTGTGC	1031-1803	773 bp
	LR3	CAGCATTAAGCACCAGGTCA		
	LF4	CCTGGTACTGGCATGGAAAT	1618-2405	788 bp
	LR4	CTCCTCACTGAAGGCTCCAC		
	LF5	GGAGAACAAGGCATCACCAT	2169-2954	786 bp
	LR5	TGAGTTCATGCCTGCTGTGT		
PDZ and LIM domain 2 (*Pdlim2*, NM_145978)	P2F1	AGCAACTGAAGAGGCAGGAG	2-693	692 bp
	P2R1	GCTGAACCTAGGGCTGGAG		
	P2F2	GCTCACCACTTGACCTACCC	571-1390	820 bp
	P2R2	CCATACGCTTTCGTGTCAAA		
Fibroblast growth factor 17 (*Fgf17*, NM_008004)	FGF17F1	GTTGCCGCATCAAACCTG	16-592	577 bp
	FGF17R1	TCTCCCCCTGTGTTTGACA		
	FGF17F2	AATCGCCCCAAGAAGTCTCT	488-1179	692 bp
	FGF17R2	TACTGGCCTCCCTGACTACG		
	FGF17F3	CTTCATCAAGCGCCTCTACC	1032-1680	649 bp
	FGF17R3	TGGTTTTATTCTGGGGCTTG		
Tumor necrosis factor receptor superfamily, member 10b (*Tnfrsf10b*, NM_020275)	T10BF1	CTGGGAGTGAGGAAATCCAG	29-828	800 bp
	T10BR1	CCAAGAGAGACGAATGCACA		
	T10BF2	ACGGGGAAGAGGAACTGACT	589-1340	752 bp
	T10BR2	CATCTTCGGGGCTCTCTACA		
Retinoic acid induced 16 (*RAI16*, AK090035)	RAI16F1	CCTGGGGAGAGCAATCTTATC	21-655	635 bp
	RAI16R1	GCAATGCTGATCTCGTCTGA		
	RAI16F2	CATAGAGGACAGCCCCCATA	578-1299	722 bp
	RAI16R2	CACCCTGACAAGCACAGAGA		
	RAI16F3	AGCCGTACAGCCTGAACCTA	1153-1967	815 bp
	RAI16R3	CTGCCGAGTCTTAGCAGCTT		
	RAI16F4	AGCTAGAGGATGGCCAGTGA	1737-2556	820 bp
	RAI16R4	GGCCTGTTGTGAGGTAATGC		
	RAI16F5	AAGGTACAGCATGGGACAGG	2359-3132	774 bp
	RAI16R5	CAAATGCCAAAGTGCATTGA		
Downstream of tyrosine kinase 2 (*Dok2*) Genomic DNA	Dok2F1	GCACACAGAGCAAGAAACCA	N/A	817 bp
	Dok2R1	TTCCCACCTCCTCTCCTTTT		
	Dok2F2	TTACCCAGCTGTGCTTACCC	N/A	770 bp
	Dok2R2	ACAGGCAGATGGCCTGTATC		
	Dok2F3	CTTCTCCCCTTTCATGACCA	N/A	804 bp
	Dok2R3	CACCAAGAAGCCAGGAAGAG		
	Dok2F4	CTCTTCCTGGCTTCTTGGTG	N/A	924 bp
	Dok2R4	ACCTTCCTCCTCGATCCACT		
	Dok2F5	AGTGGATCGAGGAGGAAGGT	N/A	781 bp
	Dok2R5	GGATCCTCCTGAATGCTGTC		
	Dok2F6	ACACGGCAATGAGATCTTCC	N/A	937 bp
	Dok2R6	TCTGGGAGCTAGAGGGACAA		

Table 4-1 Continued

Genes	Primers	Sequences	Positions	Size
Glial cell line derived neurotrophic factor 2 (*GFRA2*, NM_008115)	GFRA2F1	AACGCCTTCTGCCTCTTCTT	13-752	740 bp
	GFRA2R1	CAGTTGGGCTTCTCCTTGTC		
	GFRA2F2	CCTGAACGACAACTGCAAGA	507-1387	881 bp
	GFRA2R2	CCAAGGTCACCATCAGGAGT		
	GFRA2F3	AGCATGGCTGACTAGGTTGG	Covering Exon 2	665 bp
	GFRA2R3	CCGTCATCCAGTTCATCCTC		
	GFRA2F4	GGGTCGTTATCATTGCTTGG	Covering exon 1	215 bp
	GFRA2R4	TCCAGTGGGCGACTGAAC		
BB150350	BB15F	CAAGCAAAGATGGGAACCTC	N/A	95 bp
	BB15R	TGTCCCAGACTTGCTTTTCC		
BC036718	HydF	CCTCCGATCCTGTGAGAGTT	N/A	140 bp
	HydR	CTGCAGGGAGGTACCATGTC		
A disintegrin and metalloprotease domain 7 (*Adam* 7, NM-007402)	ADAM7F1	TGTTTCCCACAGGTATATTTTTGA	2-695	694 bp
	ADAM7R1	AAATTGACCATCCCCCAAAT		
	ADAM7F2	AATGTCAAGGCACCCTATGC	475-1340	866 bp
	ADAM7R2	CAGCACTCTCCTTCCACACA		
	ADAM7F3	GGAAGCATCCCTGCAATAAA	1084-1957	874 bp
	ADAM7R3	CTTCCTCACACTGGCACTCA		
	ADAM7F4	ACGTGACCATCAAATGCAGA	1748-2375	628 bp
	ADAM7R4	ACGGAGGATTAGCCCAGTCT		
	ADAM7F5	TGACCGATATCCATCCCCTA	2180-2931	752 bp
	ADAM7R5	CACCCAGTGTGTCTCCCTTT		
	ADAM7F6	AGGCTGAGGCAGTAGGATCA	2759-3426	668 bp
	ADAM7R6	AGGATGGGGGAAAAATCATC		
Adam28, NM_176991	ADAM28F	GTTGGAGCAGAAGCAACCTC	65-714	650 bp
	ADAM28R	GTGCAAAGGGTTCTGACGAT		
RIKEN cDNA 1700020M16	170F1	CTCTTGGGGACCCTGAGC	5-810	806 bp
	170R1	CGCATCCCATGACTCCTATT		
	170F2	AAAAGGAACAAGGGGCTGAG	723-1632	910 bp
	170R2	CCATAGCAGCTCCAGTGAGG		
RIKEN cDNA 4930506C02	493F	GGGGAGAGGGCAGTCATATT	688-1252	565 bp
	493R	GCATTCAGCACACAGAAACA		
microRNA-320	M320F	GGCGGAAGTGACATCAAGG	N/A	215 bp
	M320R	GAGGACCGCACCTCTACTCC		
microRNA-124a1	MR124F	TCCTCCCTCTCTTCCATCCT	N/A	238 bp
	MR124R	TGTGCTGGGTCGATCCTT		

N/A: not available

required to form potent hair fibers (Botchkarev and Kishimoto, 2003). It is possible, therefore, that alterations in the expression levels of a key transcription factor could disrupt hair follicle gene expression and cause dystrophic hairs as seen in Hr^n/Hr^n mice. Thus, a regulatory mutation outside the *Hr* coding region could underlie the near naked phenotype. Northern blots and quantitative RT-PCR (qPCR) were used to assay levels of *Hr* expression in Hr^n mutants and wild type littermates. For these assays 7 day-old mice were used to represent the visual onset of the phenotype and to dissociate results from the secondary phenotypic changes that ensure as the phenotype progresses. Northern blot hybridization to a probe spanning exons 5-12 indicated that the Hr^n mutation did not alter *Hr* transcript size, but that expression levels were slightly but significantly increased relative to +/+. Quantitative RT-PCR was used to for further determination of *Hr* expression. *Hr* expression in 7-day animals was significantly increased in $Hr^n/+$ (~ 2-fold over +/+) and further elevated in Hr^n/Hr^n (~ 3-fold over +/+). However, its expression in 5-week mice was significantly decreased in $Hr^n/+$ (~ 3-fold over +/+) and further down in Hr^n/Hr^n (~ 7-fold over +/+). This suggests that the Hr^n phenotype might be due to altered *Hr* expression. The phenotype in skin of near naked mice is marked, and expression levels of numerous genes (not only *Hr*) are likely to be altered. However, to further explore the upregulation of *Hr* expression revealed by qRT-PCR, *in situ* hybridization was applied to determine if the elevation in *Hr* expression was ectopically detected. As shown in figure 4-11, wild type mice showed strong *Hr* expression in matrix cells and in the inner and outer root sheaths, as did $Hr^n/+$ mice. *Hr* expression appeared to be stronger in the outer and inner root sheath of Hr^n/Hr^n mice. A considerable proportion of fibroblasts in the cavernous sinus also appeared to express *Hr*, unlike those in wild type animals. Therefore, the elevated expression of *Hr* seen with qPCR appears to be due to both ectopic expression (in fibroblasts) and to elevated expression in normal locations (IRS and ORS). Consistent with HE staining, the numbers of matrix cells appeared to be significantly reduced in Hr^n/Hr^n.

Microarray expression profiling

As part of a larger emphasis on the study of skin and hair biology, focused arrays were developed and fabricated, representing genes important in skin and hair biology, as

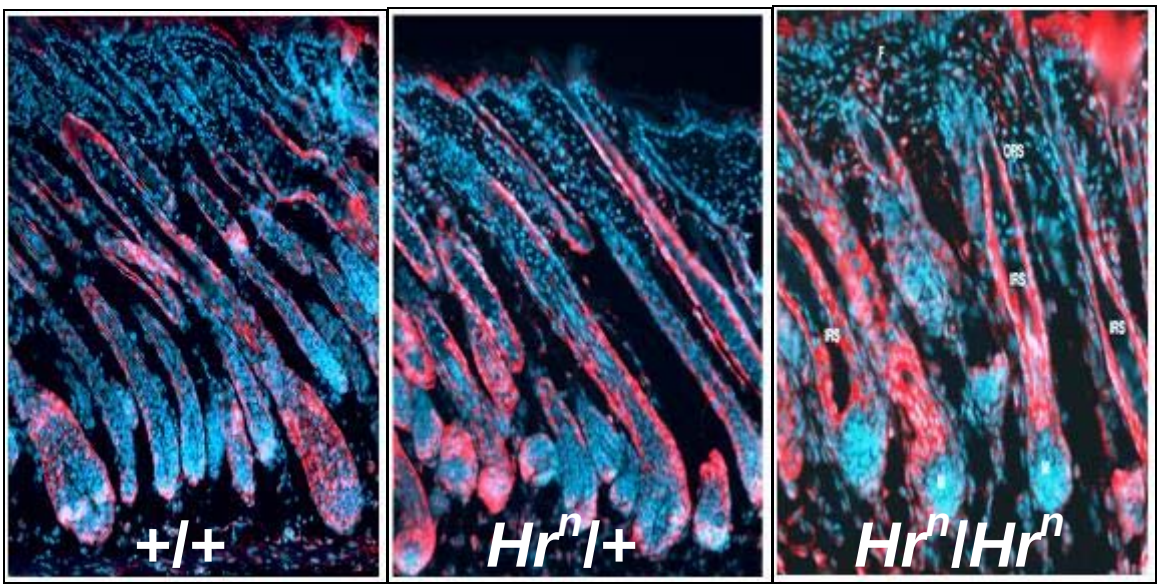

Figure 4-11 *In situ* hybridization of 7-day old mice with *Hr* probe.

well as in skin cancer. Arrays consisted of approximately 300 sequence-verified genes with multiple functional assignments, including epithelial differentiation, hair structure, cell cycle, apoptosis, and DNA repair, and of uncharacterized clones sequenced from a skin cDNA library. These arrays were used to identify the set of genes with altered expression in skin of *Hr*^{n} mutants at 5 weeks of age as a next step to understanding the basis for the near naked phenotype. We were only able to reliably produce homozygous animals by outcrossing to FVB/N and then intercrossing F1 animals, and we were concerned that the mixed genetic background from this strategy would confound interpretation of microarray results. Therefore we used a 2-step strategy for differential expression studies, first profiling expression with microarrays in wild type and *Hr*^{n}/+ mice congenic on Balb/cRL and then screening mice of all 3 genotypes (but on the mixed background) to determine the range of expression changes altered by heterozygosity and homozygosity, and at 2 ages (7 days and 5 weeks). A subset of genes highlighted by microarrays was validated first by qRT-PCR in the same RNA samples to verify the microarray results. Microarrays identified many genes that were significantly differentially expressed ($p<0.05$) across a panel of 3 pairs of wild type and *Hr*^{n}/+ mice (Table 4-2). This set of genes includes several hair keratins and keratin-associated proteins (KRTAPs) and *S100A3*, a Ca^{2+} binding protein expressed specifically in postmitotic differentiated cells of the hair follicle (Kizawa and Ito, 2005), all of which were downregulated in *Hr*^{n}/+ mice. In addition to keratins and KRTAPs, *Rab27b*, a Ras-like monomeric GTPase involved in vesicular transport, and sequestosome 1, a scaffold protein involved in signaling through atypical protein kinases Cs (aPKCs), were also downregulated in *Hr*^{n} mutants. Genes with increased expression included cytochrome b and sequestosome 1, a scaffolding protein that interacts with multiple signaling pathways. Aside from the common structural functions of keratins and krtaps, differentially expressed genes were enriched in the GO category of cellular proliferation (BP).

We then screened the expression levels of these genes with qRT-PCR in wild type, *Hr*^{n}/+ and *Hr*^{n}/*Hr*^{n} mice at 7 days of age to identify genes differentially expressed at the onset of the visible phenotype as shown in table 4-2. Most of the keratins and keratin-

Table 4-2 Genes with altered expressions in 5-week and 7-day old mice from microarray analysis and real time PCR experiments

Gene Name	7 days		5 weeks	
	Hr^{n}/+ vs. +/+	*Hr*^{n}/*Hr*^{n} vs. +/+	*Hr*^{n}/+ vs. +/+	
	RT-PCR	RT-PCR	Array	RT-PCR
KRT 1-C29	-1.5	-2.4	-2.9	-8.4
KRT 1-2	0	0	-2.3	-3.2
KRT 2-1	1.5	2.9	N/A	9.6
KRT2-4	N/A	-2.7	-1.9	0
KRT 2-6	0	-3.6	N/A	-4.4
KRT1-13	1.4	2.1	-1.7	0
KRTAP3-1	N/A	N/A	-1.7	N/A
KRTAP 6-1	0	-2.6	N/A	-13.8
KRTAP 6-2	0	-3.3	N/A	-8.4
KRTAP 8-1	-15.8	-22.3	-2.7	-73
KRTAP 8-2	-2.4	-8.4	N/A	-14
KRTAP 9-1	0	-2.7	N/A	-5.5
KRTAP16-5	-1.8	-6.3	-1.8	-2.7
KRTAP 16-10	-3.1	-17	N/A	-16.2
Ccna2	0	0	N/A	-1.7
Cct7	0	0	-3.4	-2.1
Stat1	0	0	N/A	1.8
Rab27b	0	0	-2.1	-3
S100A3	-1.6	-1.9	-1.9	-4.1
SPRR1B	N/A	N/A	N/A	-1.7
Cytochrome B	N/A	N/A	N/A	1.6
Sequestosome	0	1.6	N/A	1.8

N/A: not available; “0” means fold change < 1.5

associated proteins except *krt2-1* are significantly downregulated in 7-day and 5-week mutant mice.

The majority of keratin-associated proteins in mouse reside in 2 large gene clusters on chromosomes 11 and 16, and the genes in this family display highly coordinated patterns of expression during hair formation (Awgulewitsch, 2003; Pruett et al., 2004). Accordingly it has been proposed that keratin and krtap genes within a cluster are regulated by locus control regions, much like what has been reported for α-globin genes and homeobox genes (Awgulewitsch, 2003; Pruett et al., 2004). Because all of the krtaps represented on our arrays were differentially expressed in Hr^n skin, and because disruption of krtap expression could result in aberrant hair fibers as manifested in Hr^n mutants, we used qRT-PCR to determine if additional krtaps also exhibited altered expression. We assayed expression levels of 10 additional Krtap genes, all of which displayed significantly lower levels of expression in Hr^n mutants than in wild type (Table 4-2). Therefore the Hr^n mutation directly or indirectly disrupts the expression levels of a large group of genes critical for normal hair structure.

Examination of hair shaft formation markers

Recently it was found that the genetic pathways containing *BMP-2*, *BMP-4*, *Foxn1*, *Msx2*, *Notch*, and *Hoxc13*, might regulate hair shaft differentiation (Ma and Cai, 2005; Mecklenburg et al., 2005). Our histological analysis suggests that hair shaft differentiation was significantly altered in Hr^n/Hr^n mutants. We used quantitative real time PCR to examine the expression levels in Hr^n/Hr^n mutants *vs.* +/+ mice and the results are shown in figure 4-12. One of the Notch effectors, *Hes1* (Hairy and enhancer of split 1), was also examined for its gene expression level. The expression of *BMP-2*, *Dsg4*, *GATA3*, *Ntc*, and *Msx2* was not altered. The expression of *BMP-4*, *Noggin*, and *β-catenin,* was increased by 2 fold. However, the expression levels of *Hoxc13*, *Foxn1*, *Hes1*, and hair keratins were significantly decreased by at least 2 fold compared to +/+ mice. The altered expression of these genes further supports that hair shaft differentiation in Hr^n/Hr^n mutants is altered and suggests that Hr^n mutation might be in the upstream of *BMP-4* in the hair follicle signaling.

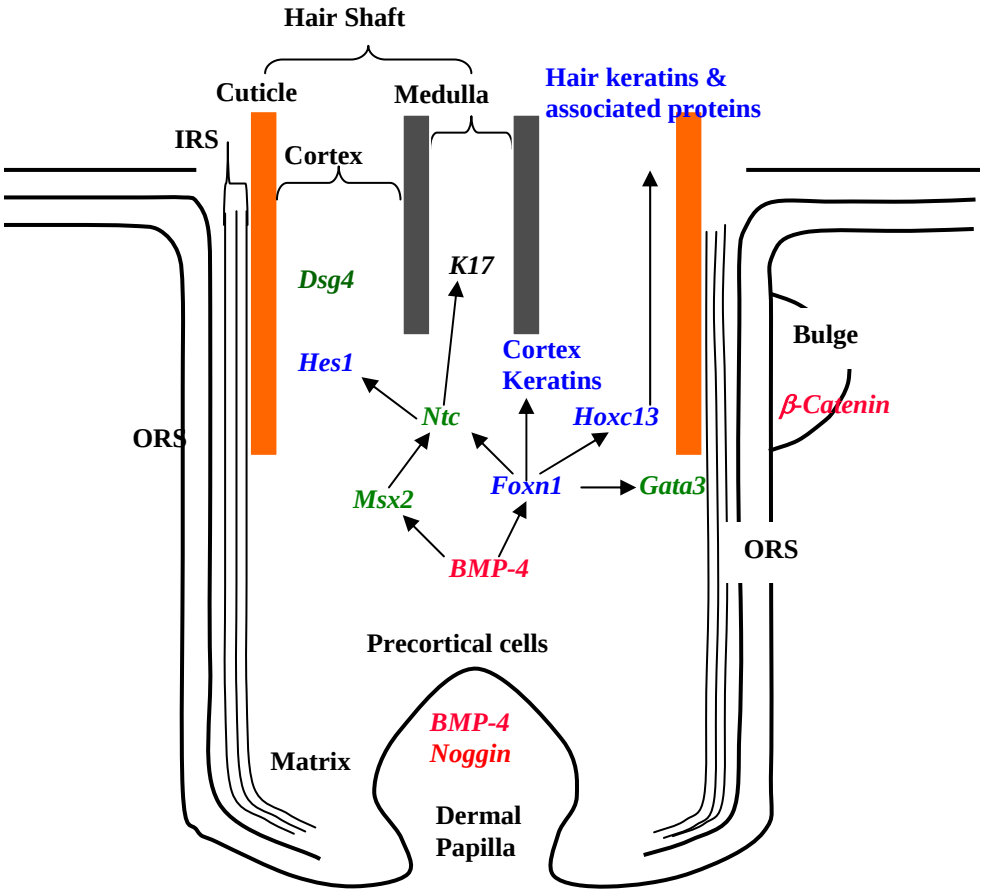

Figure 4-12 Schematic illustration of checkpoints for hair shaft formation in 7-day Hr^n/Hr^n mice with altered expressions. Red: increased expression; Blue: decreased expression; Green: no expression change

Discussion

A novel spontaneous mouse mutation was characterized here. This mutation was originally mapped to the *Hr* locus but results in a phenotype markedly different from other *Hr* mutants (Stelzner, 1983). The Hr^n mutation displays semi-dominant inheritance and prevents the initial growth of a normal coat of hair. In both respects, it differs not only from mutant alleles of *Hr* (Ahmad et al., 1999b; Ahmad et al., 1999c) but also from the majority of spontaneous mutations that have been shown to alter the pelage (Irvine and Christiano, 2001; Lane and McLean, 2004; Porter, 2003).

Delayed body growth in Hr^n mutants was observed in both Hr^n/Hr^n and $Hr^n/+$ at most of the ages tested with less body weight and smaller body length. This retarded development was first documented at 7 days of age. Hair coat does not affect mouse development and growth; therefore, the delayed growth in Hr^n mutant mice was due to the mutation, not due to the loss of hair coating. Hematology analysis was done at 9, 13, 15, and 35 days of age to determine if there were any obvious abnormalities in red and white blood cells, and platelets. No abnormalities were found (data not shown).

The structure of hair fiber in Hr^n/Hr^n mice is altered due to the mutation as shown under scanning electron microscope. Pili multigemini was observed in 5-week and 5-month old $Hr^n/+$ mice, but not in 8-day old $Hr^n/+$ mice, indicating that pili multigemini might be related with hair cycles. Histological analysis with 5-week $Hr^n/+$ mice suggests that either multiple hair follicles were associated together or multiple hair shafts were formed in one hair follicle during the early anagen of hair cycle. It has been reported that a kinetic dermal papilla changes its form from single-tipped to double-tipped producing two hair shafts that separately grow from the same piliary canal on the skin surface during anagen (Whiting, 1987). This would support the idea that multiple hair shafts were formed in one hair follicle during anagen.

Pili multigemini is actually very useful for hair transplantation in clinics to produce more hairs with a limited number of hair follicles. It was found that the entire hair follicle is not necessary to generate hair growth (Gho et al., 2004). Even just the upper part of hair follicle is enough to grow a normal hair. It was found there are two different sites containing stem cells (Gho et al., 2004), either of which is able to induce

normal hair growth, suggesting that two hairs could grow from one hair follicle. Unpublished data from GHO clinic (http://www.ghoclinic.com/) found that two or more hair follicles could be developed from a single hair follicle, producing two or three normal hairs. It was also found that three or even five hairs were developed when one or two upper parts of hair follicles were implanted. These observations might help explain the pili multigemini in 5-week and 5-month Hr^n/+ mice. It could be that the Hr^n mutation alters hair follicle stem cell populations. Alternatively, pili multigemini might be triggered by the separation of the upper part of the follicle from the bulge during first catagen.

Based on the initial allelism testing with *Hr*, we began by sequencing the *Hr* gene, including all introns and exons, 1483 bp of the 3'-UTR and 8414 bp upstream to the next gene. Despite *Hr* as an obvious candidate for hair loss in this region of mouse chromosome 14, no mutation was identified in any portion of *Hr*. Therefore we are left to conclude that another gene near *Hr* on chromosome 14 underlies the Hr^n mutant phenotype. It is also possible that the Hr^n phenotype results from a regulatory mutation in *Hr*. *Hr* mRNA levels were increased in Hr^n/Hr^n animals at 7 days of age, although the effect was relatively modest (3-fold). *Hr* encodes a transcriptional co-repressor(Potter et al., 2001; Zarach et al., 2004), and even small alterations in a transcription factor can have significant effects on its target genes. In the hair follicle, a very tightly coordinated sequence of events controls the transition from proliferation to differentiation and the formation of concentric hair fiber layers from a pool of precursor keratinocytes (Botchkarev and Kishimoto, 2003). It has been suggested that even subtle alterations in the transcription factors responsible for hair formation might dramatically impact the hair fiber phenotype (Fuchs, 1998; Jamora et al., 2003; Rendl et al., 2005). Therefore it is possible that an as yet unidentified mutation that increases expression of *Hr* is sufficient to disrupt the normal pattern of expression of its target genes and lead to a dysmorphic hair follicle. Consistent with this possibility, all of the hair keratin and keratin associated protein genes with altered expression in Hr^n skin were downregulated, as might be predicted from increased expression of a transcriptional co-repressor. By contrast, the vast majority of genes differentially expressed in skin of *Hr* null mice were upregulated,

including *keratin 10*, *loricrin, filaggrin, caspase 14, calmodulin 4*, and *keratinocyte differentiation-associated protein* (Zarach et al., 2004) due to the loss of transcriptional co-repressor.

Transgenic mice expressing *Hr* under the control of a keratin 14 promoter were recently created to rescue the hair growth in *Hr* null mice (Beaudoin et al., 2005). Under the control of keratin 14 promoter, *Hr* is mainly expressed in the outer root sheath including bulge region. These mice displayed shorter hairs and, like Hr^n, decreased proliferation of matrix cells, and thicker epidermis, suggesting delayed epidermal differentiation. These authors concluded that *Hr* normally promotes differentiation toward hair cell fate and suppress the differentiation into epidermis(Beaudoin et al., 2005), which is consistent with the apparent premature differentiation and increased keratinization reported in Hr^n hair fibers. Unlike Hr^n mice, K14-*rHr* transgenic mice did not lose hair although they have shorter hair. However, the expression pattern produced by driving *Hr* with the K14 promoter does not completely reproduce endogenous *HR* expression. Overexpression was primarily in the outer root sheath, while endogenous *Hr* is expressed in the inner and outer root sheath, and the matrix. Therefore, it is still possible that elevated *Hr* expression in its normal sites could produce the Hr^n phenotype.

The profile of KRTAP expression in Hr^n mice resembles that seen in transgenic mice overexpressing *Hoxc13*, in which the Krtap16 family of genes was uniformly downregulated. *Hoxc13* binding sites have been reported in promoter regions of Krtaps from the 10, 12 and 16 families, suggesting that these genes are direct transcriptional targets of *Hoxc13* (Awgulewitsch et al. 2004; Rogers 2004 JID). Like many Krtaps, *Hoxc13* expression was also significantly decreased in skin of Hr^n mice. In hair follicles, *Hoxc13* is expressed in the rapidly dividing and differentiating keratinocytes directly apical to the dermal papilla, where it has been suggested to control proliferation and/or differentiation of matrix keratinocytes as they progress into formation of layers of the hair fiber (Godwin and Capecchi, 1998). This expression pattern overlaps the region of the initial morphological changes in Hr^n follicles, and the putative function of *Hoxc13* is consistent with the apparent disruption of the proliferation-differentiation transition in Hr^n mutants. These collective findings place the Hr^n gene upstream of *Hoxc13*.

The hair loss phenotype of *Hr*^{n} mice appears to be due to a striking and premature increase in keratinocyte differentiation that occurs very early in hair fiber development. The early increase in differentiation is paralleled by decreased proliferation of matrix cells, suggesting that the underlying mutation alters the signaling mechanism that normally guides a gradual transition to differentiation and keratinization of the hair fiber. In this respect, hair of *Hr*^{n} mutants resembles that of *Dsg4* mutants (Kljuic et al., 2003). Loss of *Dsg4* disrupted normal intercellular adhesion in the medulla and inner root sheath, leading to premature, abnormal and rapid keratinization of hair fibers (Kljuic et al., 2003). In addition, *Dsg4* mutants also displayed downregulation of *Hoxc13* and *hHb2* and *hHa4* keratins. *Dsg4* gene is upstream of *Hoxc13*. The expression of *Dsg4* gene in *Hr*^{n}/*Hr*^{n} mice was examined with real time PCR and no difference was found between *Hr*^{n}/*Hr*^{n} and +/+ mice, suggesting no direct involvement of *Dsg4* in *Hr*^{n} mutant mice.

Members of the TGF-β super family including *BMP-2* and *BMP-4* have been implicated in the induction and progression of various stages of the hair follicle cycle. *BMP-2* and *-4* are expressed in the hair shaft precursors, i.e. the precortical matrix, and dermal papilla, and regulate hair follicle cycling. Ectopic expression of *BMP-4* in the outer root sheath of hair and whisker follicles inhibits hair matrix proliferation and accelerates the differentiation program in the outer root sheath (Blessing et al., 1993). Increased expression of *BMP-4* in *Hr*^{n}/*Hr*^{n} mutants is consistent with the decreased proliferation in the precortex and matrix region shown in Ki-67 staining. The expression pattern of cytokeratins was also disturbed in some hair follicles (Blessing et al., 1993), which was also present in *Hr*^{n} mutants. Increased expression of *BMP-4* suggests its direct involvement in *Hr*^{n} mutant mice. Recently it was found that *Hr* triggers reactivation of hair growth by repressing *Wise*, a modulator of Wnt signaling, and promoting Wnt signaling (Beaudoin et al., 2005). Accordingly, if *Hr*^{n} is a pro-regulatory mutation in *Hr*, *Wise* expression should be repressed in *Hr*^{n}/*Hr*^{n} relative to +/+. However, we failed to detect changes of the expression of *Wise* in skin of 7-day old *Hr*^{n}/*Hr*^{n} mice by quantitative real time PCR.

Mouse models are usually used to study human diseases and *Hr*^{n} may be a novel model for a relative rare human hair syndrome. The only human hair syndrome (other

than those due to known mutations in *Hr*) that maps to the same genomic region as Hr^n is Marie Unna hereditary hypotrichosis (MUHH) (Cichon et al., 2000; Green et al., 2003). MUHH is a rare disorder characterized by coarsely textured hair that is progressively lost with age, beginning in early adulthood, with no other obvious phenotypic consequences (Roberts et al., 1999). SEM images of hair fibers from MUHH patients revealed a longitudinal groove and an irregular form (Kim et al., 2001), similar to that seen in 8-day Hr^n/Hr^n mice (figure 4-13). For both models, mutations within the *HR* coding region have been excluded as the cause of the hair phenotype (Cichon et al., 2000; He et al., 2004; Lefevre et al., 2000; van Steensel et al., 1999). Recent studies even suggest that the phenotypes of MUHH are due to mutations in other or multiple loci in the human genome (Yan et al., 2004; Yang et al., 2005). This might be true with MUHH or due to the difficulties to distinguish MUHH patients from other similar diseases in clinics (Green et al., 2003). It is possible that mutations in a homologous gene underlie these two models, or that they are both due to a regulatory mutation in *Hr*. MUHH has been described as autosomal dominant (Argenziano et al., 1999), while Hr^n is semi-dominant (Stelzner, 1983). However, given the low incidence of MUHH and the relatively small number of affected individuals within the population, it is possible that this disorder is also semi-dominant and that individuals homozygous for the underlying mutation would display a much more severe phenotype.

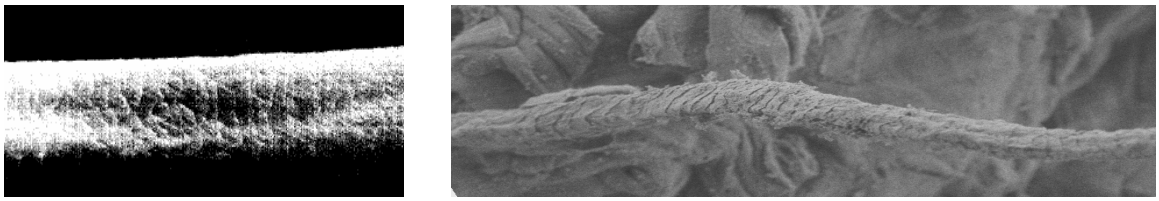

(A) (B)

Figure 4-13 Longitudinal grooving in hairs of MUHH patients and 8-day Hr^n/Hr^n mice through scanning electron microscopy. (A) hair from MUHH patients (Kim et al., 2001); (B) hair from 8-day old Hr^n/Hr^n mice.

Chapter 5 Early molecular and histological alterations in *Hr*^{n} mice

The data from mice at 0-5 days of age, included in this chapter, are being drafted into a manuscript that will focus on gene regulatory networks that are altered by *Hr*^{n}.

Introduction

The *Hr*^{n} mutation first manifests itself at postnatal day 6-7 as a sparse (*Hr*^{n}/+) or virtually absent (*Hr*^{n}/*Hr*^{n}) coat of hair. In many cases, homozygous mice can be distinguished from the other two genotypes at 4-5 day by their shiny skin, smaller body size and reduced vibrissae. Therefore we are certain that *Hr*^{n} has effects on the phenotype much earlier than postnatal day 7. In this chapter, we describe our efforts to identify the earliest phenotype of gene expression changes that result from the *Hr*^{n} mutation. Without having identified the mutation, we did not have access to a strategy for genotyping mixed litters at early ages. On the BALB/C background, litter sizes are very small (~3-5) and mating between homozygous parents did not produce offspring. However, we outcrossed *Hr*^{n} to FVB/N mice and litter sizes were large (up to 13). Mating of *Hr*^{n}/*Hr*^{n} parents produced offspring, although the females still had difficulty nursing the pups. We were able to cross-foster one of three such litters (n=10) onto a DBA/B6 mom, who cared for the offspring normally. From this litter we obtained mice that allowed us to examine the very early histological and gene expression changes at *Hr*^{n} mutants. We present the results from postnatal days 0, 1, 3, and 7 in this chapter.

Results

Histological analysis of young mutant mice

Histological analysis plays an important role in characterizing the mouse mutant. Dorsal skins from 0-, 1-, and 3-day old +/+ and *Hr*^{n}/*Hr*^{n} mice were fixed in 10% neutral buffered formalin, embedded in paraffin, sectioned, and stained with hematoxylin & eosin (HE) (figure 5-1). Hair follicles in wild type mice at day 0 after birth appear normal with obvious inner root sheath, outer root sheath, dermal papilla, and cortex region. There is no hair shaft formed at this time (It would form and grow out from the piliary canal). Epidermis is normal with cornified layers. The keratinization zone in +/+ hair follicles is organized and located in the top of pre-cortex region. Hair follicles at 0-day *Hr*^{n}/*Hr*^{n} mutant mice are structurally normal with inner root sheath, outer root

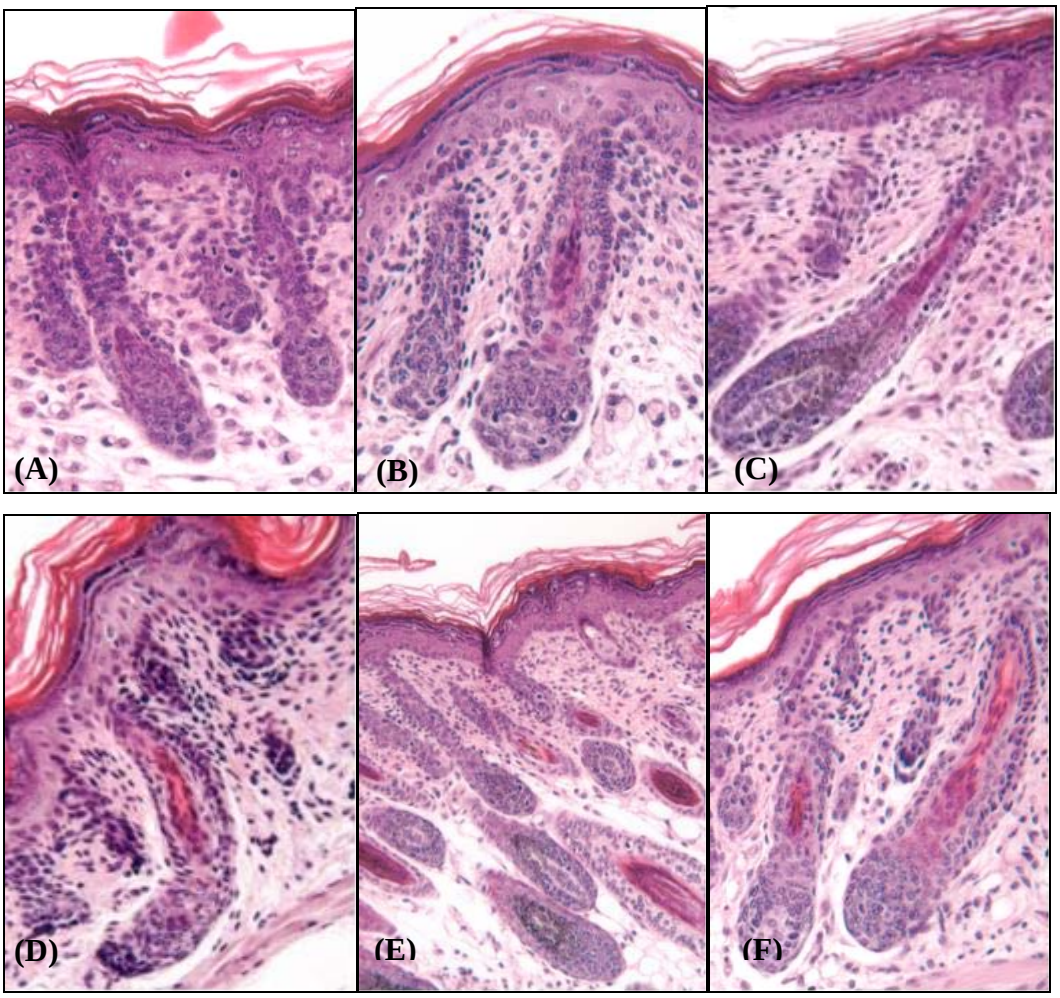

Figure 5-1 Histology of 0-, 1-, and 3-day Hr^n/Hr^n and +/+ mice with HE staining. (A) 0 day +/+ mice; (B) 0 day Hr^n/Hr^n mice; (C) 1 day +/+ mice skin; (D) 1 day Hr^n/Hr^n mice skin; (E) Histology of 3-day old +/+ mice; (F) Histology of 3-day old Hr^n/Hr^n mice.

sheath, and dermal papilla. Even at this early stage, hyperkeratosis is apparent in and apical to the pre-cortex, indicating that premature keratinization is one of (or the) earliest morphological change in Hr^n follicle. The keratinization in hair follicles of 0-day Hr^n/Hr^n mice was not localized to the keratinization zone seen in 0-day +/+ mice; instead it occurs in a wider region and is disorganized. One day later, in +/+ mice, the keratinocytes in the pre-cortex region begin to differentiate and form a line of nuclei of keratinocytes, which will later form the hair shaft. However in 1-day old Hr^n/Hr^n mice, the hair follicle is increasingly disorganized. There is increased keratinization inside the hair follicles. There are no formations of lined nuclei of differentiated keratinocytes. Instead, this region is full of cornified materials. In addition, there are still subtle but noticeable cornified materials in the pre-cortex region. By the age of 3 days, the hair follicles in Hr^n/Hr^n mice are filled with more cornified materials in the region where a normal hair shaft forms in +/+ mice. The keratinization in the pre-cortex region becomes more significant. These findings indicate that hyperkeratosis begins immediately after birth (or perhaps even before birth) and becomes more severe with age.

Microarray analysis with 0-day mutant mice

What causes hyperkeratosis in Hr^n/Hr^n mice is still unknown since the underlying genetic mutation remains unclear. However, the genes involved into the hyperkeratosis might be studied through genome-wide gene expression assays and provide a clue to the basis for the Hr^n phenotype. Therefore, microarray analysis was applied to 0-day old Hr^n/Hr^n and +/+ mice to identify the earliest changes in gene expression due to the unknown Hr^n mutation. About 60 genes were identified as differentially expressed in Hr^n/Hr^n mice, based on a 99% confidence level (table 5-1). Amongst these sixty genes, four genes are related with immunoglobin or T cell receptor, which means some sort of altered immunological function.

The differentially expressed genes were uploaded to DAVID 2.1 (Database for Annotation, Visualization and Integrated Discovery) (http://david.abcc.ncifcrf.gov/) (Dennis et al., 2003) for functional annotation including Gene Ontology (GO) analysis. It was shown that several categories were enriched, including odorant binding, tryptase activity, extracellular space, transporter activity, phospholipid binding (table 5-2). It was

Table 5-1 Differentially expressed genes from the microarray analysis with 0-day Hr^n/Hr^n mice compared to wild type mice. The data was analyzed with ImaGene and GeneSight based on 99% confidence interval and fold change of 1.6 ($2^{0.7}$).

Gene ID	Gene Name	Fold change
M16355	major urinary protein I (*MUP* I)	-8.7
M16356	major urinary protein II (*MUP* II)	-8.3
M16357	major urinary protein III (*MUP* III)	-6.6
AK020171	12 days embryo male wolffian duct includes surrounding region cDNA	-6.6
NM_009947	copine 6 (*Cpne6*)	-4.4
M16360	major urinary protein V (*MUP* V)	-4.1
M29241	U5 small nuclear RNA, clone 1	-3.4
J03299	liver transferring	-3.2
M17763	major urinary protein pseudogene (G2-4), exon 1	-3.1
M27608	major urinary protein	-3.0
M23016	Transferring segment 4_	-2.8
NM_007606	carbonic anhydrase 3 (*Car3*)	-2.8
NM_008648	major urinary protein 4 (*Mup4*)	-2.7
NM_026358	RIKEN cDNA 4930583H14 gene (4930583H14Rik)	-2.6
NM_020281	melanoma antigen, family A, 7 (*Magea7*)	-2.5
NM_016792	thioredoxin-like (32kD) (*Txnl*)	-2.5
AB037540	CYP4F14 mRNA for leukotriene B4 omega-hydroxylase	-2.5
AK006259	1700023A20Rik, RIKEN cDNA 1700023A20 gene	-2.4
AK020601	9530049O05Rik, RIKEN cDNA 9530049O05 gene	-2.4
M12449	cell adhesion molecule (*CAM*) uvomorulin	-2.3
NM_013805	claudin 5 (*Cldn5*)	2.3
NM_009265	small proline-rich protein 1B (*Sprr1b*)	2.4
BC004653	SWI/SNF related, matrix associated, actin dependent regulator of chromatin, subfamily a, member 2 (*Smarca2*)	2.4
AF375885	protein o-fucosyltransferase (*Pofut1*)	2.4
AF108215	5_-AMP-activated protein kinase beta subunit	2.4
AK019736	4930544I03Rik, RIKEN cDNA 4930544I03 gene	2.5
NM_008476	Keratin complex 2, gene 6a (*Krt2-6a*)	2.5
NM_013473	annexin A8 (*Anxa8*)	2.5
AK021197	C330013E15Rik, RIKEN cDNA C330013E15 gene	2.6
NM_013808	cysteine-rich protein 3 (*Csrp3*)	2.6
NM_020591	RIKEN cDNA A030009H04 gene (A030009H04Rik)	2.6
AK014850	hypothetical Leucine-rich repeat/bZIP (Basic-leucine zipper) transcription factor family/Leucine-rich repeat, typical subtype containing protein	2.6
AK004778	Transmembrane protein 43 (*Tmem43*)	2.6

Table 5-1 continued

Gene ID	Gene Name	Fold change
AK004796	weakly similar to pol polyprotein (fragment) [simian sarcoma-associated virus, SSAV]	2.7
NM_013545	hemopoietic cell phosphatase (*Hcph*)	2.8
NM_011363	SH2-B PH domain containing signaling mediator 1 (*Sh2bpsm1*)	2.8
NM_010789	myeloid ecotropic viral integration site 1 (*Meis1*)	2.9
AK017885	Ras homolog gene family, member H (*Rhoh*)	3.0
AK005497	1600019K03Rik, RIKEN cDNA 1600019K03 gene	3.2
AK015086	spermidine/spermine N1-acetyl transferase-like 1 (*Satl1*)	3.3
NM_011607	tenascin C (*Tnc*)	3.4
AL136158	dM538M10.5 (novel 7 transmembrane receptor (olfactory receptor like) protein similar to human HS6M1-28)	3.4
L00653	mast cell protease-7 (*Mcpt7*)	3.6
AK017047	4933433N18Rik, RIKEN cDNA 4933433N18 gene	4.2
AK009746	Kaptin (actin-binding protein)	4.8
NM_010781	mast cell protease 6 (*Mcpt6*)	4.9
L04961	nuclear-localized inactive X-specific transcript (*Xist*)	5.8
AK009793	2310043P16Rik, RIKEN cDNA 2310043P16 gene	19.7
AF242214	38C2 immunoglobulin light chain variable domain	-2.7
V00808	Part of the murine gene for kappa-immunoglobulin leader peptide and variable part (cell line MOPC41).	-2.5
AF318436	clone 490.08 immunoglobulin heavy chain variable region gene	2.7
Z12222	rearranged T-cell receptor beta chain Vbeta8 repertoire (VDJ).	3.0

Table 5-2 Functional annotation for the microarray data from 0-day Hr^n/Hr^n mice

Enriched Categories	Enriched Genes	
ODORANT BINDING	M16355	major urinary protein 1
	M16356	major urinary protein 2
	M16357,M27608	major urinary protein 3
	NM_008648	major urinary protein 4
	M16360	major urinary protein 5
TRYPTASE ACTIVITY	NM_010781	mast cell protease 6
	L00653	mast cell protease 7
EXTRACELLULAR SPACE	NM_013805	claudin 5
	AB037540	cytochrome P450, family 4, subfamily f, polypeptide 14
	NM_008648	major urinary protein 4
	M16360	major urinary protein 5
	NM_010781	mast cell protease 6
	L00653	mast cell protease 7
	AF375885	protein O-fucosyltransferase 1
	NM_011607	tenascin C
	J03299,M23016	transferrin
TRANSPORTER ACTIVITY	M16355	major urinary protein 1
	M16356	major urinary protein 2
	M16357,M27608	major urinary protein 3
	NM_008648	major urinary protein 4
	M16360	major urinary protein 5
	NM_016792	thioredoxin-like 1
PHOSPHOLIPID BINDING	NM_013473	annexin A8
	NM_009947	copine VI

very surprised to notice that many proteins called major urinary proteins 1-5 were downregulated significantly. These proteins are related with odorant binding and transport of small molecules.

Microarray analysis with 7-day mice

Seven-day old homozygous and heterozygous mutant mice were distinguished phenotypically from wild type mice. It was found in the previous chapter that premature keratinization occurred in the pre-cortex region of hair follicles in both Hr^n/Hr^n and $Hr^n/+$ mice. As an additional step to catch the very early molecular changes in Hr^n/Hr^n mutant mice, microarray analysis was done in Hr^n/Hr^n and +/+ mice with slides containing about 21,000 (22k) mouse genes and with slides containing about 15,000 (15k) mouse genes (15k is a subset of 22k). It was found that about 130 genes were differentially expressed in Hr^n/Hr^n mice compared to wild type mice (listed in table 5-3). Most of the differentially expressed genes in table 5-1 were downregulated and only 12 genes, 10% of the total genes were upregulated. Expression of *Hr* in 7-day old Hr^n/Hr^n mice was increased by 2-3 fold compared to wild type mice by real time PCR earlier. Since *Hr* has been shown to be a transcriptional co-repressor (Potter et al., 2001; Zarach et al., 2004), it would be expected that increased expression of *Hr*, even just 2-3 fold, would decrease expression of genes that are *Hr* targets. This might help to explain why most of the differentially expressed genes were upregulated. This might suggest that the Hr^n mutation could be related to a regulatory mutation in *Hr* gene.

It was noticed that many genes related with immune function were differentially expressed from the microarray analysis (table 5-4). Most of these genes are related with either immunoglobin or T cell receptor (including both α and β chain). All mice were maintained in a SPF (specific-pathogen-free) facility, so these changes are not due to dermal pathogens. Some forms of alopecia areata have been linked to autoimmune type changes. Therefore, it is possible that differential expression of these immune-related genes play some role in hair loss in Hr^n.

The differentially expressed genes were uploaded to DAVID 2.1 for functional annotation including GO analysis. One of the features of this program is that it can generate clusters of genes based on their cytobands in the genome. The program

Table 5-3 Differentially expressed genes from microarray analysis of 7-day old Hr^n/Hr^n mice compared with +/+ mice. The data was analyzed with ImaGene and GeneSight from BioDiscovery based on 99% confidence interval and fold change of 1.6.

Gene ID	Gene name	Fold change
NM_025602	DNA segment, Chr 10, ERATO Doi 718, expressed	-4.2
X75650	keratin, hair, acidic, 3B	-4.1
D89901	keratin associated protein 6-3	-4.1
NM_011199	Parathyroid hormone receptor 2	-4.0
NM_008124	gap junction membrane channel protein beta 1	-3.9
NM_028333	angiopoietin-like 1	-3.7
NM_008177	gastrin releasing peptide receptor	-3.7
BC006914	leucine zipper domain protein	-3.6
AK017244	trichohyalin-like 1	-3.6
NM_019400	rabaptin, RAB GTPase binding effector protein 1	-3.4
NM_023907	forkhead box I1	-3.4
AK021201	protein kinase C binding protein 1	-3.4
AK002671	protein phosphatase 1, regulatory (inhibitor) subunit 2	-3.3
AK021005	AT rich interactive domain 1B (Swi1 like)	-3.3
AK013609	zinc finger, DHHC domain containing 4	-3.3
AK021149	potassium voltage-gated channel, subfamily H (eag-related), member 3	-3.3
NM_025562	tetratricopeptide repeat domain 11	-3.2
D86424	keratin associated protein 3-1	-3.2
NM_008536	transmembrane 4 superfamily member 1	-3.1
AK020505	early B-cell factor 2	-3.1
AK017895	SET domain and mariner transposase fusion gene	-3.1
AK014721	ATPase, H+ transporting, V0 subunit D, isoform 2	-3.1
NM_008237	hairy and enhancer of split 3 (Drosophila)	-3.1
AB031959	solute carrier organic anion transporter family, member 1b2	-3.1
U46027	CREB transcription factor, novel spliced form	-3.1
NM_019960	heat shock protein 3	-3.0
X99143	keratin, hair, basic, 6 (monilethrix)	-3.0
NM_009254	serine (or cysteine) proteinase inhibitor, clade B, member 6a	-3.0
NM_009294	syntaxin 4A (placental)	-2.9
AF345291	keratin associated protein 16-1	-2.9
NM_008215	hyaluronan synthase1	-2.9
NM_015756	Shroom	-2.9
AL021127	centrin 2	-2.9
NM_018815	nucleoporin 210	-2.9
M15525	laminin B1 subunit 1	-2.9
AK019761	GLIS family zinc finger 1	-2.8
BC013550	TAF5-like RNA polymerase II, p300/CBP-associated factor (PCAF)-associated factor	-2.8

Table 5-3 Continued

Gene ID	Gene name	Fold change
NM_010676	keratin associated protein 8-2	-2.8
AK011693	ring finger protein 157	-2.8
NM_010670	keratin associated protein 12-1	-2.8
U50960	clone TSAP2 p53-induced apoptosis differentially expressed mRNA sequence.	-2.8
NM_008891	Pinin	-2.8
NM_026402	APG3 autophagy 3-like (S. cerevisiae)	-2.8
NM_010561	interleukin enhancer binding factor 3	-2.8
NM_009010	RAD23a homolog (S. cerevisiae)	-2.8
AK009447	vacuolar protein sorting 24 (yeast)	-2.7
NM_008412	Involucrin	-2.7
BC002226	hook homolog 2 (Drosophila)	-2.7
NM_008579	meiosis expressed gene 1	-2.7
BC012520	pantothenate kinase 4	-2.7
NM_026320	interleukin enhancer binding factor 2	-2.7
D30748	protein tyrosine phosphatase, non-receptor type 15	-2.7
NM_016716	cullin 3	-2.7
AK005136	phosphatase and actin regulator 3	-2.7
AK003884	protein phosphatase 1F (PP2C domain containing)	-2.7
AF340231	EGL nine homolog 2 (C. elegans)	-2.7
NM_009063	regulator of G-protein signaling 5	-2.7
NM_008838	phosphatidylinositol glycan, class F	-2.7
NM_010885	NADH dehydrogenase (ubiquinone) 1 alpha subcomplex, 2	-2.7
AF357392	t-complex protein 1	-2.7
NM_007478	ADP-ribosylation factor 3	-2.7
AK011461	BTB (POZ) domain containing 4	-2.7
AK007207	myosin, light polypeptide kinase	-2.7
NM_016857	exocyst complex component 7	-2.7
AF418208	docking protein 5	-2.7
L09600	nuclear factor, erythroid derived 2	-2.7
BC005669	expressed sequence R74862	-2.6
NM_008904	peroxisome proliferative activated receptor, gamma, coactivator 1 alpha	-2.6
AK012212	Procollagen, type XVI, alpha 1	-2.6
AY044153	histamine receptor H 3	-2.6
NM_010807	MARCKS-like protein	-2.6
NM_007994	fructose bisphosphatase 2	-2.6
AK017747	SMC2 structural maintenance of chromosomes 2-like 1 (yeast)	-2.6
NM_031872	taste receptor, type 1, member 3 (Tas1r3)	-2.6
BC011407	golgi autoantigen, golgin subfamily a, 2	-2.6
NM_007520	BTB and CNC homology 1	-2.6

Table 5-3 Continued

Gene ID	Gene name	Fold change
AK018152	KH-type splicing regulatory protein	-2.6
M27134	MHC class I H-2K1-k pseudogene	-2.6
AF166265	glucagon-like peptide 2 receptor	-2.6
NM_011104	protein kinase C, epsilon	-2.6
S37491	Angiotensin receptor 1b	-2.6
S43865	protein phosphatase 3, regulatory subunit B, alpha isoform (calcineurin B, type II)	-2.6
AF053628	D3Mm3e (D3Mm3e)	-2.5
NM_007526	BarH-like homeobox 1	-2.5
AK004406	MAF1 homolog	-2.5
NM_021789	trafficking protein particle complex 4	-2.5
NM_026924	zinc finger protein 339	-2.5
AF357419	RNA, U68 small nucleolar	-2.5
NM_009446	Tubulin, alpha 7	-2.5
NM_023136	thymidylate kinase (Tmk)	-2.5
AK018638	diptheria toxin resistance protein required for diphthamide biosynthesis (Saccharomyces)-like 2	-2.5
BC006661	debranching enzyme homolog 1 (S. cerevisiae)	-2.5
AK012914	Leucine rich repeat protein 1, neuronal	-2.5
NM_010919	NK2 transcription factor related, locus 2 (Drosophila)	-2.5
L10370	neurofibromatosis 1	-2.5
NM_008762	olfactory receptor 15	-2.5
NM_025681	limb expression 1 homolog (chicken)	-2.5
NM_007423	Alpha fetoprotein	-2.5
NM_010634	fatty acid binding protein 5, epidermal	-2.5
NM_009229	syntrophin, basic 2	-2.5
BC004738	Similar to dual specificity phosphatase 9, clone MGC	-2.5
NM_015741	keratin associated protein 9-1	-2.5
AK006697	methionine sulfoxide reductase A	-2.5
NM_009282	stromal antigen 1	-2.4
AL133159	olfactory receptor 107	-2.4
NM_011062	3-phosphoinositide dependent protein kinase-1	-2.4
AB041350	procollagen, type IV, alpha 5	-2.4
M18589	pseudo-kallikrein gene, exon 2, clone mGK-10._	-2.4
NM_007654	CD72 antigen	-2.4
NM_009501	ventral anterior homeobox containing gene 1	-2.4
NM_009396	tumor necrosis factor, alpha-induced protein 2	-2.4
NM_010659	keratin complex 1, acidic, gene 1	-2.4
NM_008553	achaete-scute complex homolog-like 1 (Drosophila)	-2.4
NM_015757	protocadherin 13 (Pcdh13)	-2.4
NM_007914	ets homologous factor	-2.4
AJ293592	Laminin, alpha 3	-2.4

Table 5-3 Continued

Gene ID	Gene name	Fold change
NM_013589	latent transforming growth factor beta binding protein 2	-2.4
V00830	keratin complex 1, acidic, gene 10	2.2
NM_008445	kinesin family member 3C	2.4
NM_013459	adipsin	2.4
AK006506	Enolase 3, beta muscle	2.5
AK019689	Unc-84 homolog A (C. elegans)	2.5
AK013576	brain-specific angiogenesis inhibitor 3	2.5
NM_013541	Glutathione S-transferase, pi 1	2.8
AB011019	EGF-like-domain, multiple 9	3.1
AK010477	polymerase (DNA-directed), delta 4	3.4
NM_019916	T-cell leukemia, homeobox 3	-2.4
AL513354	DNA segment, Chr 15, Brigham & Women's Genetics 0669 expressed	3.5
AK011423	glucosamine (N-acetyl)-6-sulfatase	5.1
NM_025358	NADH dehydrogenase (ubiquinone) 1 alpha subcomplex, 9	10.8

Table 5-4 Differentially expressed Ig- or TCR- related genes in 7-day Hr^n/Hr^n mice compared with +/+ mice. Microarray data was analyzed with ImaGene and GeneSight from BioDiscovery based on 99% confidence interval and fold change of 1.6.

Gene ID	Gene name	Fold change
M36743	immunoglobulin heavy chain 6 (heavy chain of IgM)	-3.8
U55578	anti-DNA immunoglobulin light chain IgM mRNA, antibody 363p.193	-3.5
U07879	T cell receptor alpha chain AV10S10 precursor	-3.4
AF131134	immunoglobulin kappa light chain variable region gene	-3.3
S74556	Ig VH_rheumatoid factor RF1-7M _clone RF1-7M	-3.1
L41881	immunoglobulin kappa chain	-3.1
X03380	mRNA for GAT (HP9) anti-idiotypic Ab2 Ig heavy chain	-3.0
X66458	IG heavy chain V region (7F2).	-2.9
Z12199	rearranged T-cell receptor beta chain Vbeta8 repertoire	-2.9
U96685	immunoglobulin-like receptor PIRA4 (6M7)	-2.8
U26780	T cell receptor Va15/Ja35 alpha chain mRNA, isolate 726-1	-2.7
U26799	T cell receptor Va8/Ja47 alpha chain mRNA, isolate 628-23	-2.7
X55826	T-cell receptor alpha-chain (clone 14.12).	-2.6
AJ222596	similar to Ig heavy-chain V region precursor	-2.5
X06530	Ig active L-chain(k) V-region	-2.4
M20465	Ig rearranged kappa chain mRNA V-region (VH11-JK5) N4	-2.4
AF012185	T-cell receptor alpha chain (TCRA)	-2.4
AF041952	infected mouse A seq 4, day 14, T cell receptor beta chain	2.9
AF041922	infected mouse A seq 6, day 10, T cell receptor beta chain	3.1
AF041935	infected mouse B seq 8, day 10, T cell receptor beta chain	3.3
AF041918	infected mouse A seq 2, day 10, T cell receptor beta chain	3.4
AF041950	infected mouse A seq 2, day 14, T cell receptor beta chain	3.6
AF041969	infected mouse C seq 4, day 14, T cell receptor beta chain	3.6
AF041962	infected mouse B seq 5, day 14, T cell receptor beta chain	3.9
AF041971	infected mouse C seq 6, day 14, T cell receptor beta chain	4.0
AF041923	infected mouse A seq 7, day 10, T cell receptor beta chain	4.6
U86728	T-cell receptor alpha V region t1g5	8.8

generated five gene clusters according to their positions in mouse genome (table 5-5). These five significant cytobands are on 5 different chromosomes, 2H4, 5G1, 11D, 16A1, and 17A3.1. Each cluster contains at least 2 different genes with differential expression. Cytoband clusters of 16A1 and 11D consist of a few keratins and/or keratin-associated proteins. These gene clusters might suggest that the expressions of the genes in each cluster are regulated in the same or similar pattern, or by the same transcriptional factors, in Hr^n/Hr^n mutant mice.

Functional annotation analysis suggests that there are several categories significantly enriched in Hr^n/Hr^n mutant mice compared to +/+ mice at 7-day after birth (table 5-6). These enriched categories include coiled coil, cytoskeleton, keratins, extracellular matrix structural constituents, calcium signaling pathway, calcium binding, transcription regulation, basement membrane, protein phosphatase inhibitor, and basic-leucine zipper transcription factor. Most of these enriched categories are closely related with hair follicle development and hair cycles. For example, categories of coiled coil, cytoskeleton, keratins, and extracellular matrix structural constituents are directly related with hair growth. Calcium binding and calcium signaling pathway are very critical to regulate the basic events such as regulation of transcription and keratinocyte differentiation. The enriched categories of transcription regulation and basic-leucine zipper transcription factor suggest that the transcriptional regulation in Hr^n/Hr^n mutant mice was systematically regulated by many different transcriptional factors. The functional annotation of microarray data suggests the possible effects of Hr^n mutation and the possible functions of unknown mutated gene for Hr^n.

Pathway and network analysis

Network analysis of these differentially expressed genes was done with the trial version of Ingenuity pathway analysis (Ingenuity Systems Inc, Mountain View, CA). The list of differentially expressed genes as well as their expression changes was uploaded to the online database of Ingenuity. The program generates all the possible networks from the uploaded genes plus the annotated genes in the online database. Figure 5-2 just shows one gene network generated from the microarray analysis by Ingenuity. Genes with red color indicate those genes downregulated in microarray analysis and those with green

Table 5-5 Clusters of differentially expressed genes in cytobands of mouse chromosomes in 7-day Hr^n/Hr^n mice. Microarray analysis was done with ImaGene and GeneSight. The cytoband analysis was through DAVID 2.1 from NIH.

Cytoband	Gene ID	Gene Name
16 A1	NM_007520	BTB and CNC homology 1
	U50960	RIKEN cDNA 1190017O12 gene
	AF345291	keratin associated protein 16-1
	NM_010676	keratin associated protein 8-2
	BC006914	leucine zipper domain protein
	AK007207	myosin, light polypeptide kinase
	NM_008762	olfactory receptor 15
	AK003884	protein phosphatase 1F (PP2C domain containing)
5 G1	NM_025562	tetratricopeptide repeat domain 11
	AK019689	unc-84 homolog A (C. elegans)
17 A3.1	NM_008215	hyaluronan synthase1
	NM_025681	limb expression 1 homolog (chicken)
2 H4	AK011461	BTB (POZ) domain containing 4
	AY044153	histamine receptor H 3
	AK005136	phosphatase and actin regulator 3
11 D	D86424	keratin associated protein 3-1
	NM_015741	keratin associated protein 9-1
	NM_010659	keratin complex 1, acidic, gene 1
	V00830	keratin complex 1, acidic, gene 10
	X75650	keratin complex 1, acidic, gene 3

Table 5-6 Functional annotation of the microarray data from 7-day Hr^n/Hr^n mice through DAVID 2.1 from NIH.

Enriched Categories	Enriched Genes	
COILED COIL	AK017747	SMC2 structural maintenance of chromosomes 2-like 1
	NM_028333	angiopoietin-like 1
	NM_016857	exocyst complex component 7
	BC011407	golgi autoantigen, golgin subfamily a, 2
	BC002226	hook homolog 2 (Drosophila)
	NM_010659	keratin complex 1, acidic, gene 1
	V00830	keratin complex 1, acidic, gene 10
	X75650	keratin complex 1, acidic, gene 3
	X99143	keratin complex 2, basic, gene 10
	NM_008445	kinesin family member 3C
	M15525	laminin B1 subunit 1
	AJ293592	laminin, alpha 3
	AK005136	phosphatase and actin regulator 3
	NM_019400	rabaptin, RAB GTPase binding effector protein 1
	NM_009294	syntaxin 4A (placental)
	AK019689	unc-84 homolog A (C. elegans)
CYTOSKELETON	AL021127	centrin 2
	BC002226	hook homolog 2 (Drosophila)
	NM_010670	keratin associated protein 12-1
	D89901	keratin associated protein 6-3
	NM_015741	keratin associated protein 9-1
	NM_010659	keratin complex 1, acidic, gene 1
	NM_008445	kinesin family member 3C
	AK007207	myosin, light polypeptide kinase
	NM_015756	Shroom
	NM_009229	syntrophin, basic 2
	AF357392	t-complex protein 1
	NM_009446	tubulin, alpha 7
KERATIN	NM_010670	keratin associated protein 12-1
	D86424	keratin associated protein 3-1
	D89901	keratin associated protein 6-3
	NM_015741	keratin associated protein 9-1
	NM_010659	keratin complex 1, acidic, gene 1
	V00830	keratin complex 1, acidic, gene 10
	X75650	keratin complex 1, acidic, gene 3
	X99143	keratin complex 2, basic, gene 10
BASEMENT MEMBRANE	M15525	laminin B1 subunit 1
	AJ293592	laminin, alpha 3
	AB041350	procollagen, type IV, alpha 5

Table 5-6 Continued

Enriched Categories	Enriched Genes	
EXTRACELLULAR MATRIX STRUCTURAL CONSTITUENT	M15525	laminin B1 subunit 1
	AJ293592	laminin, alpha 3
	AB041350	procollagen, type IV, alpha 5
	AK012212	procollagen, type XVI, alpha 1
CALCIUM SIGNALING PATHWAY	S37491	angiotensin receptor 1b
	U46027	cAMP responsive element binding protein 1
	NM_008177	gastrin releasing peptide receptor
	AK007207	myosin, light polypeptide kinase
	S43865	protein phosphatase 3, regulatory subunit B, alpha isoform (calcineurin B, type II)
CALCIUM ION BINDING	AB011019	EGF-like-domain, multiple 9
	AL513354	RIKEN cDNA 4931407K02 gene
	AL021127	centrin 2
	M15525	laminin B1 subunit 1
	NM_013589	latent transforming growth factor beta binding protein 2
	S43865	protein phosphatase 3, regulatory subunit B, alpha isoform (calcineurin B, type II)
	NM_009229	syntrophin, basic 2
	AK017244	trichohyalin-like 1
TRANSCRIPTION REGULATION	AK011461	BTB (POZ) domain containing 4
	NM_007520	BTB and CNC homology 1
	NM_007526	BarH-like homeobox 1
	AK019761	GLIS family zinc finger 1
	AK004406	MAF1 homolog
	NM_010919	NK2 transcription factor related, locus 2 (Drosophila)
	BC013550	TAF5-like RNA polymerase II, p300/CBP-associated factor (PCAF)-associated factor
	U46027	cAMP responsive element binding protein 1
	AK020505	early B-cell factor 2
	NM_008237	hairy and enhancer of split 3 (Drosophila)
	NM_010561	interleukin enhancer binding factor 3
	L09600	nuclear factor, erythroid derived 2
	NM_008904	peroxisome proliferative activated receptor, gamma, coactivator 1 alpha
	AK021201	protein kinase C binding protein 1
BASIC-LEUCINE ZIPPER (BZIP) TRANSCRIPTION FACTOR	NM_007520	BTB and CNC homology 1
	U46027	cAMP responsive element binding protein 1
	L09600	nuclear factor, erythroid derived 2
PROTEIN PHOSPHATASE INHIBITOR	M15525	laminin B1 subunit 1
	AJ293592	laminin, alpha 3

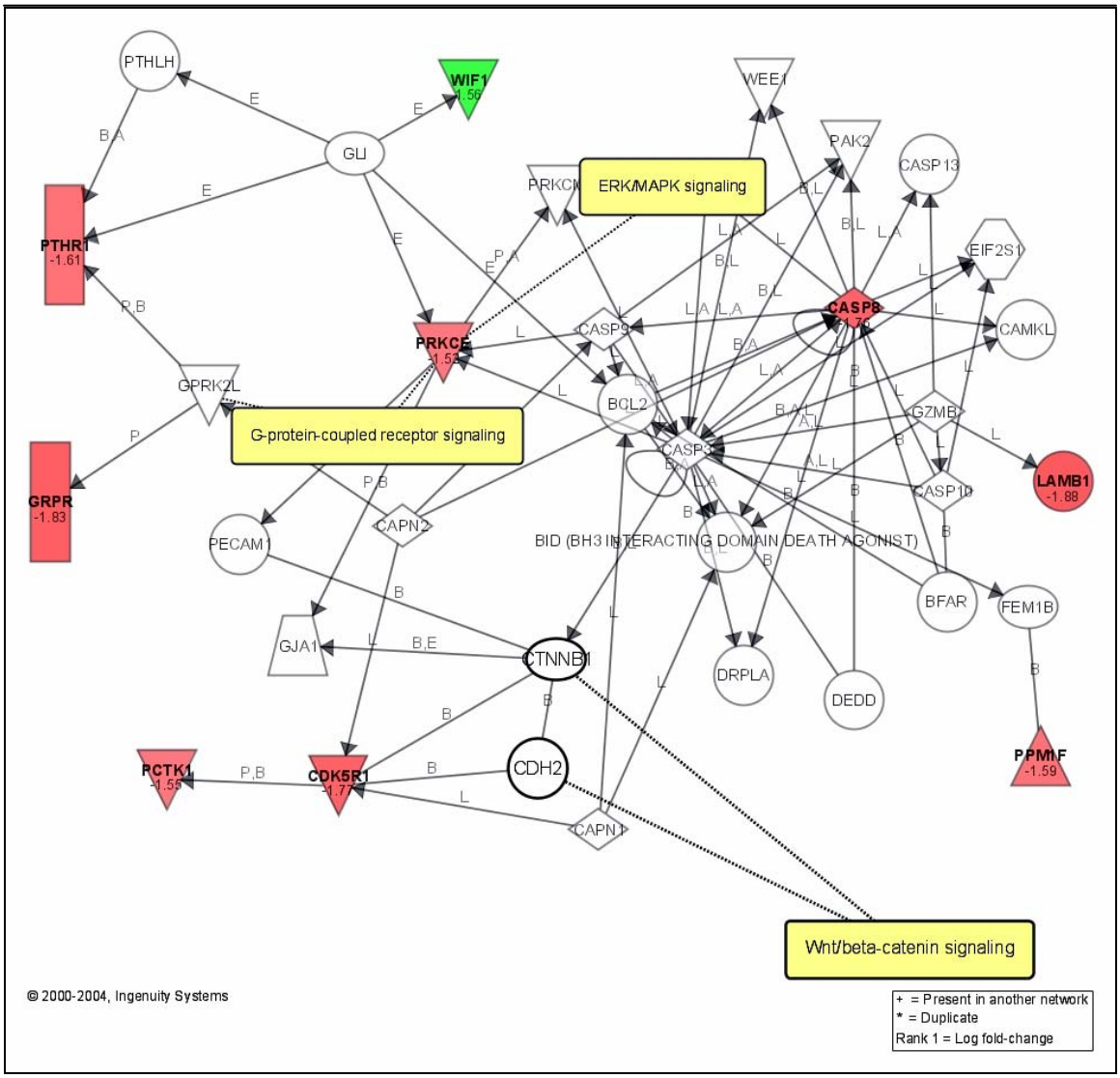

Figure 5-2 One network generated from the differentially expressed genes in microarray analysis at 7 days of age with trial version of Ingenuity. Red: downregulated expression; Green: upregulated expression.

color are for the genes with upregulation. The program is able to identify the signaling pathways connected through the networks. For example, the network shown in figure 5-2 indicated that three signaling pathways, ERK/MAPK signaling, G-protein-coupled receptor signaling, and Wnt/β-catenin signaling pathways are affected by Hr^n mutation. Altogether, there are more than 10 different networks generated by network analysis using Ingenuity. Totally there are seven different signaling pathways affected in Hr^n/Hr^n mutant mice: Wnt/β-catenin signaling, ERK/MAPK signaling, apoptosis signaling, TGF-β signaling, *NF-κB* signaling, P38 MAPK signaling, G protein coupled receptor signaling. All these pathways play important roles in cell cycle and growth. Wnt/β-catenin (Fuchs, 1998; Jamora et al., 2003; Lowry et al., 2005) and TGF-β (Peters et al., 2005) signaling pathways are critically involved in hair follicle development and hair cycle. The analysis of signal pathways suggests the possible roles of Hr^n mutation due to either the over-expression of *Hr* gene or another unknown gene mutation.

At the same time, PathwayAssist software from Stratagene was also used to analyze the differentially expressed genes at 7 days of age (figure 5-3). Instead of deriving many separate networks in Ingenuity, PathwayAssist generates a large network based on the gene lists by extracting biological interactions from the scientific literature. The uncharacterized genes within the uploaded gene list were listed as separate nodes outside of the network. The cellular processes affected in the networks include focal contact, motility, differentiation, proliferation, assembly, secretion, oxidative phosphorylation, and apoptosis. The functional classes affected include protein kinase C, SAP kinase, antisense RNA, porin, caspase, ubiquitin, hydrolase, and protein serine/threonine kinase. The cell objects affected in the network include plasma membrane, cytoskeleton, intermediate filament, adhesion junctions, and chromatin. The network also lists the small molecules working in the network, such as glucose and dexamethasome. Compared to the analysis with Ingenuity, the information generated from the network is less reliable since the interactions extracted from literature text mining while the interactions in Ingenuity is curated and updated very often in its online database. Altogether, the analyses with both softwares suggest the alteration of proliferation, differentiation, and apoptosis as well as the related signaling pathways.

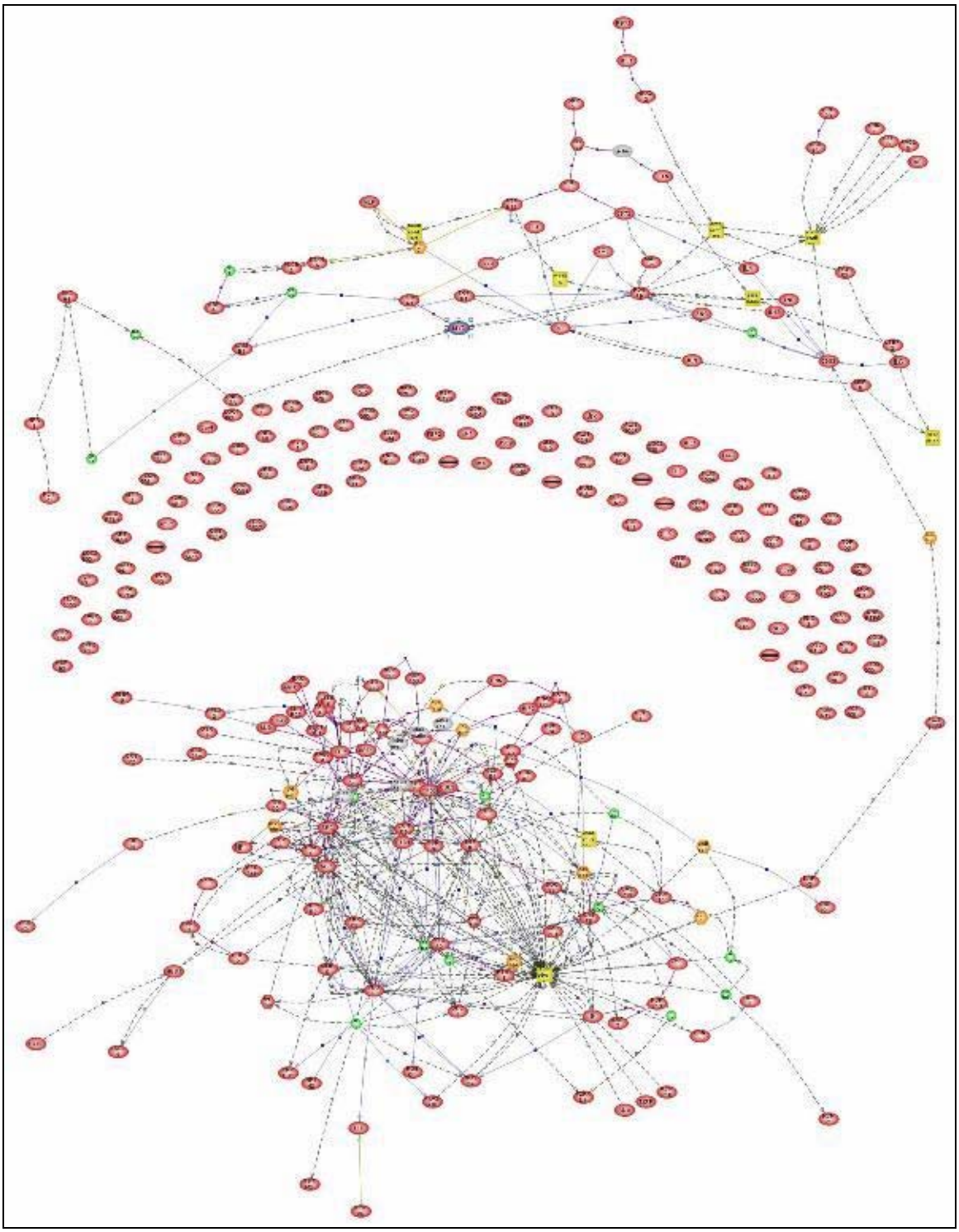

Figure 5-3 Pathway analysis with the differentially expressed genes at 7 days of age through the trial version of PathwayAssist from Stratagene.

Discussion

Histological analysis with mutant mice from 0 to 4 days after birth suggests that there is abnormal pre-mature keratinization occurring in the cortex region of hair follicles that begins right after or even before birth. It is not known what occurred during the embryogenesis stages since it is still very difficult to get a homozygous litter and we have not performed timed matings. Premature keratinization may be the initial event that leads to hair loss in Hr^n mice. The premature keratinization in the hair follicle of 0 to 4 days old mutant mice validates the previous finding in older mice of abnormal hyperkeratosis in the hair follicles and the formation of mineralized dermal cysts. This histological change is due to either a regulatory mutation in Hr^n in *Hr* or an unknown mutation in another gene.

Microarray analysis with 0 day mutant mice provides more explanation about the phenotypes in Hr^n mutants. Two thirds of the genes with altered expression are upregulated in the mutants and others are downregulated. Among the list, one interesting gene is keratin 2-6a with more than 2 fold increased expression. As reported in the previous chapter, numerous keratins and keratin-associated proteins are dysregulated in older Hr^n mice. *Krt2-6a* is the first of this class of genes to show altered expression. *Krt2-6a* usually forms a heterodimer with keratin 1-16 or keratin 1-17. *Krt2-6a* is constitutively expressed in the various stratified epithelia, including the companion cell layer of the hair follicle, tongue, footpad, nail bed, oral mucosa t (Mahony et al., 2000; Rothnagel et al., 1999). In addition, the expression of keratin 2-6a is inducible in response to different stimulus, for example, wounding, diseases states including skin tumors and psoriasis (Stoler et al., 1988), phorbol esters and all trans-retinoic acid (Rothnagel et al., 1999). The induction results in its expression in the outer root sheath of hair follicle and throughout the epidermis, including the basal layer. The increased expression of keratin 2-6a in Hr^n/Hr^n mice might be directly or indirectly due to the Hr^n mutation. A mutation that caused loss of mouse keratin 2-6a results in the collapse of keratin filaments, the destruction of hair follicles and eventually alopecia, indicating that the innermost outer root sheath cells are uniquely sensitive to even slightly altered keratin 2-6a proteins (Baker et al., 1997; Wojcik et al., 1999). Therefore, the increased

expression of mouse keratin 2-6a might cause abnormal keratinization in outer root sheath of hair follicle in Hr^n/Hr^n mice, which results into the destruction of hair follicle and eventual formation of alopecia.

Another gene called *Sprr1b* (small proline-rich protein 1B) was upregulated with more than 2 fold in Hr^n/Hr^n than +/+ mice. Sprr proteins are the primary constituents of the cornified envelope (Martin et al., 2004). *Sprr1b* locates in a region called epidermal differentiation complex in chromosome 1 consisting of *S100A10*, *trichohyalin*, *profilaggrin*, *involucrin*, *SPRR3*, *SPRR1B*, *SPRR2A*, *loricrin*, *S100A9*, *S100A9*, *S100A8*, *S100A6*, which are related with the terminal differentiation of epidermis (Mischke et al., 1996). The increase expression of *Sprr1b* indicates the increased cornified materials, which suggests hyperkeratosis occurrence in Hr^n/Hr^n mice.

Another one interesting differentially expressed gene is called *Smarca2*, SWI/SNF related, matrix associated, actin dependent regulator of chromatin, subfamily a, member 2. It was shown that *Smarca2* homologs in human are transcriptional coactivators cooperating with the estrogen receptor, the retinoic acid receptor (Chiba et al., 1994), and the glucocorticoid receptor (Muchardt and Yaniv, 1993). Its expression was upregulated by 2-fold in Hr^n/Hr^n mice compared to +/+ mice. This gene has been identified as a gene correlated with an anti-hair growth pattern, with sharp expression rising at catagen (Lin et al., 2004). Increased expression of *Smarca2* might underlie reduced hair growth in Hr^n/Hr^n mice.

Major urinary proteins (MUPs) are members of lipocalin family proteins mainly produced by the liver. They are secreted into the urine and bind to small-molecular-weight volatile pheromones. In rodents, they play important roles in individual recognition, territorial marking, social behavior, and transport of small molecules (Beynon and Hurst, 2003). Increased expression at 0-day Hr^n/Hr^n mice might be due to the unbalanced ratio of male and female mice between +/+ and Hr^n/Hr^n mice as we did not establish the gender of pups used at this age. Another possible explanation is that the increased expression of these major urinary proteins is due to Hr^n mutation or part of the Hr^n phenotype. Recently, an increased expression (5-fold) of major urinary protein 1 was reported in $Hr^{-/-}$ mice compared to wild type mice through the microarray analysis, which

was also verified by the northern blot (7-fold) (Zarach et al., 2004). In addition, it was also reported that this group of proteins was upregulated in our Hr^{rhR}/Hr^{rhR} mice through microarray analysis (mentioned in Chapter 6). MUPs have been shown to be expressed in skin, and their function there has been linked to transport of small molecules (Held et al., 1989). The transgenic mice with a fusion of ~2.5 kb of 5' flanking region from the *MUP BL6-11* gene with *SV40 T* antigen coding sequence expressed the transgene in the skin sebaceous glands and the preputial gland, a modified sebaceous gland, which is consistent with the presence of MUP mRNA in the skin and a putative role for MUPs in the transport and excretion of small molecules (Held et al., 1989). This validates our microarray experiments in terms of the expression of MUP gene in the skin and suggests a possible function related with skin and hair growth. It was also found that the expression of major urinary protein 2 (*MUP2*) was suppressed by 3-methylcholanthrene (*MC*) through aryl hydrocarbon receptor (*AhR*)-mediated disruption of the growth hormone (*GH*) receptor signaling pathway (Nukaya et al., 2004). The function of *AhR* is known to interact with *Hr*. All of these suggest that the down-regulation of major urinary proteins in Hr^{n}/Hr^{n} mice might be related with the over-expression of *Hr* gene or another unknown gene mutation.

Another gene, *SH2-B* PH domain containing signaling mediator 1 (*Sh2bpsm1* or *Sh2-B*) was differentially expressed at 0-day mutant mice with increased expression. The isoforms of *Sh2-B* form a family of signaling proteins with other proteins including *APS* and *LNK*. The functions of *Sh2-B* have been described as activators, mediators, or inhibitors of cytokine and growth factor signaling. *Sh2-B* is an endogenous enhancer of leptin sensitivity and required for maintaining normal energy metabolism and body weight in mice (Ren et al., 2005). *Sh2-B* homozygous null mice were severely hyperphagic and obese while the overexpression of *Sh2-B* counteracted *PTP1B*-mediated inhibition of leptin signaling in cultured cells (Ren et al., 2005). The expression of *Sh2-B* was significantly increased by almost 3 fold in Hr^{n}/Hr^{n} mutant mice compared to +/+ mice, which might be related with the retarded body growth in Hr^{n} mutant mice. *Sh2-B* also regulates the activity of a variety of transporters under normal and pathological conditions (Jiang et al., 2005), which might play important roles in skin or hair growth.

Sh2-B also specifically activates *JAK2* and it may serve as adapter proteins for all three *JAK*s (*JAK*1-3) independent of any role they have in JAK activity (O'Brien et al., 2002). The adapter protein *Sh2-B* in human was found to interact with *FGFR3* (fibroblast growth factor receptor 3) to mediate *FGFR3*-dependent signaling. The increased expression of human *Sh2-B* in 293T cells activates *FGFR3*, which causes the phosphorylation and nuclear translocation of *STAT5* (Kong et al., 2002b). *Sh2-B* was shown having roles in mast cell development (Kubo-Akashi et al., 2004). Here we observed two mast cell proteases with differential expression in Hr^n mutants, which might suggest the possible involvement of *Sh2-B* in the mutants.

One gene called tenascin C (*Tnc*) was upregulated in 0-day mutants. It is an extracellular matrix protein with a spatially and temporally restricted tissue distribution. In the embryo it is present in dense mesenchyme surrounding developing epithelia, in tendon anlagen, and in developing cartilage and bone. In the adult tenascin remains present in tendons and myotendinous junctions in the perichondrium and periosteum, as well as in smooth muscle. It was shown that this gene is enriched in the outer root sheath (ORS), as one of the molecular signatures of ORS (Rendl et al., 2005). *Tnc* induces the expression of *Mmp*-9 (matrix metalloproteinase 9) in the collaboration of *TGFβ 1* in breast cancer cells (Ilunga et al., 2004; Kalembeyi et al., 2003), suggesting that the increased expression might directly involve into the phenotype development of the Hr^n mutants.

Claudin 5 (*Cldn5*), also called transmembrane protein deleted in velocardiofacial syndrome (TMVCF), was also upregulated in Hr^n mutants at 0 day of age. Claudins are components of tight junction strands. Tight junctions constitute continuous seals around cells that serve as a physical barrier preventing solutes and water from passing freely through the paracellular space. Other members of claudin family, *Cldn1* and *Cldn3* decreased solute permeability in overexpressing cells, while *Cldn5* increased permeability (Coyne et al., 2003). *Cldn5* exists predominantly in pentameric and hexameric configurations and forms specific heterophilic interactions with *Cldn1* and *Cldn3* (Coyne et al., 2003). *Cldn1*, *Cldn4*, and *Cldn10* are found to be the signature genes of the matrix in hair follicles (Rendl et al., 2005) and skin lacking *Cldn1* displays

abnormally short hairs and wrinkled skin (Furuse et al., 2002). The increased expression of *Cldn5* might abolish the heterophilic protein complex with *Cldn1* and *Cldn3* and contribute to the phenotype development of Hr^n mutants.

It was very interesting to notice that several genes in the 0-day list, including hemopoietic cell phosphatase (*Hcph*), mast cell proteases (*Mcpt6* and *Mcpt7*), and cysteine-rich protein 3 (*Csrp3*), are upregulated. These genes were recently found to have an expression pattern inversely correlated with hair growth, with decreased expression in anagen and increased expression in catagen phase of normal hair cycles (Lin et al., 2004). Increased expression of these genes might be related to the reduced hair growth. Another gene called carbonic anhydrase 3 (*Car3*) was downregulated in 0-day mutants. The expression of *Car3* drops at catagen in normal hair follicle cycles (Lin et al., 2004). The decreased expression of *Car3* suggests abnormal hair growth in the mutants.

Microarray analysis with mice at 7 days of age identified a larger set of differentially expressed genes, including many keratins and keratin-associated proteins that are directly related to hair growth. The down-regulation of hair keratins and keratin-associated proteins is consistent with the loss of hair in mutant animals. Most of these genes are significantly downregulated in Hr^n mutants, suggesting that the overexpression of *Hr* as a transcriptional co-repressor might be a cause of the Hr^n phenotype. Several cytobands on different mouse chromosomes, including 2H4, 5G1, 11D, 16A1, and 17A3.1, were enriched with many differentially expressed genes, suggesting the genes in each cytoband might be regulated by a common promoter or a similar mechanism. Cytobands 16A1 and 11D contain many structural proteins including many keratins and keratin-associated proteins. It is possible that the expression of these genes might be the immediate downstream events of Hr^n mutation.

Functional annotation of the microarray results suggests that many categories were significantly enriched, indicating the importance of these categories in hair growth, including keratins, extracellular matrix structural constituent, calcium signaling pathway, and transcription regulation. Several of the genes with differential expression were suggested previously as molecular signatures of hair matrix (*Krt1-1* and *krt2-10*), outer root sheath (*Col4a5*), and dermal papilla (*Lama3*, *Pdgfra*) (Rendl et al., 2005). The

expression of all these signature genes was downregulated in Hr^n mutants, possibly suggesting reduced proliferation in hair matrix, outer root sheath, and dermal papilla, consistent with our histological findings.

Network analysis of the microarray data suggests that the Hr^n mutation affects Wnt/β-catenin, apoptosis, and TGF-β signaling pathways in skin of Hr^n/Hr^n mutants. It has been shown that these signaling pathways plays very important roles in hair follicle morphogenesis, hair growth and hair follicle cycles (Fuchs, 1998; Paus and Foitzik, 2004; Rogers, 2004; Shimizu and Morgan, 2004; Stenn and Paus, 2001). Genes related with Wnt/β-catenin signaling pathways are downregulated, suggesting repressed Wnt signaling. Recently it was found that *Hr* triggers reactivation of hair growth by repressing Wise, a modulator of Wnt signaling, and promoting Wnt signaling (Beaudoin et al., 2005). *Hr* overexpression in 7-day Hr^n/Hr^n mice should promote Wnt/β-catenin signaling pathway. However, we were unable to detect the expression changes of *Wise* in 7-day Hr^n/Hr^n mice. One reason for this is that the location of *Hr* expression is different between the transgenic *Hr* mice generated for reactivating hair growth (Beaudoin et al., 2005) and our Hr^n/Hr^n mutants. *Hr* expression in the transgenic mice is in the outer root sheath and hair bulb as the follicles enter catagen and is under the control of keratin 14 promoter (Beaudoin et al., 2005). However, in Hr^n/Hr^n mutant mice, *Hr* is expressed in the outer root sheath, inner root sheath, matrix cells, and fibroblasts in the sinus. Thus, it is very difficult to compare these two mouse models.

Pathway and network analysis from the microarray data also suggests that many cellular processes including focal adhesion, differentiation, proliferation, assembly, and apoptosis are altered in skin of Hr^n/Hr^n mutants. Focal adhesion is critical for outer root sheath to adhere to, synthesize, and remodel its adjacent basement membranes. The alteration of focal adhesion in skin suggests the change in outer root sheath. *Dsg4* null mice are an example of how loss of an adhesion molecule in hair follicles lead to hair loss, and in fact these mice display a phenotype very similar to that of Hr^n. Changes of proliferation and differentiation in skin are consistent with the histological analysis, which indicates reduced proliferation and abnormal switch from proliferation to differentiation in hair follicle precortical region. The alteration of assembly might suggest

the abnormal assembly of hair keratins and keratin-associated proteins, leading to the premature keratinization in the precortex region and aberrant hair shaft formation. Changes of apoptosis in skin might reflect the change of cell proliferation and the failure of hair shaft formation. The affected cellular objects from pathway analysis including cytoskeleton, intermediate filament, adhesion junctions, and chromatin, are consistent with the functional annotation of the microarray data, which suggests the similar categories are enriched and altered due to the Hr^n mutation.

It is very surprising to notice that so many genes responsible for immune function are differentially expressed at both 0 and 7 day-old mice. Hair follicle has a very complex immunologic profile with matrix cells in its base and perifollicular macrophages, mast cells, Langerhan's cells, and other immunocytes. It is possible that the alteration of immune profiling might be secondary to the hair follicle phenotype. However, it is also possible that the immune changes observed with microarray analysis are due to the Hr^n mutation. It has been shown recently that *hairless* could trigger reactivation of hair growth in hair follicle by promoting Wnt signaling (Beaudoin et al., 2005) and it was found that Wnt/β-catenin signaling pathway was altered in the mutants. If the Hr^n phenotype is related with the overexpression of *Hr* gene, then Wnt signaling pathway should be affected. *Tcf1* (T-cell factor 1) and *Lef1* (lymphoid enhancing factor-1) are critical for the development of T cells (Verbeek et al., 1995). Homologs of *Tcf1/Lef1* has been shown to interact with *Wnt* effector *β-catenin* to mediate axis formation in Xenopus (Molenaar et al., 1996). It was shown that interaction of *Tcf1* with *β-catenin* was required for thymocyte differentiation, and that this interaction was shown to be mediated by *Wnt1* and *Wnt4* (Staal et al., 2001). Based on this, many genes related with T-cell differentiation and development could be differentially expressed due to Hr^n mutation and not secondary to the phenotype.

In summary, the Hr^n mutation was characterized with the histological analysis of young animals and microarray analysis of mice at different ages. Although the genetic mutation has not been identified, we have studied the signaling pathways affected by this mutation. The microarray analysis might provide useful clues to explore the molecular targets of HR and help to finally identify the underlying genetic mutation.

Chapter 6 Molecular and physiological basis for hair loss in mice carrying a novel nonsense mutation in *Hr*

The results presented in this chapter are being prepared as a manuscript that will be submitted to Journal of Investigative Dermatology.

Introduction

The first description of rhino mice was reported by Gaskoin in 1856 (Gaskoin, 1856) as "rhinoceros" with hair loss and wrinkled skin. Later, the mouse called hairless arose spontaneously in 1939 at McGill University in Montreal, Canada (Sundberg, 1994). Shortly thereafter it was shown that *rhino* and *hairless* were allelic (Howard, 1940). The phenotype in rhino mice (Hr^{rh}) is more severe than that of hairless mice (Hr^{hr}), and this is thought to be due to more severe effects of the mutation on *Hr* protein levels. The classical mutation Hr^{hr} is caused by the insertion of a provirus into intron 6 of Hr, resulting in aberrant splicing and significantly reduced expression (Jones et al., 1993). All cloned Hr^{rh} mutations are nonsense mutations that cause nonsense-mediated decay of *Hr* mRNA (Panteleyev et al., 1998b) and virtually complete loss of mRNA.

Rhino alleles of *Hr* are so named because of the excessive skin wrinkling of Hr^{rh} mutants. The wrinkling is due to large utricles and dermal cysts filled with keratins that form in the dermis from the remnants of hair follicle (Mann, 1971; Panteleyev et al., 1998b; Sundberg, 1994; Sundberg and Boggess, 1998). Dermal cysts originate from undifferentiated epithelial cells of the deepest part of the hair follicle with the peripheral cells developing into sebocyte-like cells and outer root sheath cells (Bernerd et al., 1996). The cysts are filled with keratins 5, 14, 6, and 17, and lipids including cholesterol esters, wax esters, and very small amounts of triglycerides, cholesterol and ceramides (Bernerd et al., 1996). As for Hr^{hr}, hair loss coincides with onset of the first postnatal anagen. Nonsense mutations in *Hr* have also been described in human patients with APL, but the excessive skin wrinkling is not present in affected human patients.

Hr^{rhR} arose spontaneously downstream of a translocation experiment, but was not due to a translocation. The male parent was a treated JH male and the female parent was an SB female. SB refers to the F1 hybrid made from SEC/E x C57BL/E. The mutant was outcrossed to BLH F1's for stock maintenance. BLH refers to C3Hf x C57BL10a.

Homozygous mutant mice are normal at birth and display a typical coat until 2-3 weeks after birth, the time at which the first hair cycle initiates. At this point they fail to initiate the first hair cycle and begin to lose their hair. By 5-weeks of age the mice are hairless and have wrinkled skin. Because the phenotype of this mutant is so similar to the known rhino (Hr^{rh}) mice (Howard, 1940; Panteleyev et al., 1998b), we sequenced the *Hr* genomic DNA and found a novel nonsense mutation in exon 12, leading to a premature stop codon. Here we report the cloning of this rhino allele of *Hr*, detailed histological and molecular characterization of the phenotype.

Results

Phenotype

The Hr^{rhR} mutant mice arose spontaneously in Oak Ridge National Lab. It was maintained in the ORNL mouse facility by mating Hr^{rhR}/Hr^{rhR} male with $Hr^{rhR}/+$ female with an inbred mixed strain background. Both genders of mutant mice appear to be fertile and viable, but the females have difficulty in nursing pups, likely due to skin lesions that develop due to thin skin. Hr^{rhR}/Hr^{rhR} mice were distinguishable from $Hr^{rhR}/+$ or +/+ as early as 2 weeks of age due to hair loss. $Hr^{rhR}/+$ mice are phenotypically normal. As the Hr^{rhR}/Hr^{rhR} mice age, they become almost completely nude and their skin becomes excessively wrinkled in a fashion similar to other Hr^{rh} alleles (Ahmad et al., 1998c; Ahmad et al., 1998d; Brancaz et al., 2004; Garcia-Atares et al., 1998; Panteleyev et al., 1998a; San Jose et al., 2001; Sundberg and Boggess, 1998) (Figure 6-1 A). One difference is that hair loss in Hr^{rhR}/Hr^{rhR} mice begins in a random manner across the body, while other *Hr* mutants lose hair in a head-to-tail manner (Panteleyev et al., 1998b). The hair on the snout, head, and both ears is the last to be lost (Figure 6-1 B), likely due to the slower cycling of follicles in these areas. The Hr^{rhR}/Hr^{rhR} mutant mice still have the vibrissae even after they are hairless. The homozygotes have longer nails compared to the heterozygotes by 4 weeks of age and become more significant with age (data not shown). Thymuses in the homozygotes are much smaller compared to those in the heterozygotes, suggesting thymic abnormalities related to the mutation.

Figure 6-1 Photos of Hr^{rhR}/Hr^{rhR} mice. (A) 6-month old Hr^{rhR}/Hr^{rhR}; (B) 5-week old Hr^{rhR}/Hr^{rhR}.

Novel nonsense mutation

The phenotype of Hr^{rhR}/Hr^{rhR} mutant mice is extremely similar to other rhino mice (Hr^{rh}/Hr^{rh}). Therefore, we began by sequencing the genomic region of *Hr* using direct sequencing of PCR products amplified using primer pairs that spanned the genomic DNA (Table 3-1). Genomic DNA was extracted from tail snips. Primers were designed to amplify overlapping fragments of about 700-900 bp in length. PCR products were separated through 1% agarose gel electrophoresis and purified with GFX columns. Sequences were extracted from raw chromatograms using Chromas software and compared to the published *Hr* sequence using BLAST (NCBI). Using this strategy, we found a base pair change from C to T in position 3134 of *Hr* mRNA (NM_021877) in the homozygous mutant mice (Figure 6-2). This change occurred in exon 12 of *Hr* gene leading to the formation of a premature stop codon from arginine 814 (R814X). As expected, heterozygotes showed a mixture of C and T at position 3134. Samples from a total of 100 animals were sequenced to confirm the mutations. Due to its distance from the terminal exon, this mutation is predicted to be degraded through nonsense-mediated decay. The mutation also abolishes a digestion site of restriction enzyme *Cac8I*, which can be used to genotype mice prior to the development of hair loss. A new pair of primers was specially designed to amplify the segment containing the mutation as well as the restriction digestion site of *Cac8I*. The amplified PCR product from wild type mouse was fully digested by *Cac8I* (figure 6-3). It showed two bands with smaller size around 200 bp in the gel electrophoresis. The PCR product from the DNA of the heterozygous mice was partially digested by *Cac8I* and three bands were seen in the gel electrophoresis. Among the three bands, the very top one is the DNA without restriction digestion by *Cac8I*. The two bands in the bottom are digested DNA fragments. The PCR product from the DNA of Hr^{rhR}/Hr^{rhR} mice was not digested by *Cac8I* due to the mutation and only one band was seen at the top of the agarose gel. The results of *Cac8I* restriction digestion were confirmed with DNA sequencing.

Significant reduction of *Hr* expression

Northern blotting was used to determine if the mutant Hr^{rhR} mRNA was degraded due to nonsense-mediated decay. Two different probes were designed, one covering the

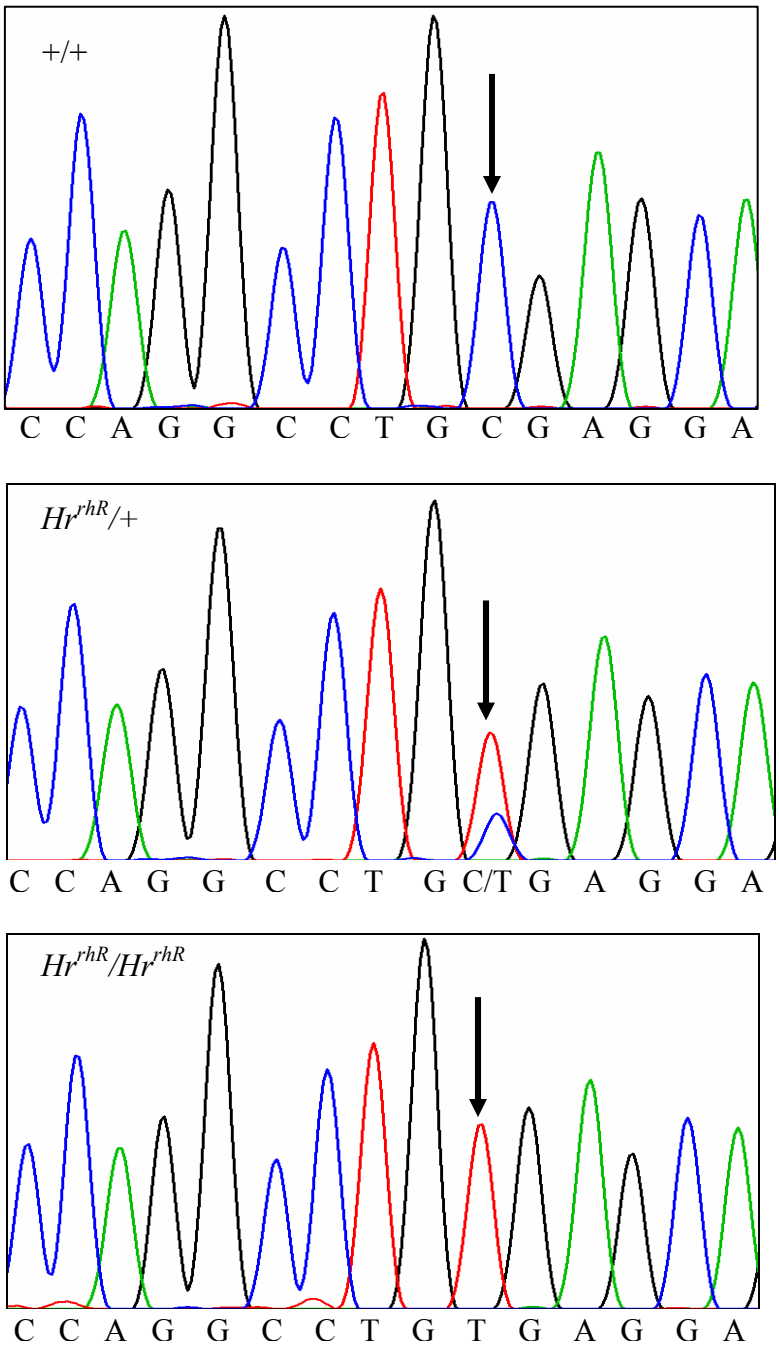

Figure 6-2 Genotyping of wild type (+/+), heterozygous (Hr^{rhR}/+), homozygous (Hr^{rhR}/Hr^{rhR}) mice in exon 12 of *Hr*. Arrows indicate the position of mutation (3134C to T of NM_021877). Wild type mice have a C at position 3134. Heterozygous mice have T/C at this position. Homozygous mice have a T at this position.

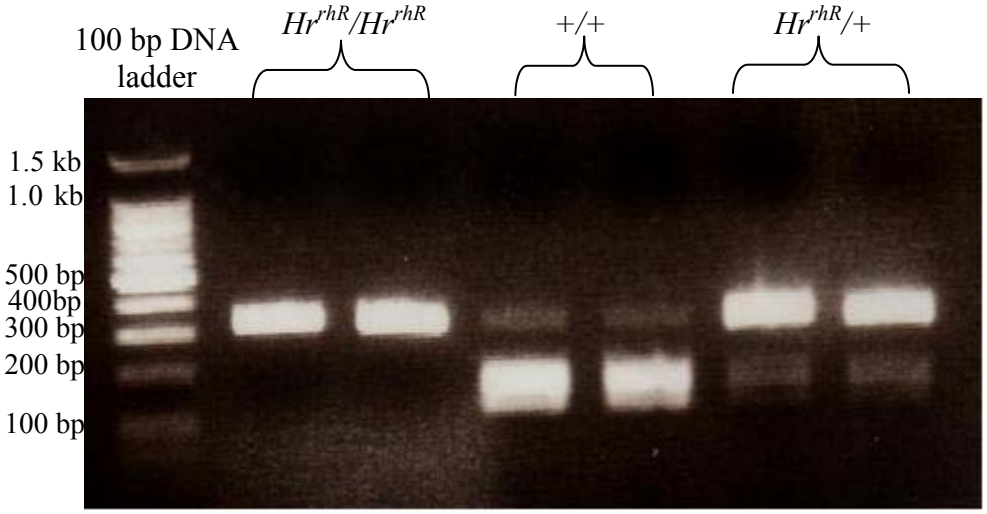

Figure 6-3 The digestion pattern of PCR products from the genomic DNA of Hr^{rhR}/Hr^{rhR}, $Hr^{rhR}/+$, and +/+ mice. The PCR products were amplified with primers called gRHF and gRHR.

exon 12 and containing the mutation site, and the other covering exons 5 to 11. Both probes were amplified through PCR, separated on gel, and purified through GFX columns. Total RNA from dorsal skin of 1, 7, 14, and 35-day old mice was extracted, separated on gels using electrophoresis, transferred overnight to the membranes using capillary effect, and crosslinked to the membranes using UV-light. Probes were randomly labeled with α-^{32}P-CTP and hybridized to membranes at 42°C overnight. Results are shown in figures 6-4 and 6-5. Results with each probe suggest that there is significant loss of *Hr* mRNA in Hr^{rhR}/Hr^{rhR} mutant mice compared to either wild type or $Hr^{rhR}/+$ mice. This significant loss of *Hr* expression was found in homozygous mice at all ages including 1-, 7-, 14-, and 35-day after birth. There is only one major band in each Northern blot, matching to the size of full-length *Hr* mRNA transcript. No other transcripts were found, indicating that no alternatively spliced transcripts correspond to these two probes. Splicing might occur in other regions of *Hr* gene not represented by these probes, such as 3' end. There is a very strong signal of *Hr* expression in 14 days after birth, consistent with its known expression pattern. Hr^{rhR}/Hr^{rhR} mutant mice exhibit much more prominent wrinkling phenotype than hairless mice (Hr^{hr}/Hr^{hr}) or rhino mice (Hr^{rh}/Hr^{rh}). The phenotype is very similar to the one in rhino-Yurlovo (Hr^{rhY}/Hr^{rhY}) (Panteleyev et al., 1998a) and the null mutant (Hr^{tm1Cct}/Hr^{tm1Cct}) (Zarach et al., 2004). This might suggest that the severe skin-wrinkling phenotype in Hr^{rhR}/Hr^{rhR} mutant mice is due to significant or complete loss of *Hr* expression.

Utricle and dermal cysts formation

It was reported previously that formation of utricles at postnatal day 12 was the first morphological change in $Hr^{-/-}$ mice (Zarach et al., 2004). A detailed histological analysis with a series of different ages of mice from postnatal day 1 to 35 was performed to identify the first recognizable change in Hr^{rhR}/Hr^{rhR} mutants. The development of hair follicles in Hr^{rhR}/Hr^{rhR} mice is normal compared to wild type at postnatal days 1 and day 7 (Figure 6-6) and overall follicle structure is normal. There is no difference in the thickness of epidermis or the number of hair follicles in the skin between Hr^{rhR}/Hr^{rhR} and $Hr^{rhR}/+$ mice. By postnatal day 10, however, the infundibulum near the top of the piliary canal become wider and contains increased keratinized material (Figure 6-7), ultimately

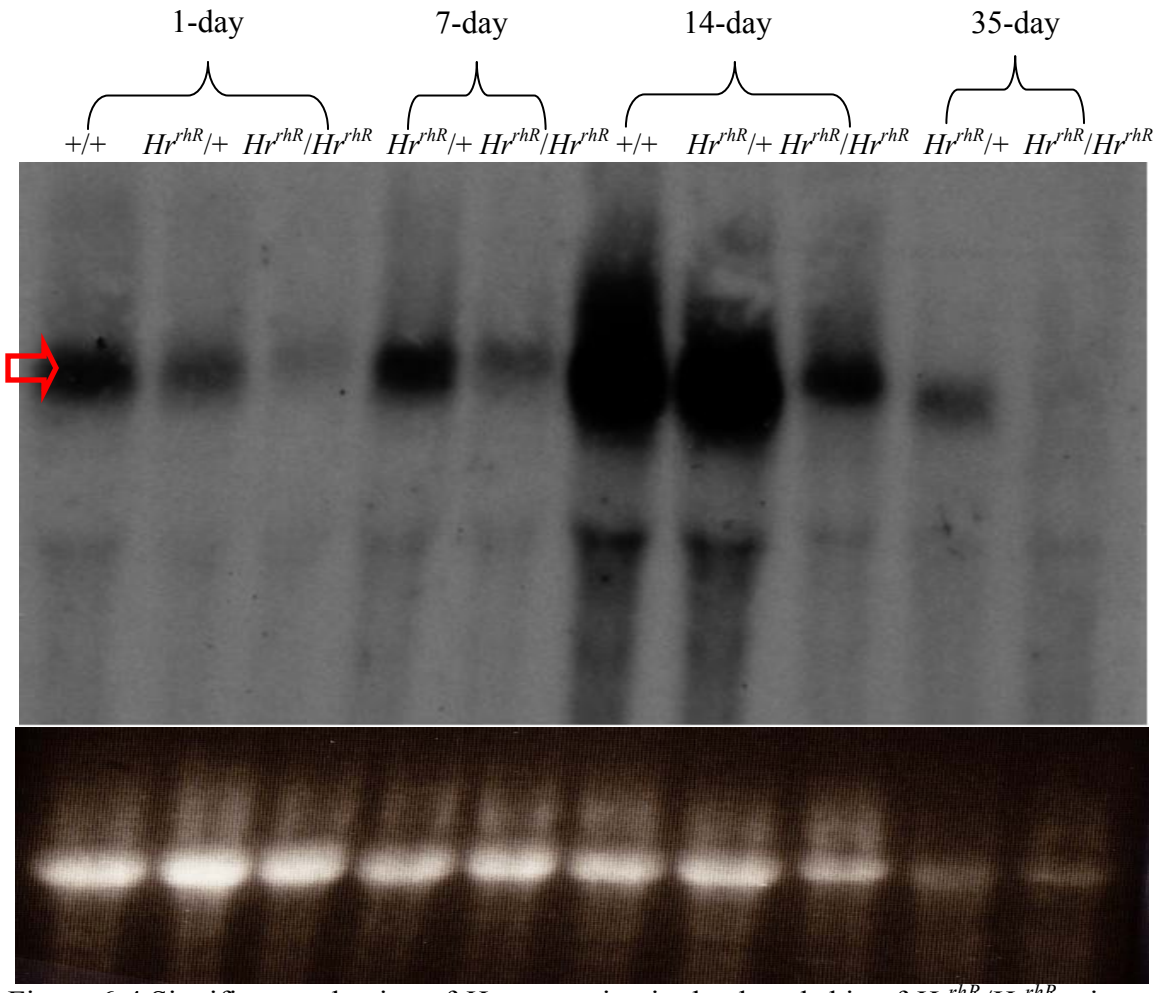

Figure 6-4 Significant reduction of *Hr* expression in the dorsal skin of Hr^{rhR}/Hr^{rhR} mice (1). The total RNA was extracted from the dorsal skin of each genotype at different ages (1, 7, 14, 35 days after birth). 20 μg of the total RNA was loaded on each lane. The probe was amplified with PCR covering exon 12 containing the mutation. The probe was randomly labeled with α-^{32}P-CTP and blot to the membrane overnight at 42°C. The red block arrow indicates the position for full-length *hairless* mRNA. The bottom panel shows the intensity of 28S band from the gel.

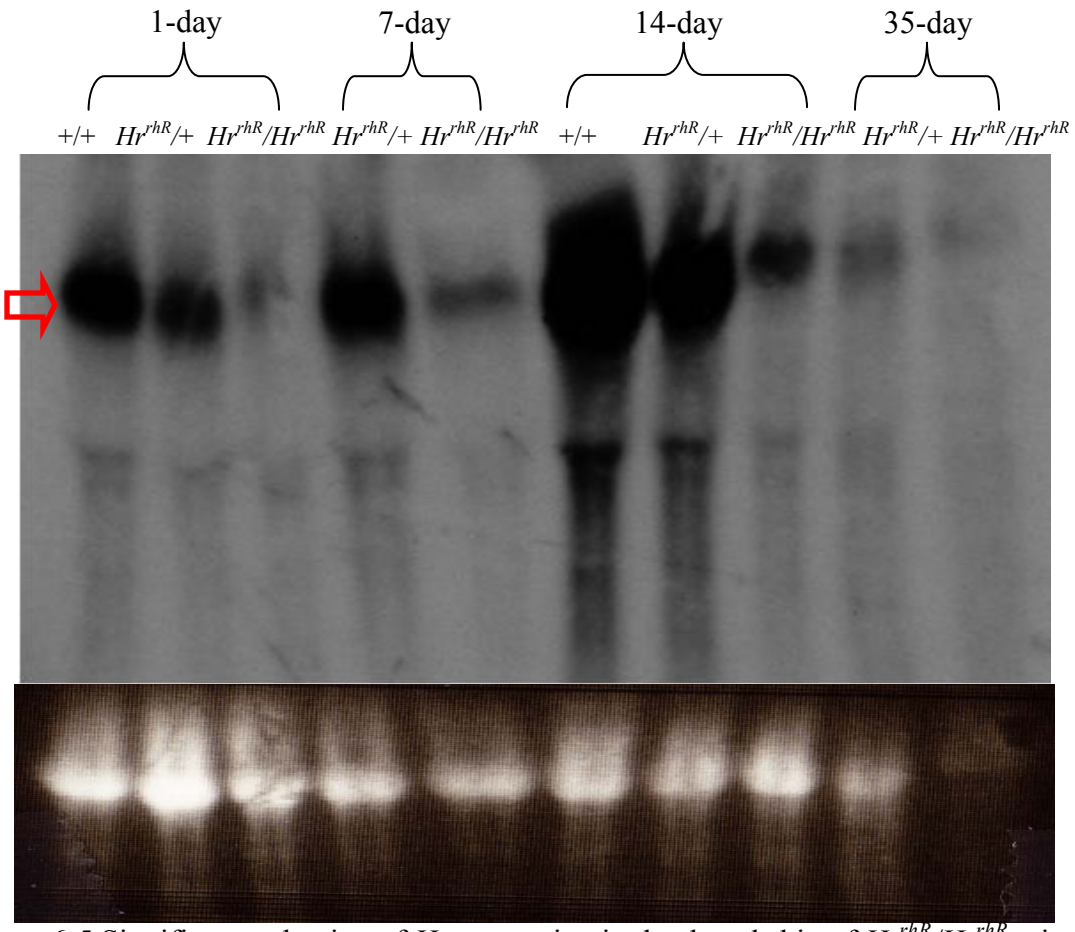

Figure 6-5 Significant reduction of *Hr* expression in the dorsal skin of Hr^{rhR}/Hr^{rhR} mice (2). The total RNA was extracted from the dorsal skin of each genotype at different ages (1, 7, 14, and 35 days after birth). Twenty μg of the total RNA was loaded on each lane. The probe was amplified with PCR covering exon 5 to exon 11. The probe was randomly labeled with α-^{32}P-CTP and blot to the membrane overnight at 42°C. The red block arrow indicates the position for full-length *hairless* mRNA. The bottom panel shows the intensity of 28S band from the gel.

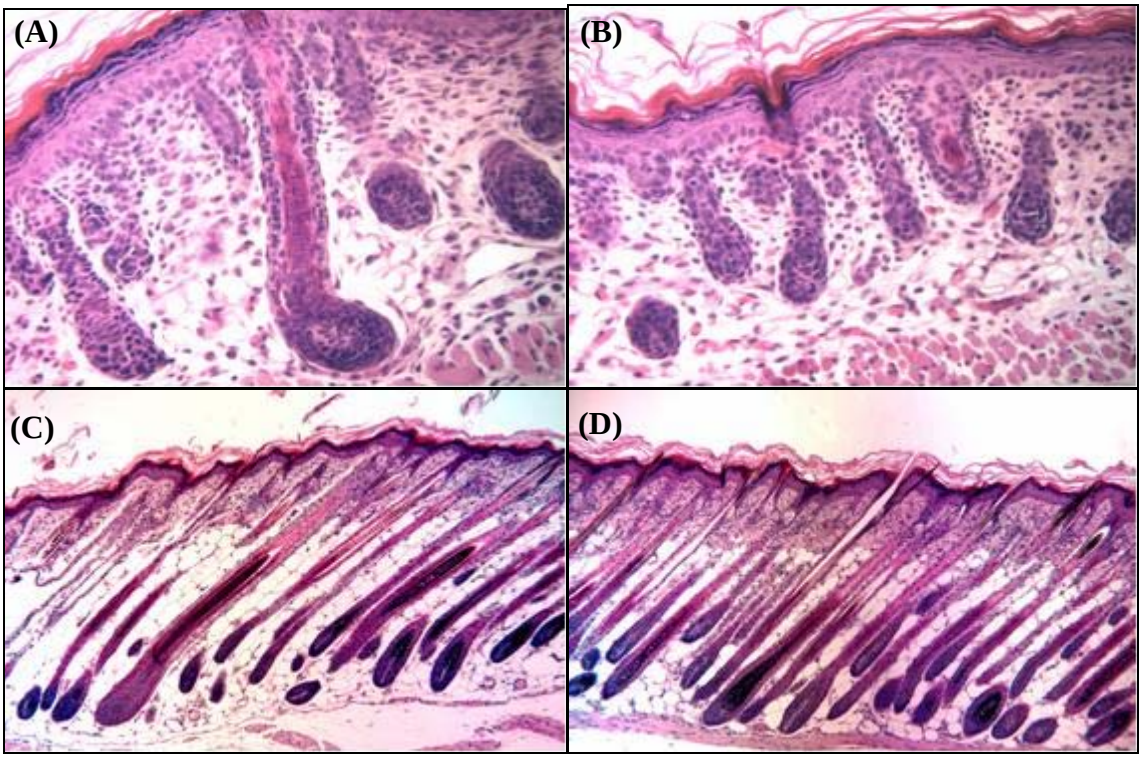

Figure 6-6 Histology of the dorsal skin from *Hr*^{rhR}/+ and *Hr*^{rhR}/*Hr*^{rhR} mice at 1 and 7 days of age. (A) Histology of the dorsal skin of 1-day old *Hr*^{rhR}/+ mouse; (B) Histology of the dorsal skin of 1-day old *Hr*^{rhR}/*Hr*^{rhR} mouse; (C) Histology of the dorsal skin of 7-day old *Hr*^{rhR}/+ mouse; (D) Histology of the dorsal skin of 7-day old *Hr*^{rhR}/*Hr*^{rhR} mouse.

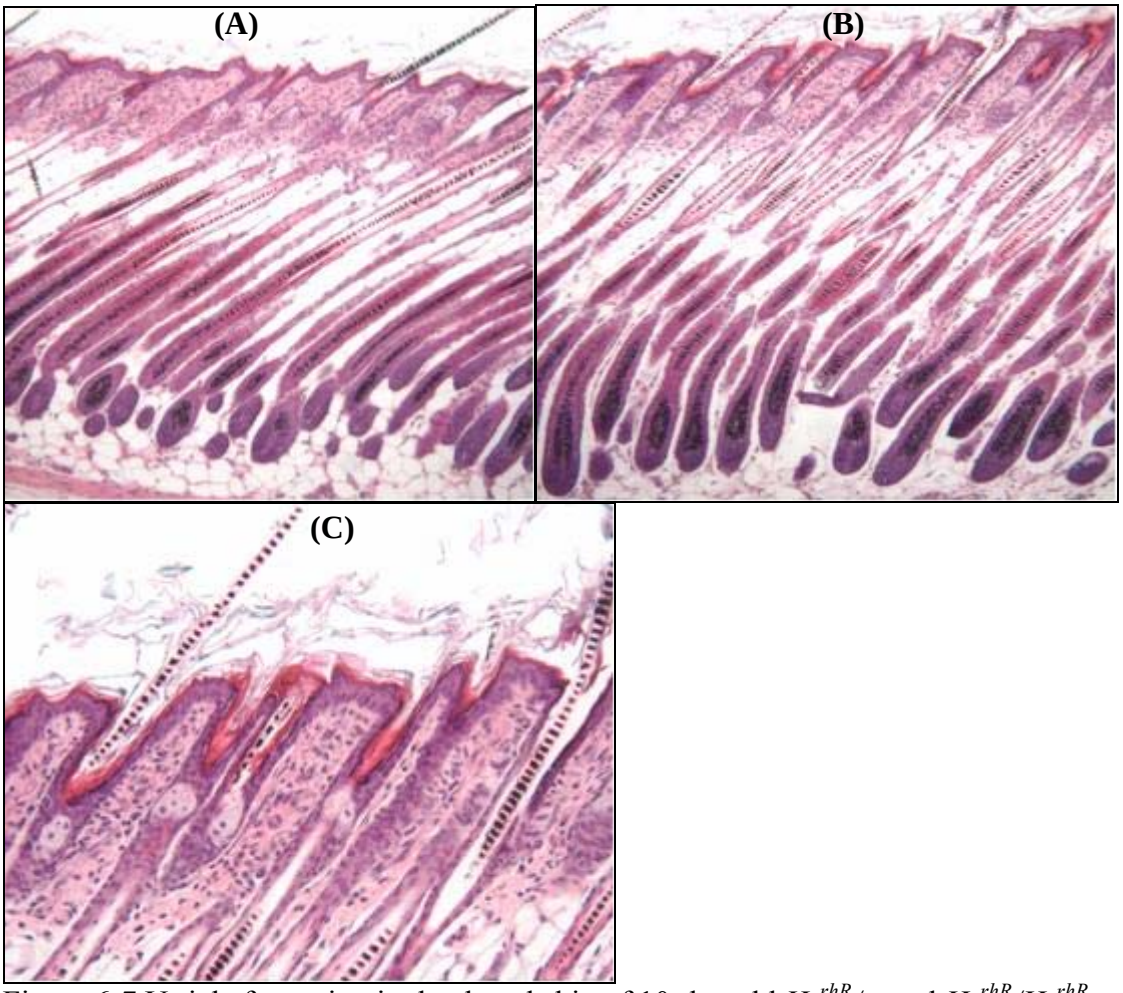

Figure 6-7 Utricle formation in the dorsal skin of 10-day old Hr^{rhR}/+ and Hr^{rhR}/Hr^{rhR} mice. (A) Histology of the dorsal skin of 10-day old Hr^{rhR}/+ mice; (B) Histology of the dorsal skin of 10-day old Hr^{rhR}/Hr^{rhR} mice; (C) Higher magnification of a local area from panel B.

leading to utricle formation in the Hr^{rhR}/Hr^{rhR} mutants. Other parts of the hair follicles in mutant mice are relatively normal compared to the heterozygous mice. These changes become more prominent by postnatal day 14 (figure 6-8) with the increase widening of the infundibulum in Hr^{rhR}/Hr^{rhR} mice. Cross sections also showed the formation of utricles. At postnatal day 18 (figure 6-9), the utricle formation is present in all the hair follicles in Hr^{rhR}/Hr^{rhR} mice, but none in $Hr^{rhR}/+$ mice. The amount of keratinized materials filling in the utricles increases progressively. The utricle formation encompasses the entire area distal to the sebaceous glands. By 3 weeks of age, the entire hair follicle becomes keratinized (figure 6-10 B). Hair follicles in Hr^{rhR}/Hr^{rhR} mice lose their connections with the dermal papilla, but no such change is seen in $Hr^{rhR}/+$ mice. Dermal cysts begin to form at this stage. By the age of 5-weeks, several layers of huge dermal cysts are formed and all hair follicles are disintegrated (figure 6-10 D). The dermal cysts are filled with a large amount of cornified materials. During the preparation of histological slides, a lot of white materials, which are cornified materials, fell out from the tissue. The size of the dermal cysts increases as the mice age, which causes progressive wrinkling of the skin.

Microarray analysis

Little is known about the molecular basis of the morphological changes in Hr^{rhR}/Hr^{rhR} mutant mice. To identify the genes with altered expression in skin of Hr^{rhR}/Hr^{rhR} mutant mice, we used microarray experiments to profile expression in the skin of 7-day, 10-day, and 5-week old mice. We used these early ages to precede (7-day) and coincide with (10-day) the appearance of the phenotype. Gene expression changes in 7-day old mice might suggest the earliest initial molecular events due to the Hr^{rhR} mutation. Differential expression at 10 days might provide the molecular basis related to formation of utricles, while the analysis with 5-week old mice might provide the molecular basis related with hair loss and the formation of dermal cysts.

Totally 10 mice (5 $Hr^{rhR}/+$ and 5 Hr^{rhR}/Hr^{rhR}) from one litter and 3 mice (1 $Hr^{rhR}/+$ and 2 Hr^{rhR}/Hr^{rhR}) from another litter were used for the microarray analyses at 7 days of age. Microarray analysis was done with ImaGene and GeneSight from Biodiscovery. No genes showed statistically significant alterations in gene expression.

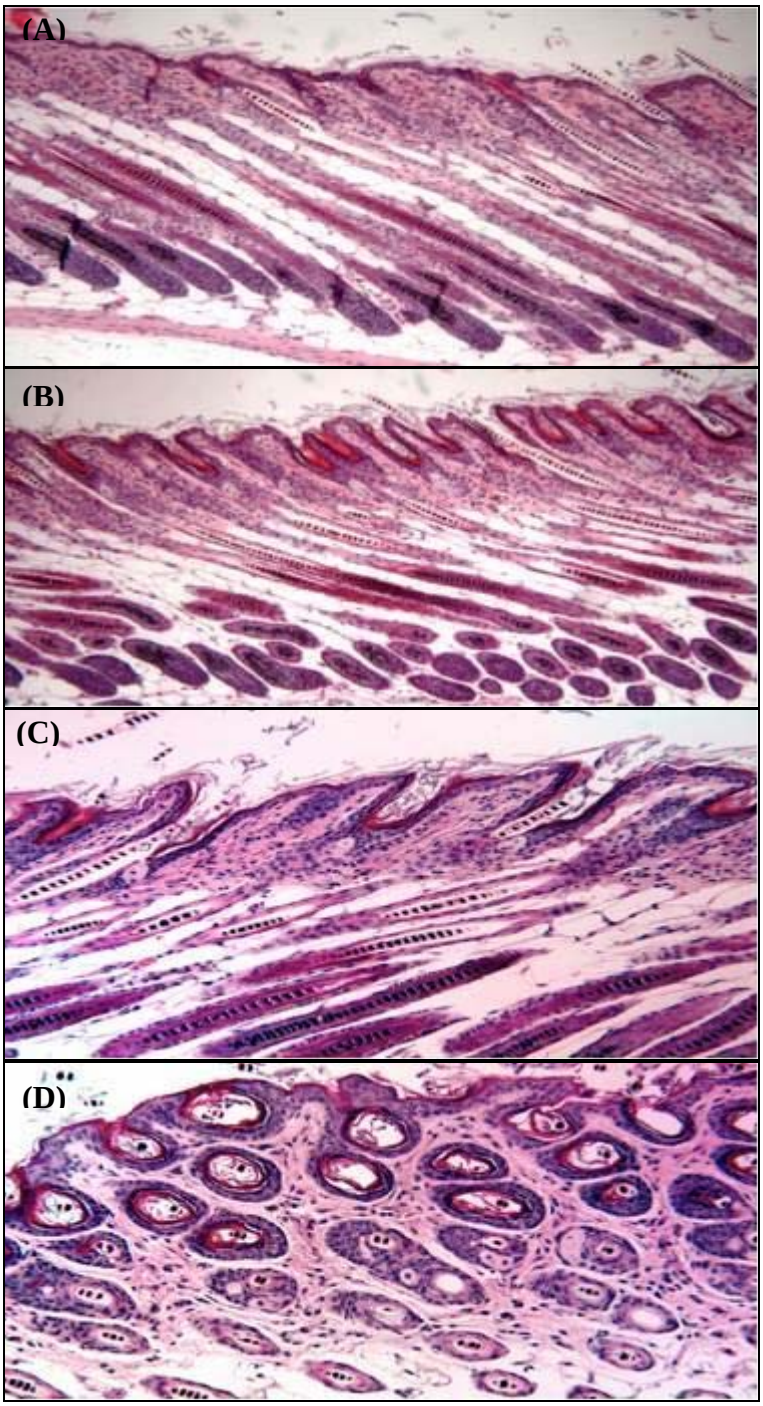

Figure 6-8 Utricle formations in the dorsal skin of 14-day old mice. (A) Histology of the dorsal skin of 14-day old Hr^{rhR}/+ mice; (B) Histology of the dorsal skin of 14-day old Hr^{rhR}/Hr^{rhR} mice; (C) Higher magnification of formed utricle in the skin of Hr^{rhR}/Hr^{rhR} mice; (D) the cross sections of the dorsal skin of 14-day old Hr^{rhR}/Hr^{rhR} mice.

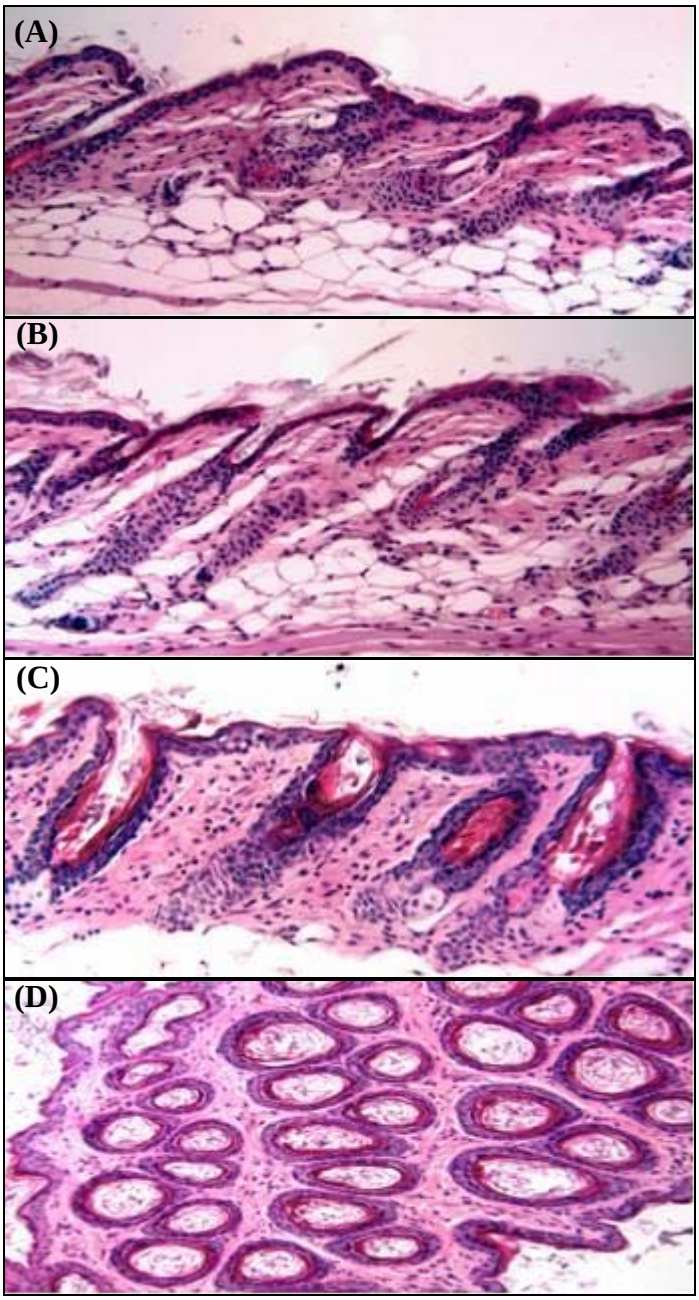

Figure 6-9. Utricle formation in the dorsal skin from 18-day old $Hr^{rhR}/+$ and Hr^{rhR}/Hr^{rhR} mice. (A) and (B) Histology of the dorsal skin from 18-day old $Hr^{rhR}/+$ mice; (C) Histology of the dorsal skin from 18-day old Hr^{rhR}/Hr^{rhR} mice; (D) Histology of the cross sections of the dorsal skin from 18-day old Hr^{rhR}/Hr^{rhR} mice.

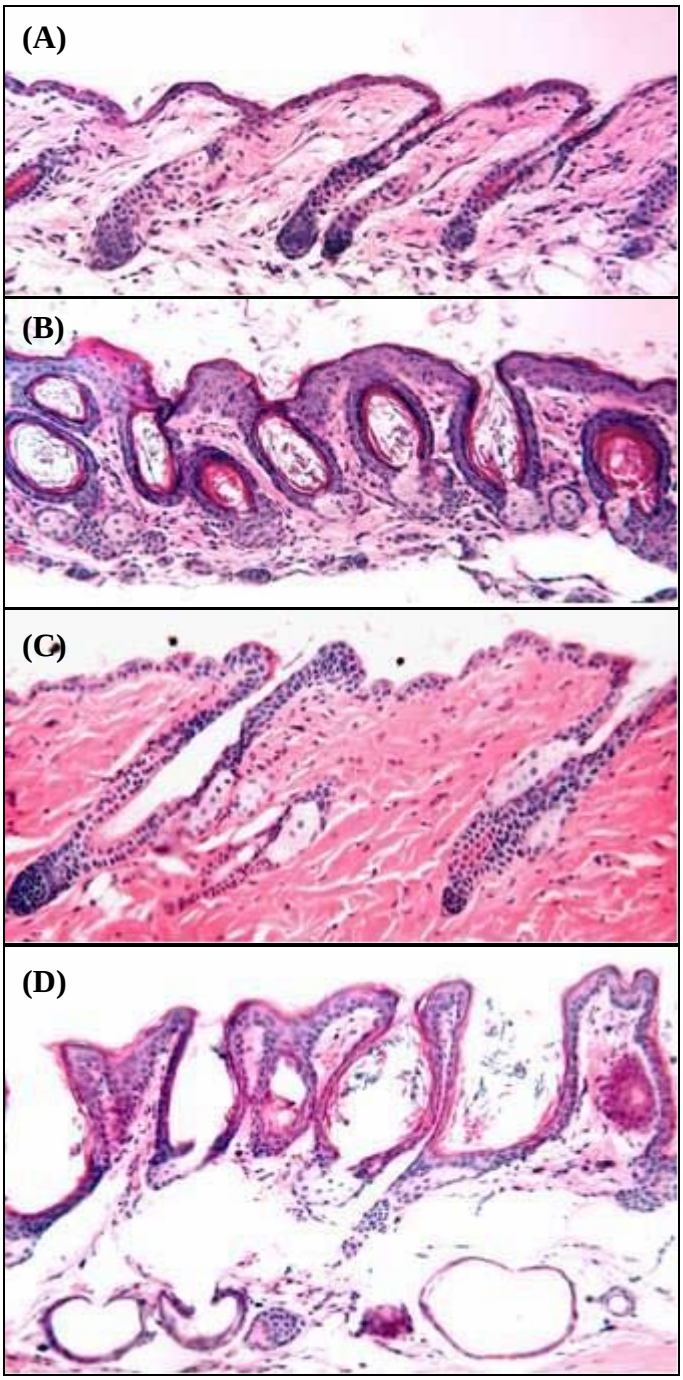

Figure 6-10 Dermal cyst formation in 21- and 35-day old Hr^{rhR}/Hr^{rhR} mice. (A) Histology of the dorsal skin from 21-day old $Hr^{rhR}/+$ mice; (B) Histology of the dorsal skin from 21-day old Hr^{rhR}/Hr^{rhR} mice; (C) Histology of the dorsal skin from 35-day old $Hr^{rhR}/+$ mice; (D) Histology of the dorsal skin from 35-day old Hr^{rhR}/Hr^{rhR} mice.

by using 95% confidence interval and a minimum fold change of 2. This might be due to the limit of the oligolibrary spotted on the array because this oligolibrary does not cover the whole mouse genome. Since there are no significant morphological changes in the skin of 7-day Hr^{rhR}/Hr^{rhR} animals, this reinstates that the phenotype develops between 7 and 10 days of age.

Unlike 7 days, significant changes in gene expression were found at 10 days, the earliest point at which the phenotypic changes were found histologically. These hybridizations used an oligo array format representing ~ 15,000 mouse genes. Six mice containing three $Hr^{rhR}/+$ and three Hr^{rhR}/Hr^{rhR} mice from one litter were used, and hybridizations with each pair of samples were done with dye swaps. All 6 slides generated high quality images. Data were analyzed with ImaGene and GeneSight from BioDiscovery to derive the list of genes with differential expression, using 99% confidence interval and a minimum fold change of 2. Differentially expressed genes were defined as those that were significant in analysis of all 6 hybridizations together and that showed a response in two of three biological replicates. Results are listed in table 6-1.

It is very intriguing to notice that most of the differentially expressed genes in table 6-1 are upregulated at 10-day after birth, which is consistent with the loss of *Hr* function as a transcriptional co-repressor (Zarach et al., 2004). This list of genes was uploaded to DAVID (Dennis et al., 2003) for functional annotation. Several categories were enriched based on the functional annotation as shown in table 6-2. These categories include cell organization and biogenesis, intermediate filament, non-membrane-bound organelle, and coiled coil. The genes in each enriched category were listed in table 6-2. Among the differentially expressed genes, two of them are keratins, *Krt2-1* and *Krt1-10*, both of which show increased expression in Hr^{rhR}/Hr^{rhR} mutants. *Krt 1-10* and *Krt 2-1* are coexpressed in terminally differentiated epidermis and heterodimerize to form intermediate filaments. Their co-upregulation indicates a disturbance of normal keratinocyte differentiation in Hr^{rhR}/Hr^{rhR} mice.

It was also found that a large number of genes related with either immunoglobulin or T cell receptor β chain are upregulated in the skin of 10-day old Hr^{rhR}/Hr^{rhR} mutants comparing to $Hr^{rhR}/+$ mice. These genes are listed in table 6-3. The increased expression

Table 6-1 List of differentially expressed genes from 10-day old Hr^{rhR}/Hr^{rhR} mice. Data was analyzed with ImaGene and GeneSight from BioDiscovery based on the 99% confidence interval and the fold change of 1.5 ($2^{0.6}$).

Gene ID	Gene name	Symbol	fold change
L04961	Xist (X inactive specific transcript)	*Xist*	-2.9
AK013594	RIKEN cDNA 2900024O10 gene		-2.6
NM_010702	Leukocyte cell-derived chemotaxin 2	*Lect2*	-2.4
NM_007740	Procollagen, type IX, alpha 1	*Col9a1*	-2.1
NM_016875	Y box protein 2 (Ybx2)	*Ybx2*	1.9
NM_011043	protocadherin 10	*Pcdh10*	1.9
NM_019402	Poly(A) binding protein, nuclear 1	*Pabpn1*	1.9
NM_013510	Erythrocyte protein band 4.1-like 1	*Epb4.1l1*	1.9
AK011423	Glucosamine (N-acetyl)-6-sulfatase	*Gns*	1.9
AK011425	Solute carrier family 25 (mitochondrial carrier, phosphate carrier), member 24	*Slc25a24*	1.9
L38249	LIM homeobox protein 3	*Lhx3*	1.9
NM_011957	cAMP responsive element binding protein 3-like 1	*Creb3l1*	2.1
V00830	Keratin complex 1, acidic, gene 10	*Krt1-10*	2.1
AK005108	RIKEN cDNA 1500002C15 gene		2.1
AK020189	Zinc finger protein 59 (Zfp59)	*Zfp59*	2.2
AK003656	lipocalin-interacting membrane receptor	*Limr*	2.3
U94828	Regulator of G-protein signaling 16	*Rgs16*	2.3
NM_008473	Keratin complex 2, basic, gene 1	*Krt2-1*	2.3
L04678	Integrin beta 4	*Itgb4*	2.4
AY036887	myeloid/lymphoid or mixed-lineage leukemia 3	*Mll3*	2.4
NM_008952	Pipecolic acid oxidase, mRNA	*Pipox*	2.4
NM_008564	Minichromosome maintenance deficient 2 mitotin (S. cerevisiae)	*Mcm2*	2.6
L76157	proline rich protein with ubiquitin-like domain	*Bat-3*	2.7
NM_021883	Tropomodulin 1 (Tmod1)	*Tmod1*	2.8
NM_018874	Pancreatic lipase related protein 1	*Pnliprp1*	2.9
NM_010552	Interleukin 17	*Il-17*	3.0

Table 6-2 Functional annotations of the differentially expressed genes in 10-day old Hr^{rhR}/Hr^{rhR} mice compared with $Hr^{rhR}/+$ mice. Enriched categories including the genes in each category was shown below. The analysis was done with DAVID from NIH.

Enriched Category Name	Enriched Genes
Cell organization and biogenesis	*Krt1-10, Krt2-1, Mcm2, Tmod1, Mll3, Pipox, Epb4.1l1*
Structural molecular activity	*Krt1-10, Krt2-1, Epb4.1l1, Col9a1*
Non-membrane-bound organelle	*Krt1-10, Krt2-1, Mcm2, Tmod1, Xist, Epb4.1l1*
Coiled-coil	*Krt1-10, Krt2-1, Mll3, Pabpn1*
mRNA binding	*Pabpn1, Ybx2*

Table 6-3 List of differentially expressed genes related with immune functions in 10-day Hr^{rhR}/Hr^{rhR} mice compared with $Hr^{rhR}/+$ mice. Microarray analysis was done with ImaGene and GeneSight softwares from BioDiscovery based on the 99% confidence interval and the fold change of 1.5 ($2^{0.6}$).

Gene ID	Gene name	fold change
Z12394	rearranged T-cell receptor beta chain Vbeta5 repertoire (VDJ)	2.5
Z12416	rearranged T-cell receptor beta chain Vbeta5 repertoire (VDJ)	2.2
Z12426	rearranged T-cell receptor beta chain Vbeta5 repertoire (VDJ)	1.9
Z12446	rearranged T-cell receptor beta chain Vbeta5 repertoire (VDJ)	2.5
Z12457	rearranged T-cell receptor beta chain Vbeta5 repertoire (VDJ)	2.1
Z12461	rearranged T-cell receptor beta chain Vbeta5 repertoire (VDJ)	2.4
Z12497	rearranged T-cell receptor beta chain Vbeta5 repertoire (VDJ)	2.4
Z12498	rearranged T-cell receptor beta chain Vbeta5 repertoire (VDJ)	2.7
Z12499	rearranged T-cell receptor beta chain Vbeta5 repertoire (VDJ)	1.9
Z12545	rearranged T-cell receptor beta chain Vbeta8 repertoire (VDJ)	2.1
Z12571	rearranged T-cell receptor beta chain Vbeta8 repertoire (VDJ)	1.9
Z12184	T-cell receptor beta, variable 13	2.1
Z12273	T-cell receptor beta, variable 13	2.5
Z12280	T-cell receptor beta, variable 13	2.7
U55582	IgG light chain gene, V region	3.8
U21569	Immunoglobulin A heavy chain variable region (IGHV gene), clone WJ17	2.2
U55699	Immunoglobulin kappa light variable region (IgKV gene)	2.1
Y11589	Immunoglobulin lambda chain, mAb 667	3.5
AF041957	infected mouse A seq 9, day 14, T cell receptor beta chain	1.9
AF041896	infected mouse B seq 5, day 7, T cell receptor beta chain	2.2
AF041910	infected mouse C seq 13, day 7, T cell receptor beta chain	2.1
AF041882	Uninfected mouse B seq 9, T cell receptor beta chain	1.9

of these genes is directly or indirectly due to the loss of *Hr* function. It suggests that there might be some significant immunological reactions occurring in the mutant mice. These immune responses might be related with the phenotypes in Hr^{rhR}/Hr^{rhR} mice although the exact functions of these genes in immune system of the skin are still not very clear.

Microarray experiments and data analysis were also applied to the 5-week old Hr^{rhR}/Hr^{rhR} and $Hr^{rhR}/+$ mice. Data were analyzed with ImaGene and GeneSight from BioDiscovery and shown in table 6-4. Most genes were upregulated due to the loss of *Hr* function since *Hr* is suggested to be a transcription co-repressor (Potter et al., 2001). There are four different keratins with differential expressions, including keratin 2-1, keratin 1-15, keratin 2-6a, and type I epidermal keratin. The expression of keratin 1-15 was downregulated while the expression of the other three was upregulated due to the loss of *Hr* function. It was also found that many genes related to immunoglobin and T-cell receptor were differentially expressed in 5-week Hr^{rhR}/Hr^{rhR} mice, which is listed in table 6-5.

The GenBank accession numbers of the differentially expressed genes were uploaded to DAVID 2.1 (http://apps1.niaid.nih.gov/david/) for functional annotation. Among the 138 differentially expressed genes, 119 genes were annotated in DAVID and used for further analysis. About ten different categories were found to be enriched based on the level 5 of gene ontology, including molecular function, biological process, and cellular component (table 6-6). These enriched categories are cytoskeleton, myofibril, intermediate filament cytoskeleton, actin cytoskeleton, cytoskeleton organization and biogenesis, anion transport, angiogenesis, cellular macromolecule catabolism, cysteine-type endopeptidase activity, and striated muscle thin filament. Most of these categories are related with cytoskeleton, which suggests that the loss of *Hr* function directly or indirectly affects the cytoskeleton.

The differentially expressed genes in 5-week old Hr^{rhR}/Hr^{rhR} mice as well as their expression alterations were uploaded to Ingenuity for pathway and network analysis. Figure 6-11 shows one network created from this analysis. Most of the genes in figure 6-11 from our microarray analysis were upregulated. This analysis revealed signaling pathways that are affected in Hr^{rhR}, based on differential expression. Altogether, it was

Table 6-4 List of the differentially expressed genes in 5-week old Hr^{rhR}/Hr^{rhR} mice compared with $Hr^{rhR}/+$ mice. Microarray analysis was done with ImaGene and GeneSight from BioDiscovery based on 99% confidence interval and fold change of 1.6 ($2^{0.7}$).

Gene ID	Gene Name	Fold change
AK002589	0610012D17Rik, RIKEN cDNA 0610012D17 gene	2.5
BC004797	0610040J01Rik, RIKEN cDNA 0610040J01 gene	-2.8
AK005108	1500002C15Rik, RIKEN cDNA 1500002C15 gene	2.5
AK005145	1500004F05Rik, RIKEN cDNA 1500004F05 gene	-2.5
AK006506	1700029K24Rik, RIKEN cDNA 1700029K24 gene	2.5
AK006707	1700047G03Rik, RIKEN cDNA 1700047G03 gene	2.6
AK006816	1700056N10Rik, RIKEN cDNA 1700056N10 gene	2.4
AK018881	1700066C05Rik, RIKEN cDNA 1700066C05 gene	2.4
AK007829	1810048J11Rik, RIKEN cDNA 1810048J11 gene	2.5
AK007938	1810062O18Rik, RIKEN cDNA 1810062O18 gene	-2.3
AK009423	2310020J12Rik, RIKEN cDNA 2310020J12 gene	-2.7
U01139	2610020N02Rik, RIKEN cDNA 2610020N02 gene	2.4
AK019584	4930425K24Rik, RIKEN cDNA 4930425K24 gene	3.2
AK015453	4930453J04Rik, RIKEN cDNA 4930453J04 gene	-2.6
AK016542	4932432N11Rik, RIKEN cDNA 4932432N11 gene	2.7
AK017060	4933434M16Rik, RIKEN cDNA 4933434M16 gene	2.4
AK017381	5430432M24Rik, RIKEN cDNA 5430432M24 gene	2.3
AK020414	9430013L17Rik, RIKEN cDNA 9430013L17 gene	2.6
AK020947	A930040O22Rik, RIKEN cDNA A930040O22 gene	4.0
NM_011062	3-phosphoinositide dependent protein kinase-1 (Pdpk1)	-2.3
NM_020561	acid sphingomyelinase-like phosphodiesterase 3a (ASML3)	2.7
NM_009672	acidic nuclear phosphoprotein 32 (Anp32)	-2.8
AK014322	AF4/FMR2 family, member 3 (Aff3)	2.7
NM_007504	ATPase, Ca++ transporting, cardiac muscle, fast twitch 1 (Atp2a1)	-2.2
Z83816	axonemal dynein heavy chain (partial, ID mdhc8).	3.3
NM_026602	Breast carcinoma amplified sequence 2 (Bcas2)	3.8
U80888	CAG trinucleotide repeat mRNA	-2.4
NM_020036	calmodulin 4 (Calm4)	3.4

Table 6-4 Continued

Gene ID	Gene Name	Fold change
AK014694	camello-like 3 (Cml3)	-3.2
AB070894	clipin E/coronin 6 type A	-2.6
NM_007779	colony stimulating factor 1 receptor (Csf1r)	-2.2
NM_007710	creatine kinase, muscle (Ckmm)	-2.2
NM_007793	cystatin B (Cstb)	2.9
AK003744	Cystatin E/M (Cst6)	4.4
NM_007830	diazepam binding inhibitor (Dbi)	2.2
AK004912	dual specificity phosphatase 23 (Dusp23)	2.3
AK021364	E130101E03Rik, RIKEN cDNA E130101E03 gene	2.4
AF277093	Elovl4 mRNA, complete cds.	4.2
M14721	epidermal profilaggrin	3
NM_010634	fatty acid binding protein 5, epidermal (Fabp5)	8.3
NM_010211	four and a half LIM domains 1 (Fhl1)	2.4
NM_019516	galectin-related inhibitor of proliferation (Grip1)	-2.3
NM_010354	gelsolin (Gsn)	-2.2
NM_008130	GLI-Kruppel family member GLI3 (Gli3)	3.1
NM_008131	glutamine synthetase (Glns)	2.2
AK012496	Hsdl1, hydroxysteroid dehydrogenase like 1	2.5
AK004007	hypothetical Aspartyl protease, retroviral-type family profile/Peptidase aspartic, active site containing protein	3
U96693	immunoglobulin-like receptor PIRB5 (6M1)	-2.2
NM_010552	interleukin 17 (Il17)	4.1
NM_008469	keratin complex 1, acidic, gene 15 (Krt1-15)	-2.8
NM_008473	Keratin complex 2, basic, gene 1 (Krt2-1)	4.8
NM_008476	keratin complex 2, gene 6a (Krt2-6a)	2.3
NM_010715	ligase I, DNA, ATP-dependent (Lig1)	-2.3
AK003656	Limb region 1 like (Lmbr1l)	3.8
AF251268	Low affinity sodium-glucose cotransporter (Slc5a4b)	-2.5
NM_025349	LSM7 homolog, U6 small nuclear RNA associated (S. cerevisiae)	-2.3
M16355	major urinary protein I (MUP I)	-2.7
M16360	major urinary protein V (MUP V)	-2.2
NM_011847	mammalian relative of DnaJ (Dnajb6)	2.4

Table 6-4 Continued

Gene ID	Gene Name	Fold change
NM_008613	meiosis-specific nuclear structural protein 1 (Mns1)	2.5
NM_008564	minichromosome maintenance deficient 2 (S. cerevisiae) (Mcm2)	4.6
BC013625	NOL1/NOP2/Sun domain family 2 (Nsun2)	3.1
AF332077	Parathyroid hormone receptor 2 (Pthr2)	2.2
NM_008987	pentaxin related gene (Ptx3)	2.4
M12289	Perinatal skeletal myosin heavy chain mRNA, 3' end.	-2.5
NM_008952	peroxisomal sarcosine oxidase (Pso)	3.8
NM_011078	PHD finger protein 2 (Phf2)	-2.4
NM_011182	pleckstrin homology, Sec7 and coiled/coil domains 3 (Pscd3)	2.9
AK011193	Plexin A1 (plxna1)	2.6
NM_019402	poly(A) binding protein, nuclear 1 (Pabpn1)	3.3
NM_007552	Polycomb group ring finger 4 (Pcgf4)	2.2
NM_007743	procollagen, type I, alpha 2 (Cola2)	-2.3
NM_031163	procollagen, type II, alpha 1 (Col2a1)	-2.2
D17546	Procollagen, type XVIII, alpha 1 (Col18a1)	3.6
AF316872	PTEN induced putative kinase 1 (Pink1)	2.3
AK003705	putative weakly similar to skin-specific protein	3.1
U94828	regulator of G-protein signaling 16 (Rgs16)	4.5
NM_011289	ribosomal protein L27 (Rpl27)	2.5
NM_026811	RIKEN cDNA 1110031B11 gene (1110031B11Rik)	7.5
NM_026394	RIKEN cDNA 1110055J05 gene (1110055J05Rik)	4.6
NM_027205	RIKEN cDNA 1600015I10 gene (1600015I10Rik)	2.2
NM_027137	RIKEN cDNA 2310037L11 gene (2310037L11Rik)	3.7
NM_029667	RIKEN cDNA 2310069N01 gene (2310069N01Rik)	4.9
NM_027622	RIKEN cDNA 4921530G04 gene (4921530G04Rik)	-2.5
AK011583	RIKEN clone 2610028E01	-2.2
AK006757	ring finger and FYVE like domain containing protein (Rffl)	-2.3
AK020481	RNA binding motif protein 12 (Rbm12)	3.5
X03766	sceletal muscle alpha-actin (pAM 91; AA 40-375)	-3.2
NM_011408	schlafen 2 (Slfn2), mRNA.	-3.2
AK017710	Similar to basic proline-rich protein	2.9

Table 6-4 Continued

Gene ID	Gene Name	Fold change
AK002609	sirtuin 5 (silent mating type information regulation 2 homolog) (S. cerevisiae),	3.4
NM_013670	small nuclear ribonucleoprotein N (Snrpn)	2.9
NM_028625	Small proline rich-like 2 (Sprrl2)	4.7
NM_025984	Small proline rich-like 3 (Sprrl3)	2.7
NM_026822	Small proline rich-like 5 (Sprrl5)	2.4
AK011425	solute carrier family 25 (mitochondrial carrier, phosphate carrier), member 24 (Slc25a24)	7.6
AY032863	solute carrier family 26, member 6	2.3
NM_009216	somatostatin receptor 1 (Smstr1)	3.6
AF407332	sperm ion channel	-2.3
NM_009261	spermatid perinuclear RNA-binding protein (Spnr)	3.1
M92417	Stefin A1 (Stfa1)	7.8
M92419	stefin A3 (Stfa3)	22.1
AF124299	Stratum corneum chymotryptic enzyme	2.7
NM_009359	testis expressed gene 9 (Tex9)	3.9
AK003152	Titin (Ttn)	-2.3
NM_009369	transforming growth factor, beta induced, 68 kDa (Tgfbi)	-2.5
BC013497	transmembrane protein 66 (Tmem66)	2.3
NM_009394	troponin C, fast skeletal (Tncs)	-2.6
NM_011620	troponin T3, skeletal, fast (Tnnt3)	-2.7
J02644	type I epidermal keratin	2.9
AK013783	Ubiquitin specific protease homolog [Homo sapiens]	-2.6

Table 6-5 List of differentially expressed genes related with immune functions in 5-week Hr^{rhR}/Hr^{rhR} mice compared with $Hr^{rhR}/+$ mice. Microarray analysis was done with ImaGene and GeneSight softwares from BioDiscovery.

Gene ID	Gene Name	Fold change
AF151729	clone 7 T-cell receptor alpha chain	2.3
M59956	Ig active kappa chain mRNA V-J region, partial cds.	2.8
AF041927	infected mouse A seq 11, day 10, T cell receptor beta chain	2.8
AF041896	infected mouse B seq 5, day 7, T cell receptor beta chain	2.5
AF041907	infected mouse C seq 10, day 7, T cell receptor beta chain.	2.8
AF041910	infected mouse C seq 13, day 7, T cell receptor beta chain	4.0
Y11589	mRNA for antibody light chain, clone library pYBM-AL6.	2.8
Z12528	Rearranged T-cell receptor beta chain Vbeta5 repertoire (VDJ)	3.5
Z12473	Rearranged T-cell receptor beta chain Vbeta5 repertoire (VDJ).	4.3
Z12427	Rearranged T-cell receptor beta chain Vbeta5 repertoire (VDJ).	3.3
Z12472	rearranged T-cell receptor beta chain Vbeta5 repertoire (VDJ).	2.7
Z12498	rearranged T-cell receptor beta chain Vbeta5 repertoire (VDJ).	2.5
Z12184	rearranged T-cell receptor beta chain Vbeta5 repertoire (VDJ).	2.9
Z12497	rearranged T-cell receptor beta chain Vbeta5 repertoire (VDJ).	2.8
Z12416	rearranged T-cell receptor beta chain Vbeta5 repertoire (VDJ).	2.7
Z12416	rearranged T-cell receptor beta chain Vbeta5 repertoire (VDJ).	2.7
Z12461	rearranged T-cell receptor beta chain Vbeta5 repertoire (VDJ).	2.5
Z12555	Rearranged T-cell receptor beta chain Vbeta8 repertoire (VDJ)	3.6
Z12581	rearranged T-cell receptor beta chain Vbeta8 repertoire (VDJ)	3.0
Z12580	Rearranged T-cell receptor beta chain Vbeta8 repertoire (VDJ).	3.1
Z12545	rearranged T-cell receptor beta chain Vbeta8 repertoire (VDJ).	2.4
Z12254	rearranged T-cell receptor beta chain Vbeta8 repertoire (VDJ).	2.2
X61756	Rearranged T-cell receptor beta variable region (Vb17a).	-2.2
AE008686	T-cell receptor alpha/delta locus section 4 of 4 of the complete region	2.2
M16120	T-cell receptor insulin B-chain reactive beta chain VNDNJC	-2.6

Table 6-6 Enriched categories and the genes in each enriched categories in 5-week old Hr^{rhR}/Hr^{rhR} mice compared with $Hr^{rhR}/+$ mice. The microarray analysis was done with ImaGene and GeneSight from BioDiscovery. The differentially expressed genes were applied to DAVID 2.1 for functional annotation based on gene ontology.

Enriched Categories	Enriched Genes	
CYTOSKELETON	J02644	Type I epidermal keratin
	X03766	actin, alpha 1, skeletal muscle
	AK003744	cystatin E/M
	Z83816	dynein, axonemal, heavy chain 3
	NM_008469	keratin complex 1, acidic, gene 15
	NM_008473	keratin complex 2, basic, gene 1
	NM_008476	keratin complex 2, basic, gene 6a
	NM_008613	meiosis-specific nuclear structural protein 1
	M12289	Myosin, heavy polypeptide 8, skeletal muscle, perinatal
	NM_009261	spermatid perinuclear RNA binding protein
	AK003152, X64700	Titin
	NM_009394	troponin C2, fast
	NM_011620	troponin T3, skeletal, fast
MYOFIBRIL	M12289	Myosin, heavy polypeptide 8, skeletal muscle, perinatal
	AK003152, X64700	Titin
	NM_009394	troponin C2, fast
	NM_011620	troponin T3, skeletal, fast
INTERMEDIATE FILAMENT CYTOSKELETON	J02644	Type I epidermal keratin
	NM_008469	keratin complex 1, acidic, gene 15
	NM_008473	keratin complex 2, basic, gene 1
	NM_008476	keratin complex 2, basic, gene 6a
	NM_008613	meiosis-specific nuclear structural protein 1
ACTIN CYTOSKELETON	X03766	actin, alpha 1, skeletal muscle
	M12289	Myosin, heavy polypeptide 8, skeletal muscle, perinatal
	AK003152, X64700	Titin
	NM_009394	troponin C2, fast
	NM_011620	troponin T3, skeletal, fast

Table 6-6 Continued

Enriched Categories	Enriched Genes	
CYTOSKELETON ORGANIZATION AND BIOGENESIS	X03766	actin, alpha 1, skeletal muscle
	Z83816	dynein, axonemal, heavy chain 3
	NM_008469	keratin complex 1, acidic, gene 15
	NM_008473	keratin complex 2, basic, gene 1
	NM_008476	keratin complex 2, basic, gene 6a
	M12289	myosin, heavy polypeptide 8, skeletal muscle, perinatal
ANION TRANSPORT	NM_007743	procollagen, type I, alpha 2
	NM_031163	procollagen, type II, alpha 1
	D17546	procollagen, type XVIII, alpha 1
	AY032863	solute carrier family 26, member 6
ANGIOGENESIS	U80888	Angiomotin
	AK011583	integrin alpha V
	D17546	procollagen, type XVIII, alpha 1
CELLULAR MACROMOLECULE CATABOLISM	NM_025349	LSM7 homolog, U6 small nuclear RNA associated (S. cerevisiae)
	Z12184, Z12254	RIKEN cDNA 1810049H19 gene
	AK004007	RIKEN cDNA 2300003P22 gene
	AK012496	RIKEN cDNA 2700067E09 gene
	AK006506	enolase 3, beta muscle
	AF124299	kallikrein 7 (chymotryptic, stratum corneum)
	AK003152, X64700	Titin
	AK013783	Ubiquitin specific protease 32
CYSTEINE-TYPE ENDOPEPTIDASE ACTIVITY	AK012496	RIKEN cDNA 2700067E09 gene
	AK003152, X64700	Titin
	AK013783	Ubiquitin specific protease 32
STRIATED MUSCLE THIN FILAMENT	NM_009394	troponin C2, fast
	NM_011620	troponin T3, skeletal, fast

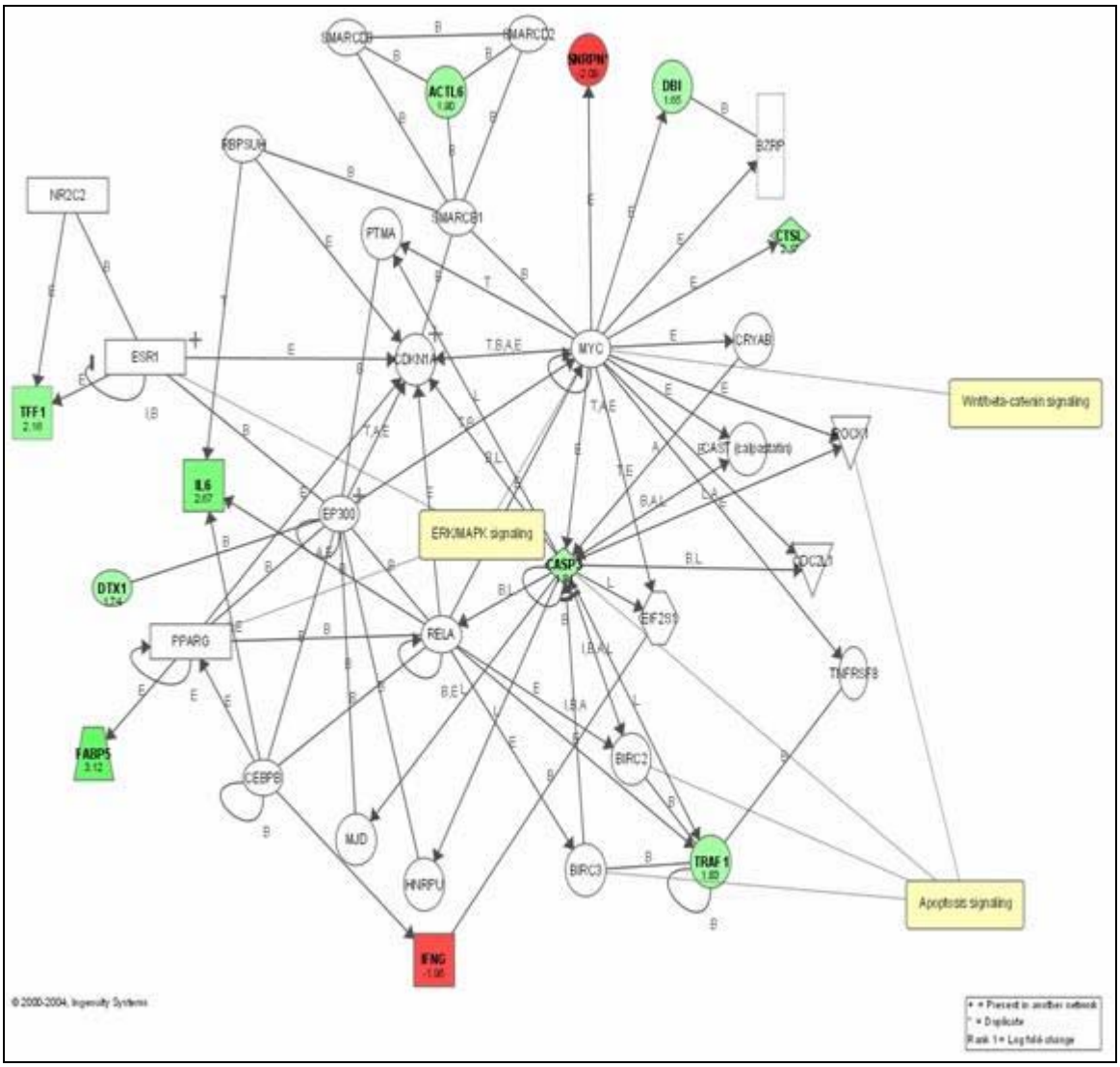

Figure 6-11 Gene networks of the differentially expressed genes from 5-week old Hr^{rhR}/Hr^{rhR} vs. $Hr^{rhR}/+$ mice analyzed with Ingenuity. The microarray analysis was done with ImaGene and GeneSight from BioDiscovery. Red: genes with downregulated expression. Green: genes with upregulated expression.

found that three signaling pathways were affected, including Wnt/β-catenin, apoptosis, and ERK/MAPK signaling pathways. All of these pathways play significant roles in hair follicle development and growth. The alteration of these pathways suggests that the function of *Hr* gene is directly or indirectly related with these signaling pathways.

Discussion

A novel nonsense mutation R814X in exon 12 of *Hr* was successfully identified in rhino-like mice that originated at Oak Ridge National Laboratory. This mutation has been designated as Hr^{rhR} in MGI (Mouse Genome Informatics) (Blake et al., 2003). The mutation has been used to genotype the mutant mice in relation to the rhino-like phenotype, across more than one hundred mice. Homozygous mice always contain the mutation in both chromosomes. Heterozygous mice are always heterozygous for the nonsense mutation, meaning a mixture of a mutated allele and a wild type allele. Wild type mice do not contain any mutations in the same region. Thus, it is confirmed that the Hr^{rhR} mutation is a disease-causing mutation that is responsible for the typical rhino phenotype of rhino-like mutant mice and that Hr^{rhR} is an allele of *Hr*. There are sixteen pathogenic *Hr* mutations (including this mutation) reported to cause the phenotype of hairless or rhino in mice (table 2-2). It indicates that there is a wide spectrum of different *Hr* mutations including nonsense mutations, insertion of a provirus in the introns, and deletions in the exons.

The mutation of Hr^{rhR} is a change of C to T in position of 3134 based on the sequence of *Hr* mRNA (NM_021877), resulting in a nonsense mutation in *Hr*, which should lead to nonsense-mediated mRNA decay (Maquat, 2005). The expression of *Hr* was examined in dorsal skin of mice aged from 1 day to 7, 14, and 35 days by Northern blotting with two probes covering different portions of *Hr* mRNA. *Hr* expression in the dorsal skin of Hr^{rhR}/Hr^{rhR} mice was significantly reduced compared to those in either +/+ or Hr^{rhR}/+ mice at all ages (day 1, 7, 14, and 35). Lack of expression of *Hr* due to *Hr* mutations leads to the complete loss of hair in mice (Cserhalmi-Friedman et al., 2004; Panteleyev et al., 1998b). Decreased expression of *Hr* has been directly linked to the hairless phenotype by topically applying *Hr*-specific catalytic oligonucleotides designed to cleave the mouse *Hr* mRNA to recapitulate the hair phenotype (Cserhalmi-Friedman et

al., 2004). Significantly reduced *Hr* expression in Hr^{rhR}/Hr^{rhR} mice validates the nonsense mutation in *Hr* responsible for the rhino-like phenotype. This novel nonsense mutation was confirmed in more than one hundred mutant mice by direct sequencing of the region containing the mutation. It has been successfully used as a basic tool to genotype the mice before they develop the phenotype of hair loss.

The phenotypic change was seen at as early as 10 days of age with widening of the infundibulum and formation of utricles in the hair follicles, which becomes more severe with age. Dermal cysts were formed by 4 weeks of age and no normal hair follicle structures were observed. The phenotype is very similar to that of $Hr^{-/-}$ mice, which develop utricles at as early as postnatal day 12 (Zarach et al., 2004). The earlier formation of utricles in our mutants suggests a similar severity of the phenotype, including the wrinkling skin. Aged Hr^{rhR}/Hr^{rhR} mutants have skin wrinkling similar in severity to $Hr^{-/-}$ mice, consistent with the extremely low level of *Hr* mRNA in Hr^{rhR}/Hr^{rhR} mutants. However, the pattern of hair loss is random in Hr^{rhR}/Hr^{rhR} mutants, which is different with the pattern in *Hr* knockout mice starting from head.

In order to identify the downstream events of Hr^{rhR} mutation, we applied microarray analysis to study the genes with altered expressions prior to (7-day), coinciding with (10-day), and after (5-week) phenotype development. We did not find genes with statistically significant alteration in expression at 7 days of age. However, many genes were found with statistically significant increased expressions in Hr^{rhR}/Hr^{rhR} mutants, which are consistent with the loss of *Hr* as a transcriptional co-repressor. Many of these differentially expressed genes are linked to hair follicle cycling, including *IL-17*, *Rgs16*, *Krt1-10*, *Krt2-1*, Lipocalin2 (interacting with *Limr*), *Itgb4*, *Mcm2*, *Mll*, and *Crebl1* (Lin et al., 2004). Functional annotation indicates that cell organization, structural molecules, and coiled-coil interactions are significantly altered in skin of 10-day old mutants.

IL-17, a proinflammatory cytokine produced by T cells, plays an important role in activating T cells in allergen-specific T cell-mediated immune responses (Nakae et al., 2002). Its expression characterizes a unique T helper linage that regulates tissue inflammation and the overexpression of *IL-17* in lung causes inflammation (Park et al.,

2005). It is known that many inflammatory cytokines, including *TNF-α*, *IL-1α*, induce drastic morphologic changes and growth arrest of hair follicles in vitro as well as in vivo (Groves et al., 1995; Mahe et al., 1996). This might suggest the involvement of the increased expression of *IL-17* in the development of dermal cysts and hair loss.

Among the differentially expressed genes, *Itgb4* (integrin β4) was upregulated in 10-day mutant mice. *Itgb4* is a glycoprotein associating with α6 integrin to form the α6/β4 complex as a receptor for laminin and plays a critical structural role in the hemidesmosome of epithelial cells. Defects in *Itgb4* cause epidermolysis bullosa letails characterized by mucocutaneous fragility and gastrointestinal atresia (Iacovacci et al., 2003), and long blistering of the skin associated with hair and tooth abnormalities (van der Neut et al., 1999). *Itgb4* was shown to be a signature gene of outer root sheath (Rendl et al., 2005) a region where *Hr* is also expressed (figure 4-11) (Panteleyev et al., 1999). It was shown that hairless phenotype in Hr^{hr}/Hr^{hr} mutant mice is due to the dyscoordination of cell proliferation in distinct hair follicle compartments, malpositioning of the proximal inner root sheath, striking atrophy of outer root sheath and failure of trichilemmal keratinization in the developing club hair (Panteleyev et al., 1999). In catagen stage, the hair bulb and central outer root sheath disintegrate into separate cell clusters in Hr^{hr}/Hr^{hr} mutants, thus disrupting all epithelial contact with the dermal papilla. The altered expression of *Itgb4* might alter the adhesion between center outer root sheath and hair bulb and lead to the formation of utricles and the failure to initiate the first hair cycle in Hr^{rhR}/Hr^{rhR} mutant mice. Therefore, the loss of *Hr* expression in the outer root sheath might induce the expression of *Itgb4* directly and lead to the phenotype of rhino mice, suggesting that *Itgb4* might be a direct target of *Hr* function, which needs to be validated in the future.

Krt2-1 and *Krt1-10*, which are coexpressed in suprabasal terminally differentiating epithelia cells, are both upregulated by about 3 fold in 10-day old Hr^{rhR}/Hr^{rhR} mutant mice. *Krt2-1* and *Krt1-10* are also expressed in the inner root sheath of hair follicles (Botchkarev and Paus, 2003). Mutations in *Krt2-1* or *krt1-10* lead to epidermolytic hyperkeratosis, epidermolysis bullosa simplex, and epidermolytic palmoplantar keratoderma in human patients (Porter et al., 1996). Increased expression of

Krt2-1 and *Krt1-10* suggests increased terminal differentiation in the inner root sheath and might lead to the altered keratinization pattern in skin of Hr^{rhR}/Hr^{rhR} mutants.

Limr, lipocalin-interacting membrane receptor, was upregulated in 10-day old Hr^{rhR}/Hr^{rhR} mutants. Lipocalins are transporters for small hydrophobic molecules, such as lipids, steroid hormones, bilins, and retinoids. The ablation of *RXR* (retinoid X receptor)-α leads to a progressive alopecia after the first pelage and the destruction of hair follicle architecture and the formation of utricles and dermal cysts in adult mice, suggesting that *RXR*α plays a key role in anagen initiation during the hair follicle cycle (Li et al., 2001). In addition, *RXR*α ablation results in epidermal interfollicular hyperplasia with keratinocyte hyperproliferation and aberrant terminal differentiation, accompanied by an inflammatory reaction of the skin (Li et al., 2001). This suggests that the transportation of retinoids might play important roles in hair growth and hair follicle cycles. The increased expression of *Limr* might affect the function of Lipocalin, the transportation of retinoids, thus the hair follicle cycles.

Hr has been found to trigger reactivation of hair growth by repressing a modulator of Wnt signaling, *Wise*, to promote Wnt signaling pathway in *Hr* knockout mice during the initiation of first hair follicle cycle(Beaudoin et al., 2005). In 10-day old mice, loss of *Hr* function did not lead to alteration of *Wise* expression change examined by quantitative real time PCR, suggesting that hair loss in Hr^{rhR}/Hr^{rhR} mutant mice may not be directly due to the expression change of *Wise*, at least in terms of utricle formation. We did find that Wnt signaling pathway was affected in 5-week mutant mice, supporting the possible relationship between *Hr* and Wnt pathway. Regulation of *Wise* gene expression is just one part of *Hr* functions in hair follicle growth and cycles. The relationship between *Hr* and *Wise* signaling may be specific to the stage of the hair cycle, and *Hr* is differentially regulated from anagen to catagen (Beaudoin et al., 2005).

Microarray analysis with 5-week old mutant mice is consistent with the phenotype of hair loss. We found that many genes encoding procollagens, keratins, transcription factors, proteinase, and kinases, were enriched with differential expressions, suggesting their involvement in the Hr^{rhR}/Hr^{rhR} phenotype. Functional annotation of microarray data indicated that categories of cytoskeleton and anion transport are enriched

in 5-week Hr^{rhR}/Hr^{rhR} mutant mice, suggesting that *Hr* is related to the regulation of the genes in these categories. Network analysis suggests that signaling through Wnt/β-catenin, ERK/MAPK, and apoptosis pathways, is altered in Hr^{rhR}/Hr^{rhR}, based on differential expression. Alteration of apoptosis has been confirmed previously in the catagen of hair follicles (Panteleyev et al., 1999) as increased apoptosis in dermal papilla of Hr^{hr}/Hr^{hr} mutant mice. This confirmation strengthens the reliability of our microarray analysis.

We also noticed that many immune-related genes display differential expression in Hr^{rhR}/Hr^{rhR} mutants at both 10 days and 5 weeks of age. We also found that the thymus in Hr^{rhR}/Hr^{rhR} mutants was significantly smaller compared to $Hr^{rhR}/+$ mice at 4-weeks and the difference is more significant as the mice age. Accelerated atrophy of the thymus with age has been reported in both $Hr^{rh\text{-}J}/Hr^{rh\text{-}J}$ and Hr^{rhsl}/Hr^{rhsl} mutants (San Jose et al., 2001; Zhang et al., 2005). Detailed immunohistochemistry analysis of the thymus in $Hr^{rh\text{-}J}/Hr^{rh\text{-}J}$ mutant mice shows relative cortical atrophy, enlargement of blood vessels, proliferation of perivascular connective tissue, and the appearance of cysts (San Jose et al., 2001). *Hr* has been reported to be expressed in thymus, suggesting the possible involvement of *Hr* in T cell development and functions (Cachon-Gonzalez et al., 1994). Skin also contains many macrophages, mast cells, and Langerhan's cells, which are related with immune systems. Atrophy of the thymus in Hr^{rh}/Hr^{rh} mutants may also cause immune changes in skin including hair follicles. Thus, the differential expression of immune-related genes in skin is associated with the loss of *Hr* function.

In summary, we have identified a novel nonsense mutation in murine *Hr* gene, leading to significantly reduced expression of *Hr* probably through nonsense-mediated decay. The phenotype of Hr^{rhR}/Hr^{rhR} mutants is very similar with $Hr^{-/-}$ mice, including extremely low levels of *Hr* expression. Microarray analysis highlighted a gene expression profile that is consistent with the development of hair loss phenotype. In particular, several candidate genes (e.g., *Itgb4*) were highlighted as potential initial downstream events due to the Hr^{rhR} mutation.

Chapter 7 Conclusions and future directions for elucidating the role of *Hr* in hair follicle development and maintenance

Molecular and physiological basis for hair loss in Hr^n mutant mice

Near naked hairless mice (Hr^n) arose spontaneously at Oak Ridge National Laboratory in the 1980s. The mutation was first reported in 1983 by Stelzner (Stelzner, 1983) as an autosomal, semi-dominant allele of the mouse *hairless* gene. Semi-dominance means that the heterozygous mutants have a less severe phenotype compared to the homozygotes. The homozygotes never develop a normal pelage, and heterozygotes have a sparse coat that is severe with age. Since then, no other studies have examined this mutant.

Both the phenotype and the molecular mechanisms involved with the phenotype were characterized systematically. It was found that Hr^n/Hr^n mutants have delayed body growth in terms of both body weight and body length. Vibrissae in Hr^n/Hr^n mutants are much shorter and curly. There are few hairs in Hr^n/Hr^n mutants. Of these few hairs, they have normal overlapping cuticles on the surface of hair shaft, with blunt and irregular ends. Pili multigemini, which means more than two hair shafts coming out of one piliary canal in skin, was found in 5-week and 5-month old $Hr^n/+$ mutants, but not in Hr^n/Hr^n mutants. Histological analysis suggests two alternative mechanisms for this: 1) during early anagen, more than two hair follicles were associated with each other and they shared one piliary canal on the surface of the skin; 2) during early anagen, more than two regions in distinct parts of hair follicles were initiated for keratinocytes proliferation and differentiation to produce hair shafts so that more than one hair shaft grows from one hair follicle.

Histological analysis with dorsal skin suggests that the premature keratinization occurs in the matrix and precortical region of hair follicle in Hr^n/Hr^n mutants after birth. Hyperkeratosis in hair follicles became more severe as the mice age. Hair follicles were completely filled with keratinized materials and the normal structure of hair follicles was totally devastated due to the pre-mature keratinization. Dermal cysts were formed and mineralized in Hr^n/Hr^n mutants. Ki-67 antigen staining suggested an abrupt change around the line of Auber from proliferation to differentiation in the pre-cortex region of

hair follicles in Hr^n/Hr^n mutants. There are also fewer proliferating cells in the matrix and pre-cortical region of hair follicles in Hr^n/Hr^n mutants. Instead of forming a normal hair shaft, a disorganized premature keratinization occurred in the precortex region.

Although the previous research suggested that Hr^n is an allele of *Hr*, no mutations were found within the murine *Hr* locus by genomic sequencing. *Hr* was differentially expressed in Hr^n/Hr^n mutants with increased expression at an early age and reduced expression in adult animals. This might suggest a regulatory mutation in *Hr*. At the same time, many other candidate genes near *Hr* locus and with either high expression in skin or hair follicle/cycle-related functions were sequenced to identify potential mutations. No mutations were found in these candidates. Some microRNAs in the region close to *Hr* locus were also considered for the effort of identifying the mutation although no mutations were found.

The gene expression profile in Hr^n/Hr^n mutants was surveyed with mouse microarray experiments. Microarray analysis was done with 0-, 7-, and 35-day old mice. A set of keratins (Krt) and keratin-associated proteins (Krtap) was found with differential expression in Hr^n/Hr^n mutants compared to +/+ mice. Most of the keratins and keratin-associated proteins, many of which are related with hair shaft formation and growth, were downregulated in Hr^n/Hr^n mutants, which is consistent with the phenotype of hair loss. Keratinization is a time- and space-controlled event in hair follicles. Any disturbance in the expression of Krt and Krtap might interfere with the balance of keratinization control and hair shaft formation. However, the working forces behind the differential expression of Krt and Krtap were not identified since the genetic mutation was not identified. Some other genes were also identified at day 0 after birth from microarray analysis. These genes include *Krt2-6a*, *Sh2-B*, *Smarac2*, *Sprr1b*, and several members of major urinary proteins (*MUP*), and some may play important roles in the development of the near naked phenotype. Microarray analysis showed that many genes normally with low expression in anagen phase displayed increased expression, which is consistent with the hair loss. Microarray analysis with 7-day old mice suggests that members of cytoskeleton, keratin, and extracellular matrix structural components displayed altered expression in the

mutants. Calcium signaling pathway and transcriptional regulation were also significantly altered in the mutant mice due to the mutation.

However, the genetic change of the *Hr*^{n} mutation has not been identified although a great effort of this dissertation research was to sequence DNA and cDNA in search for potential mutations. It suggests that either a regulatory mutation that increases *Hr* expression or an unknown gene mutation regulates the expression of *BMP-4* and affects the expression of down-stream effectors including *Foxn1*, β-catenin, *Hes1*, distinct keratins and keratin-associated proteins. These alterations disturb the balance of proliferation and differentiation in the matrix and precortical region of hair follicle, leading to premature keratinization in these regions and finally the formation of mineralized dermal cyst.

The *Hr*^{n} mutation could be used as a model to study human diseases. Marie Unna hereditary hypotrichosis (MUHH) maps to the same genomic region as *Hr*^{n} (Cichon et al., 2000; Green et al., 2003). Patients with MUHH manifest a similar phenotype as *Hr*^{n} mutant mice. For both models, mutations within the *HR* coding region have been excluded as the cause of the hair phenotype (Cichon et al., 2000; He et al., 2004; Lefevre et al., 2000; van Steensel et al., 1999). It is possible that mutations in a homologous gene underlie these two models, or that they are both due to a regulatory mutation in *Hr*. MUHH has been described as autosomal dominant (Argenziano et al., 1999), while *Hr*^{n} is semi-dominant (Stelzner, 1983). However, given the low incidence of MUHH and the relatively small number of affected individuals within the population, it is possible that this disorder is also semi-dominant and that individuals homozygous for the underlying mutation would display a much more severe phenotype. Characterization of *Hr*^{n} mutation might help to identify the mutation in MUHH patients and to find new ways to improve or cure the hair loss in these patients. Microarray analysis with *Hr*^{n} mutation provides the molecular clues of the phenotype development and helps to improve the understanding of hair growth and hair follicle cycle.

Molecular mechanisms underlying hair loss in *Hr*^{rhR} mutant mice

The mutation in *Hr*^{rhR} mutant mice also arose spontaneously in Oak Ridge National Laboratory, several generations downstream of a translocation experiment. The

mutation is autosomal recessive, and only homozygous mutants have the phenotype of hair loss. Mutants have normal hair follicle morphogenesis, but fail to initiate the first hair cycle. Utricles begin to form at 10 days after birth and the infundibulum becomes wider. The hair follicles are filled with keratinized materials so that the structure of hair follicles is destroyed and dermal cysts are formed. The skin becomes wrinkled and severe with age. The mutation was successfully identified as a nonsense mutation, leading to dramatically reduced expression of *Hr* in the homozygotes, as evidenced by Northern blotting.

Microarray analysis was used to identify the downstream molecular events of this nonsense mutation. Mice at an age prior to the formation of utricles (7 days) and an age that coincided with the formation of utricles (10 days) were used in the microarray analysis to identify the earliest changes in gene expression due to the Hr^{rhR} mutation. Differentially expressed genes, including *IL-17*, *Krt1-10*, *Krt2-1*, *Limr*, and *Itgb4*, were identified in mutant mice at 10 days, but not at 7 days. These differentially expressed genes might provide useful information for the potential molecular target of *Hr* in hair follicles. *IL-17*, as a pro-inflammatory cytokine, may play important roles in hair growth and hair follicle cycles. *Krt1-10* and *Krt2-1* are important for the terminal differentiation of keratinocytes in skin. *Itgb4*, as a signature gene of outer root sheath, manifests increased expression, coinciding with the disintegration of hair bulb and the outer root sheath and loss of *Hr* expression in the outer root sheath. It suggests that *Hr* might regulate the expression of *Itgb4* in the outer root sheath to help initiate the first hair cycle. Microarray analysis with mice at both 10 days and 5 weeks of age suggests the alteration of immune function in skin, indicating the involvement of *Hr* in immune system, which is consistent with the accelerated atrophy of the thymus in homozygous mutants. The network and pathway analysis of the microarray data shows that signaling through Wnt/β-catenin, ERK/MAPK, and apoptosis pathway is altered in Hr^{rhR}/Hr^{rhR} mice, suggesting the possible function of *Hr* to regulate these pathways.

Hypothesis for the distinct roles of *Hr* in both Hr^{n} and Hr^{rhR} mutant mice

Hr protein is reported to translocate to the nucleus (Djabali et al., 2001), to associate with nuclear matrix, and to form a repressor complex with other nuclear

receptors, including thyroid hormone receptors (Potter et al., 2002), vitamin D receptors (Hsieh et al., 2003), ROR-α (Moraitis et al., 2002). *Hr* is also associated with histone deacetylases (HDACs), indicating its potential roles in chromatin remodeling (Beaudoin et al., 2005; Potter et al., 2002). It is reported recently that *Hr* promotes the Wnt signaling pathway to initiate the first hair cycle, by repressing the expression of gene *WISE*, an inhibitor of Wnt signaling (Beaudoin et al., 2005). The distinct roles of *Hr* in our two mutant mice are summarized in figure 7-1. Briefly, the loss of *Hr* in Hr^{rhR}/Hr^{rhR} mutant mice significantly alters Wnt/β-catenin, apoptosis, and ERK/MAPK signaling pathways, leads to increased expression of many genes including *Itgb4*, *IL-17*, *Krt2-1*, and *Krt1-10*, which might be associated with widening of infundibulum of hair follicle and formation of utricles. The normal structures of hair follicles were completely destroyed in Hr^{rhR}/Hr^{rhR} mutants by 5 weeks of age, associated with the decreased expression of hair keratins and keratin-associated proteins and hair loss. However, the roles of *Hr* in Hr^{n} mutants are different compared to those in Hr^{rhR} mutants, which are shown in figure 7-1. *Hr* expression is upregulated at early days in homozygous mutants either due to a regulatory mutation in *Hr* or an unknown gene mutation, which directly or indirectly leads to the increased expression of *BMP-4* and the reduced proliferation in hair matrix. The increased expression of *BMP-4* results in the decreased expression of *Foxn1*, *Hoxc13*, hair keratins, and keratin-associated proteins, and premature keratinization, which leads to abnormal hair shaft differentiation, finally the formation of dermal cysts, destruction of hair follicles, and hair loss.

Future directions

To identify the Hr^{n} mutation, transgenic mice need to be generated with the overexpression of *Hr* in the inner and outer root sheath and the matrix of hair follicles as well as the fibroblasts in the sinus, if possible. The overexpression of *Hr* in these regions matches with the Hr^{n} mutant mice and can be used to validate if the Hr^{n} mutation is due to *Hr* overexpression. The problem for this is to find the correct promoter to express *Hr* in these regions. Otherwise, it is not very useful for the validation of Hr^{n} mutation. Another way to characterize the Hr^{n} mutation is through fine genetic mapping by crossing to re-map the locus for Hr^{n} mutation on the chromosome. This task is not

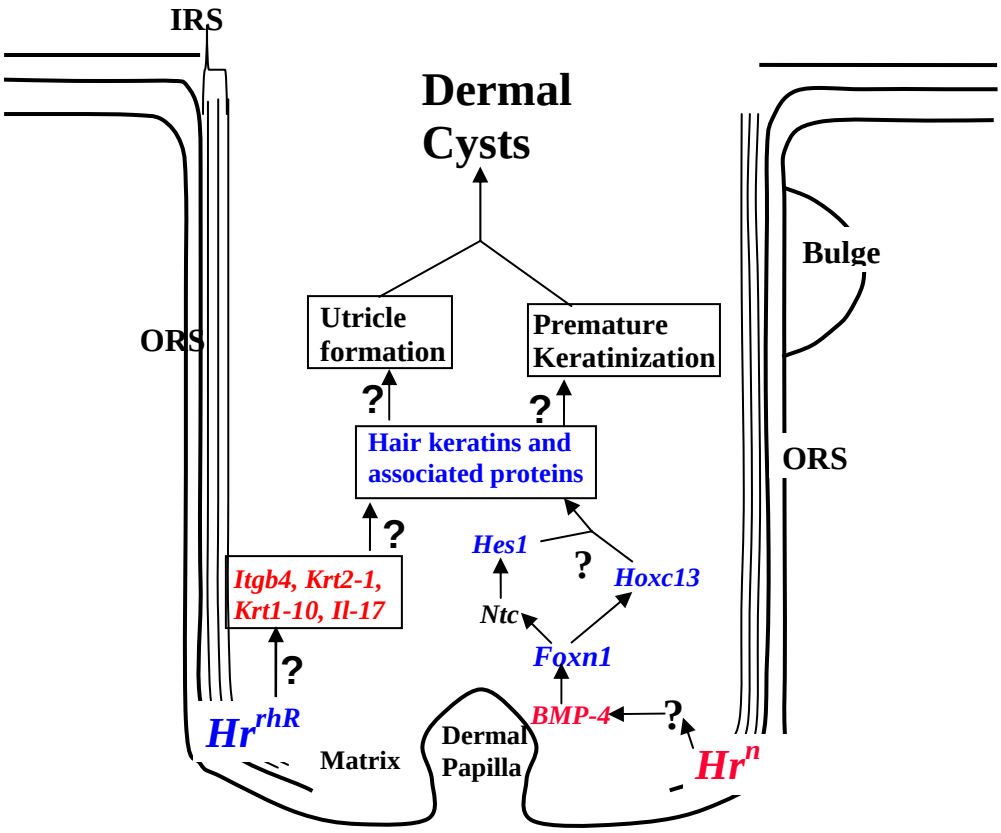

Figure 7-1 Schematic illustration of the hypothesized roles of *Hr* in Hr^{n} and Hr^{rhR} mutant mice. Red color indicates increased expression and blue indicates decreased expression. The question mark (?) indicates unknown mechanisms.

challenging, but very labor-intensive. The outcome of this approach is also not guaranteed to identify the mutation. There is a good chance to find the mutation if the mutation maps to a different region. This work seems too risky to do in the future. Both of the approaches are based on the assumption that Hr^n is a single gene mutation in either the regulatory sequence or the coding region. If the Hr^n mutation is a nonsense mutation in the coding region of a single gene, microarray covering the whole mouse genome, at least all the genes on mouse chromosome 14 could be done to check expression levels of all the genes around *Hr*. The assumed nonsense mutation should lead to the degradation of mutated mRNA through nonsense-mediated decay. A gene or transcript with significant reduction of expression in Hr^n/Hr^n mutants might carry the mutation. This strategy has been used with our microarray analysis though our microarray just covers about 50% of genes in mouse genome.

To characterize the molecular functions of *Hr*, the Hr^{rhR}/Hr^{rhR} mutant mice need to be studied with more details. We have identified a set of genes with differential expression in skin of 10-day old mutants. The alterations in expression need to be validated with either real time PCR or *in situ* hybridization on the tissue dissections. If the expression changes of *IL-17*, *Itgb4*, *Krt2-1*, and *Krt1-10* could be confirmed with *in situ* hybridization, then the expression of these genes could be examined by reporter assay with the overexpression of *Hr*. These reporter assays help to identify the genetic interactions of *Hr* and possibly the interacting proteins.

List of references

Ahmad, W., Faiyaz ul Haque, M., Brancolini, V., Tsou, H. C., ul Haque, S., Lam, H., Aita, V. M., Owen, J., deBlaquiere, M., Frank, J., *et al.* (1998a). Alopecia universalis associated with a mutation in the human hairless gene. Science *279*, 720-724.

Ahmad, W., Irvine, A. D., Lam, H., Buckley, C., Bingham, E. A., Panteleyev, A. A., Ahmad, M., McGrath, J. A., and Christiano, A. M. (1998b). A missense mutation in the zinc-finger domain of the human hairless gene underlies congenital atrichia in a family of Irish travellers. Am J Hum Genet *63*, 984-991.

Ahmad, W., Nomura, K., McGrath, J. A., Hashimoto, I., and Christiano, A. M. (1999a). A homozygous nonsense mutation in the zinc-finger domain of the human hairless gene underlies congenital atrichia. J Invest Dermatol *113*, 281-283.

Ahmad, W., Panteleyev, A., and Christiano, A. M. (1999b). Molecular basis of congenital atrichia in humans and mice. Cutis *64*, 269-276.

Ahmad, W., Panteleyev, A. A., and Christiano, A. M. (1999c). The molecular basis of congenital atrichia in humans and mice: mutations in the hairless gene. J Investig Dermatol Symp Proc *4*, 240-243.

Ahmad, W., Panteleyev, A. A., Henson-Apollonio, V., Sundberg, J. P., and Christiano, A. M. (1998c). Molecular basis of a novel rhino (hr(rhChr)) phenotype: a nonsense mutation in the mouse hairless gene. Exp Dermatol *7*, 298-301.

Ahmad, W., Panteleyev, A. A., Sundberg, J. P., and Christiano, A. M. (1998d). Molecular basis for the rhino (hrrh-8J) phenotype: a nonsense mutation in the mouse hairless gene. Genomics *53*, 383-386.

Ahmad, W., Ratterree, M. S., Panteleyev, A. A., Aita, V. M., Sundberg, J. P., and Christiano, A. M. (2002). Atrichia with papular lesions resulting from mutations in the rhesus macaque (Macaca mulatta) hairless gene. Lab Anim *36*, 61-67.

Ahmad, W., Zlotogorski, A., Panteleyev, A. A., Lam, H., Ahmad, M., ul Haque, M. F., Abdallah, H. M., Dragan, L., and Christiano, A. M. (1999d). Genomic organization of the human hairless gene (HR) and identification of a mutation underlying congenital atrichia in an Arab Palestinian family. Genomics *56*, 141-148.

Aita, V. M., Ahmad, W., Panteleyev, A. A., Kozlowska, U., Kozlowska, A., Gilliam, T. C., Jablonska, S., and Christiano, A. M. (2000). A novel missense mutation (C622G) in the zinc-finger domain of the human hairless gene associated with congenital atrichia with papular lesions. Exp Dermatol *9*, 157-162.

Argenziano, G., Sammarco, E., Rossi, A., Delfino, M., and Calvieri, S. (1999). Marie Unna hereditary hypotrichosis. Eur J Dermatol *9*, 278-280.

Ashoor, G. G., Greenstein, R. M., Lam, H., Martinez-Mir, A., Zlotogorski, A., and Christiano, A. M. (2005). Novel compound heterozygous nonsense mutations in the hairless gene causing atrichia with papular lesions. J Dermatol Sci *40*:29-33.

Awgulewitsch, A. (2003). Hox in hair growth and development. Naturwissenschaften *90*, 193-211.

Ayoub, N., Noma, K., Isaac, S., Kahan, T., Grewal, S. I., and Cohen, A. (2003). A novel jmjC domain protein modulates heterochromatization in fission yeast. Mol Cell Biol *23*, 4356-4370.

Bailey, D., and Bunker, H. (1973). Spontaneous mutation to hr. Mouse News Lett *49*, 31.

Baker, S. E., Skalli, O., Goldman, R. D., and Jones, J. C. (1997). Laminin-5 and modulation of keratin cytoskeleton arrangement in FG pancreatic carcinoma cells: involvement of IFAP300 and evidence that laminin-5/cell interactions correlate with a dephosphorylation of alpha 6A integrin. Cell Motil Cytoskeleton *37*, 271-286.

Balciunas, D., and Ronne, H. (2000). Evidence of domain swapping within the jumonji family of transcription factors. Trends Biochem Sci *25*, 274-276.

Beaudoin, G. M., 3rd, Sisk, J. M., Coulombe, P. A., and Thompson, C. C. (2005). Hairless triggers reactivation of hair growth by promoting Wnt signaling. Proc Natl Acad Sci U S A *102*, 14653-14658.

Bergman, R., Schein-Goldshmid, R., Hochberg, Z., Ben-Izhak, O., and Sprecher, E. (2005). The alopecias associated with vitamin D-dependent rickets type IIA and with hairless gene mutations: a comparative clinical, histologic, and immunohistochemical study. Arch Dermatol *141*, 343-351.

Bernerd, F., Schweizer, J., and Demarchez, M. (1996). Dermal cysts of the rhino mouse develop into unopened sebaceous glands. Arch Dermatol Res *288*, 586-595.

Beynon, R. J., and Hurst, J. L. (2003). Multiple roles of major urinary proteins in the house mouse, Mus domesticus. Biochem Soc Trans *31*, 142-146.

Blake, J. A., Richardson, J. E., Bult, C. J., Kadin, J. A., and Eppig, J. T. (2003). MGD: the Mouse Genome Database. Nucleic Acids Res *31*, 193-195.

Blessing, M., Nanney, L. B., King, L. E., Jones, C. M., and Hogan, B. L. (1993). Transgenic mice as a model to study the role of TGF-beta-related molecules in hair follicles. Genes Dev *7*, 204-215.

Botchkarev, V. A., and Kishimoto, J. (2003). Molecular control of epithelial-mesenchymal interactions during hair follicle cycling. J Investig Dermatol Symp Proc *8*, 46-55.

Botchkarev, V. A., and Paus, R. (2003). Molecular biology of hair morphogenesis: development and cycling. J Exp Zoolog B Mol Dev Evol *298*, 164-180.

Brajac, I., Tkalcic, M., Dragojevic, D. M., and Gruber, F. (2003). Roles of stress, stress perception and trait-anxiety in the onset and course of alopecia areata. J Dermatol *30*, 871-878.

Brancaz, M. V., Iratni, R., Morrison, A., Mancini, S. J., Marche, P., Sundberg, J., and Nonchev, S. (2004). A new allele of the mouse hairless gene interferes with Hox/LacZ transgene regulation in hair follicle primordia. Exp Mol Pathol *76*, 173-181.

Brooke, H. C. (1926). Hairless mice. J Hered *17*, 173-174.

Bultman SJ, M. E., Woychik RP. (1992). Molecular characterization of the mouse agouti locus. Cell *71*, 1195-1204.

Cachon-Gonzalez, M. B., Fenner, S., Coffin, J. M., Moran, C., Best, S., and Stoye, J. P. (1994). Structure and expression of the hairless gene of mice. Proc Natl Acad Sci U S A *91*, 7717-7721.

Cachon-Gonzalez, M. B., San-Jose, I., Cano, A., Vega, J. A., Garcia, N., Freeman, T., Schimmang, T., and Stoye, J. P. (1999). The hairless gene of the mouse: relationship of phenotypic effects with expression profile and genotype. Dev Dyn *216*, 113-126.

Calin, G. A., Dumitru, C. D., Shimizu, M., Bichi, R., Zupo, S., Noch, E., Aldler, H., Rattan, S., Keating, M., Rai, K., *et al.* (2002). Frequent deletions and down-regulation

of micro- RNA genes miR15 and miR16 at 13q14 in chronic lymphocytic leukemia. Proc Natl Acad Sci U S A *99*, 15524-15529.

Calin, G. A., Ferracin, M., Cimmino, A., Di Leva, G., Shimizu, M., Wojcik, S. E., Iorio, M. V., Visone, R., Sever, N. I., Fabbri, M.*, et al.* (2005). A MicroRNA signature associated with prognosis and progression in chronic lymphocytic leukemia. N Engl J Med *353*, 1793-1801.

Calin, G. A., Liu, C. G., Sevignani, C., Ferracin, M., Felli, N., Dumitru, C. D., Shimizu, M., Cimmino, A., Zupo, S., Dono, M.*, et al.* (2004). MicroRNA profiling reveals distinct signatures in B cell chronic lymphocytic leukemias. Proc Natl Acad Sci U S A *101*, 11755-11760.

Cash, T. F., Price, V. H., and Savin, R. C. (1993). Psychological effects of androgenetic alopecia on women: comparisons with balding men and with female control subjects. J Am Acad Dermatol *29*, 568-575.

Chase, H. B. (1954). Growth of the hair. Physiol Rev *34*, 113-126.

Chiba, H., Muramatsu, M., Nomoto, A., and Kato, H. (1994). Two human homologues of Saccharomyces cerevisiae SWI2/SNF2 and Drosophila brahma are transcriptional coactivators cooperating with the estrogen receptor and the retinoic acid receptor. Nucleic Acids Res *22*, 1815-1820.

Christiano, A. M. (2004). Epithelial stem cells: stepping out of their niche. Cell *118*, 530-532.

Cichon, S., Anker, M., Vogt, I. R., Rohleder, H., Putzstuck, M., Hillmer, A., Farooq, S. A., Al-Dhafri, K. S., Ahmad, M., Haque, S.*, et al.* (1998). Cloning, genomic organization, alternative transcripts and mutational analysis of the gene responsible for autosomal recessive universal congenital alopecia. Hum Mol Genet *7*, 1671-1679.

Cichon, S., Kruse, R., Hillmer, A. M., Kukuk, G., Anker, M., Altland, K., Knapp, M., Propping, P., and Nothen, M. M. (2000). A distinct gene close to the hairless locus on chromosome 8p underlies hereditary Marie Unna type hypotrichosis in a German family. Br J Dermatol *143*, 811-814.

Cotsarelis, G., and Millar, S. E. (2001). Towards a molecular understanding of hair loss and its treatment. Trends Mol Med *7*, 293-301.

Coyne, C. B., Gambling, T. M., Boucher, R. C., Carson, J. L., and Johnson, L. G. (2003). Role of claudin interactions in airway tight junctional permeability. Am J Physiol Lung Cell Mol Physiol *285*, L1166-1178.

Cserhalmi-Friedman, P. B., Panteleyev, A. A., and Christiano, A. M. (2004). Recapitulation of the hairless mouse phenotype using catalytic oligonucleotides: implications for permanent hair removal. Exp Dermatol *13*, 155-162.

Cunliffe, V. T., Furley, A. J., and Keenan, D. (2002). Complete rescue of the nude mutant phenotype by a wild-type Foxn1 transgene. Mamm Genome *13*, 245-252.

del Castillo, V., Ruiz-Maldonado, R., and Carnevale, A. (1974). Atrichia with papular lesions and mental retardation in two sisters. Int J Dermatol *13*, 261-265.

Dennis, G., Jr., Sherman, B. T., Hosack, D. A., Yang, J., Gao, W., Lane, H. C., and Lempicki, R. A. (2003). DAVID: Database for Annotation, Visualization, and Integrated Discovery. Genome Biol *4*, P3.

Djabali, K., Aita, V. M., and Christiano, A. M. (2001). Hairless is translocated to the nucleus via a novel bipartite nuclear localization signal and is associated with the nuclear matrix. J Cell Sci *114*, 367-376.

Djabali, K., and Christiano, A. M. (2004). Hairless contains a novel nuclear matrix targeting signal and associates with histone deacetylase 3 in nuclear speckles. Differentiation *72*, 410-418.

Djabali, K., Zlotogorski, A., Metzker, A., Ben-Amitai, D., and Christiano, A. M. (2004). Interaction of hairless and thyroid hormone receptor is not involved in the pathogenesis of atrichia with papular lesions. Exp Dermatol *13*, 251-256.

Engelhard, A., and Christiano, A. M. (2004). The hairless promoter is differentially regulated by thyroid hormone in keratinocytes and neuroblastoma cells. Exp Dermatol *13*, 257-264.

Fernandez, A., Silio, L., Noguera, J. L., Sanchez, A., and Ovilo, C. (2003). Linkage mapping of the porcine hairless gene (HR) to chromosome 14. Anim Genet *34*, 317-318.

Finocchiaro, R., Portolano, B., Damiani, G., Caroli, A., Budelli, E., Bolla, P., and Pagnacco, G. (2003). The hairless (hr) gene is involved in the congenital hypotrichosis of Valle del Belice sheep. Genet Sel Evol *35 Suppl 1*, S147-156.

Flanagan, S. P. (1966). 'Nude', a new hairless gene with pleiotropic effects in the mouse. Genet Res *8*, 295-309.

Frank, J., Pignata, C., Panteleyev, A. A., Prowse, D. M., Baden, H., Weiner, L., Gaetaniello, L., Ahmad, W., Pozzi, N., Cserhalmi-Friedman, P. B.*, et al.* (1999). Exposing the human nude phenotype. Nature *398*, 473-474.

Fuchs, E. (1998). Beauty is skin deep: the fascinating biology of the epidermis and its appendages. Harvey Lect *94*, 47-77.

Furuse, M., Hata, M., Furuse, K., Yoshida, Y., Haratake, A., Sugitani, Y., Noda, T., Kubo, A., and Tsukita, S. (2002). Claudin-based tight junctions are crucial for the mammalian epidermal barrier: a lesson from claudin-1-deficient mice. J Cell Biol *156*, 1099-1111.

Garber, E. (1952). Bald, a second allele of hairless in the house mouse. J Hered *43*, 45-46.

Garcia-Atares, N., San Jose, I., Cabo, R., Vega, J. A., and Represa, J. (1998). Changes in the cerebellar cortex of hairless Rhino-J mice (hr-rh-j). Neurosci Lett *256*, 13-16.

Gaskoin, J. S. (1856). On a peculiar variety of *Mus musculus*. Proc Zool Soc London *24*, 38.

Gho, C. G., Braun, J. E., Tilli, C. M., Neumann, H. A., and Ramaekers, F. C. (2004). Human follicular stem cells: their presence in plucked hair and follicular cell culture. Br J Dermatol *150*, 860-868.

Godwin, A. R., and Capecchi, M. R. (1998). Hoxc13 mutant mice lack external hair. Genes Dev *12*, 11-20.

Green, J., Fitzpatrick, E., de Berker, D., Forrest, S. M., and Sinclair, R. D. (2003). Progressive patterned scalp hypotrichosis, with wiry hair, onycholysis, and intermittently associated cleft lip and palate: clinical and genetic distinction from Marie Unna. J Investig Dermatol Symp Proc *8*, 121-125.

Groves, R. W., Mizutani, H., Kieffer, J. D., and Kupper, T. S. (1995). Inflammatory skin disease in transgenic mice that express high levels of interleukin 1 alpha in basal epidermis. Proc Natl Acad Sci U S A *92*, 11874-11878.

Gurlek, A., Pittelkow, M. R., and Kumar, R. (2002). Modulation of growth factor/cytokine synthesis and signaling by 1alpha,25-dihydroxyvitamin D(3): implications in cell growth and differentiation. Endocr Rev *23*, 763-786.

Hadshiew, I. M., Foitzik, K., Arck, P. C., and Paus, R. (2004). Burden of hair loss: stress and the underestimated psychosocial impact of telogen effluvium and androgenetic alopecia. J Invest Dermatol *123*, 455-457.

Hardy, M. H. (1992). The secret life of the hair follicle. Trends Genet *8*, 55-61.

Harmon, C. S., Nevins, T. D., and Bollag, W. B. (1995). Protein kinase C inhibits human hair follicle growth and hair fibre production in organ culture. Br J Dermatol *133*, 686-693.

Harmon, C. S., Nevins, T. D., Ducote, J., and Lutz, D. (1997). Bisindolylmaleimide protein-kinase-C inhibitors delay the decline in DNA synthesis in mouse hair follicle organ cultures. Skin Pharmacol *10*, 71-78.

Haussler, M. R., Whitfield, G. K., Haussler, C. A., Hsieh, J. C., Thompson, P. D., Selznick, S. H., Dominguez, C. E., and Jurutka, P. W. (1998). The nuclear vitamin D receptor: biological and molecular regulatory properties revealed. J Bone Miner Res *13*, 325-349.

He, P. P., Zhang, X. J., Yang, Q., Li, M., Liang, Y. H., Yang, S., Yan, K. L., Cui, Y., Shen, Y. Y., Wang, H. Y.*, et al.* (2004). Refinement of a locus for Marie Unna hereditary hypotrichosis to a 1.1-cM interval at 8p21.3. Br J Dermatol *150*, 837-842.

Held, W. A., Mullins, J. J., Kuhn, N. J., Gallagher, J. F., Gu, G. D., and Gross, K. W. (1989). T antigen expression and tumorigenesis in transgenic mice containing a mouse major urinary protein/SV40 T antigen hybrid gene. Embo J *8*, 183-191.

Henn, W., Zlotogorski, A., Lam, H., Martinez-Mir, A., Zaun, H., and Christiano, A. M. (2002). Atrichia with papular lesions resulting from compound heterozygous mutations in the hairless gene: A lesson for differential diagnosis of alopecia universalis. J Am Acad Dermatol *47*, 519-523.

Hillmer, A. M., Kruse, R., Betz, R. C., Schumacher, J., Heyn, U., Propping, P., Nothen, M. M., and Cichon, S. (2001). Variant 1859G-->A (Arg620Gln) of the "hairless" gene: absence of association with papular atrichia or androgenic alopecia. Am J Hum Genet *69*, 235-237.

Hillmer, A. M., Kruse, R., Macciardi, F., Heyn, U., Betz, R. C., Ruzicka, T., Propping, P., Nothen, M. M., and Cichon, S. (2002). The hairless gene in androgenetic alopecia: results of a systematic mutation screening and a family-based association approach. Br J Dermatol *146*, 601-608.

Howard, A. (1940). "Rhino", an allele of hairless in the house mouse. J Hered *31*, 467-470.

Hsieh, J. C., Sisk, J. M., Jurutka, P. W., Haussler, C. A., Slater, S. A., Haussler, M. R., and Thompson, C. C. (2003). Physical and functional interaction between the vitamin D receptor and hairless corepressor, two proteins required for hair cycling. J Biol Chem *278*, 38665-38674.

Hunt, N., and McHale, S. (2005). The psychological impact of alopecia. BMJ *331*, 951-953.

Iacovacci, S., Cicuzza, S., Odorisio, T., Silvestri, E., Kayserili, H., Zambruno, G., Puddu, P., and D'Alessio, M. (2003). Novel and recurrent mutations in the integrin beta 4 subunit gene causing lethal junctional epidermolysis bullosa with pyloric atresia. Exp Dermatol *12*, 716-720.

Ilunga, K., Nishiura, R., Inada, H., El-Karef, A., Imanaka-Yoshida, K., Sakakura, T., and Yoshida, T. (2004). Co-stimulation of human breast cancer cells with transforming growth factor-beta and tenascin-C enhances matrix metalloproteinase-9 expression and cancer cell invasion. Int J Exp Pathol *85*, 373-379.

Indelman, M., Bergman, R., Lestringant, G. G., Peer, G., and Sprecher, E. (2003). Compound heterozygosity for mutations in the hairless gene causes atrichia with papular lesions. Br J Dermatol *148*, 553-557.

Irvine, A. D., and Christiano, A. M. (2001). Hair on a gene string: recent advances in understanding the molecular genetics of hair loss. Clin Exp Dermatol *26*, 59-71.

Jamora, C., DasGupta, R., Kocieniewski, P., and Fuchs, E. (2003). Links between signal transduction, transcription and adhesion in epithelial bud development. Nature *422*, 317-322.

Janes, S. M., Ofstad, T. A., Campbell, D. H., Watt, F. M., and Prowse, D. M. (2004). Transient activation of FOXN1 in keratinocytes induces a transcriptional programme that promotes terminal differentiation: contrasting roles of FOXN1 and Akt. J Cell Sci *117*, 4157-4168.

Jave-Suarez, L. F., Winter, H., Langbein, L., Rogers, M. A., and Schweizer, J. (2002). HOXC13 is involved in the regulation of human hair keratin gene expression. J Biol Chem *277*, 3718-3726.

Jiang, W., Prokopenko, O., Wong, L., Inouye, M., and Mirochnitchenko, O. (2005). IRIP, a new ischemia/reperfusion-inducible protein that participates in the regulation of transporter activity. Mol Cell Biol *25*, 6496-6508.

John, P., Aslam, M., Rafiq, M. A., Amin-Ud-Din, M., Haque, S., and Ahmad, W. (2005). Atrichia with papular lesions in two Pakistani consanguineous families resulting from mutations in the human hairless gene. Arch Dermatol Res 297:226-30.

Johns, S. A., Soullier, S., Rashbass, P., and Cunliffe, V. T. (2005). Foxn1 is required for tissue assembly and desmosomal cadherin expression in the hair shaft. Dev Dyn *232*, 1062-1068.

Jones, J. M., Elder, J. T., Simin, K., Keller, S. A., and Meisler, M. H. (1993). Insertional mutation of the hairless locus on mouse chromosome 14. Mamm Genome *4*, 639-643.

Kalembeyi, I., Inada, H., Nishiura, R., Imanaka-Yoshida, K., Sakakura, T., and Yoshida, T. (2003). Tenascin-C upregulates matrix metalloproteinase-9 in breast cancer cells: direct and synergistic effects with transforming growth factor beta1. Int J Cancer *105*, 53-60.

Kim, H. S., Kim, S. C., and Lee, W. S. (2001). Marie Unna hypotrichosis in an Asian family. J Dermatol *28*, 149-152.

Kizawa, K., and Ito, M. (2005). Characterization of epithelial cells in the hair follicle with S100 proteins. Methods Mol Biol *289*, 209-222.

Klein, I., Bergman, R., Indelman, M., and Sprecher, E. (2002). A novel missense mutation affecting the human hairless thyroid receptor interacting domain 2 causes congenital atrichia. J Invest Dermatol *119*, 920-922.

Kljuic, A., Bazzi, H., Sundberg, J. P., Martinez-Mir, A., O'Shaughnessy, R., Mahoney, M. G., Levy, M., Montagutelli, X., Ahmad, W., Aita, V. M., *et al.* (2003). Desmoglein 4 in hair follicle differentiation and epidermal adhesion: evidence from inherited hypotrichosis and acquired pemphigus vulgaris. Cell *113*, 249-260.

Knutson, J. C., and Poland, A. (1982). Response of murine epidermis to 2,3,7,8-tetrachlorodibenzo-p-dioxin: interaction of the ah and hr loci. Cell *30*, 225-234.

Kong, J., Li, X. J., Gavin, D., Jiang, Y., and Li, Y. C. (2002a). Targeted expression of human vitamin d receptor in the skin promotes the initiation of the postnatal hair follicle cycle and rescues the alopecia in vitamin D receptor null mice. J Invest Dermatol *118*, 631-638.

Kong, M., Wang, C. S., and Donoghue, D. J. (2002b). Interaction of fibroblast growth factor receptor 3 and the adapter protein SH2-B. A role in STAT5 activation. J Biol Chem *277*, 15962-15970.

Kopf-Maier, P., Mboneko, V. F., and Merker, H. J. (1990). Nude mice are not hairless. A morphological study. Acta Anat (Basel) *139*, 178-190.

Kruse, R., Cichon, S., Anker, M., Hillmer, A. M., Barros-Nunez, P., Cantu, J. M., Leal, E., Weinlich, G., Schmuth, M., Fritsch, P., *et al.* (1999). Novel Hairless mutations in two kindreds with autosomal recessive papular atrichia. J Invest Dermatol *113*, 954-959.

Kubo-Akashi, C., Iseki, M., Kwon, S. M., Takizawa, H., Takatsu, K., and Takaki, S. (2004). Roles of a conserved family of adaptor proteins, Lnk, SH2-B, and APS, for mast cell development, growth, and functions: APS-deficiency causes augmented degranulation and reduced actin assembly. Biochem Biophys Res Commun *315*, 356-362.

Kulessa, H., Turk, G., and Hogan, B. L. (2000). Inhibition of Bmp signaling affects growth and differentiation in the anagen hair follicle. Embo J *19*, 6664-6674.

Lane, E. B., and McLean, W. H. (2004). Keratins and skin disorders. J Pathol *204*, 355-366.

Lefevre, P., Rochat, A., Bodemer, C., Vabres, P., Barrandon, Y., de Prost, Y., Garner, C., and Hovnanian, A. (2000). Linkage of Marie-Unna hypotrichosis locus to chromosome 8p21 and exclusion of 10 genes including the hairless gene by mutation analysis. Eur J Hum Genet *8*, 273-279.

Letunic, I., Goodstadt, L., Dickens, N. J., Doerks, T., Schultz, J., Mott, R., Ciccarelli, F., Copley, R. R., Ponting, C. P., and Bork, P. (2002). Recent improvements to the SMART domain-based sequence annotation resource. Nucleic Acids Res *30*, 242-244.

Li, M., Chiba, H., Warot, X., Messaddeq, N., Gerard, C., Chambon, P., and Metzger, D. (2001). RXR-alpha ablation in skin keratinocytes results in alopecia and epidermal alterations. Development *128*, 675-688.

Li, Y. C., Pirro, A. E., Amling, M., Delling, G., Baron, R., Bronson, R., and Demay, M. B. (1997). Targeted ablation of the vitamin D receptor: an animal model of vitamin D-dependent rickets type II with alopecia. Proc Natl Acad Sci U S A *94*, 9831-9835.

Lin, K. K., Chudova, D., Hatfield, G. W., Smyth, P., and Andersen, B. (2004). Identification of hair cycle-associated genes from time-course gene expression profile data by using replicate variance. Proc Natl Acad Sci U S A *101*, 15955-15960.

Lindner, G., Botchkarev, V. A., Botchkareva, N. V., Ling, G., van der Veen, C., and Paus, R. (1997). Analysis of apoptosis during hair follicle regression (catagen). Am J Pathol *151*, 1601-1617.

Lowry, W. E., Blanpain, C., Nowak, J. A., Guasch, G., Lewis, L., and Fuchs, E. (2005). Defining the impact of beta-catenin/Tcf transactivation on epithelial stem cells. Genes Dev *19*, 1596-1611.

Ma, L., and Cai, J. (2005). Genetic pathways regulating hair shaft differentiation. J Invest Dermatol *124*, A105.

Ma, L., Liu, J., Wu, T., Plikus, M., Jiang, T. X., Bi, Q., Liu, Y. H., Muller-Rover, S., Peters, H., Sundberg, J. P.*, et al.* (2003). 'Cyclic alopecia' in Msx2 mutants: defects in hair cycling and hair shaft differentiation. Development *130*, 379-389.

Mahe, Y. F., Buan, B., Billoni, N., Loussouarn, G., Michelet, J. F., Gautier, B., and Bernard, B. A. (1996). Pro-inflammatory cytokine cascade in human plucked hair. Skin Pharmacol *9*, 366-375.

Mahony, D., Karunaratne, S., Cam, G., and Rothnagel, J. A. (2000). Analysis of mouse keratin 6a regulatory sequences in transgenic mice reveals constitutive, tissue-specific expression by a keratin 6a minigene. J Invest Dermatol *115*, 795-804.

Mann, S. J. (1971). Hair loss and cyst formation in hairless and rhino mutant mice. Anat Rec *170*, 485-499.

Maquat, L. E. (2005). Nonsense-mediated mRNA decay in mammals. J Cell Sci *118*, 1773-1776.

Martin, N., Patel, S., and Segre, J. A. (2004). Long-range comparison of human and mouse Sprr loci to identify conserved noncoding sequences involved in coordinate regulation. Genome Res *14*, 2430-2438.

Masse, M., Ashoor, G., Michailidis, E., Greenstein, R., Paradisi, M., Pedicelli, C., Theos, A., Martinez-Mir, A., Zlotogorski, A., and Christiano, A. M. (2005a). Identification of five novel hairless mutations underlying atrichia with papular lesions. J Invest Dermatol *124*, A104.

Masse, M., Martinez-Mir, A., Lam, H., Geraghty, M. T., and Christiano, A. M. (2005b). Identification of a recurrent mutation in the human hairless gene underlying atrichia with papular lesions. Clin Exp Dermatol *30*, 363-365.

Mecklenburg, L., Tychsen, B., and Paus, R. (2005). Learning from nudity: lessons from the nude phenotype. Exp Dermatol *14*, 797-810.

Miller, J., Djabali, K., Chen, T., Liu, Y., Ioffreda, M., Lyle, S., Christiano, A. M., Holick, M., and Cotsarelis, G. (2001). Atrichia caused by mutations in the vitamin D receptor gene is a phenocopy of generalized atrichia caused by mutations in the hairless gene. J Invest Dermatol *117*, 612-617.

Mischke, D., Korge, B. P., Marenholz, I., Volz, A., and Ziegler, A. (1996). Genes encoding structural proteins of epidermal cornification and S100 calcium-binding proteins form a gene complex ("epidermal differentiation complex") on human chromosome 1q21. J Invest Dermatol *106*, 989-992.

Molenaar, M., van de Wetering, M., Oosterwegel, M., Peterson-Maduro, J., Godsave, S., Korinek, V., Roose, J., Destree, O., and Clevers, H. (1996). XTcf-3 transcription factor mediates beta-catenin-induced axis formation in Xenopus embryos. Cell *86*, 391-399.

Moraitis, A. N., Giguere, V., and Thompson, C. C. (2002). Novel mechanism of nuclear receptor corepressor interaction dictated by activation function 2 helix determinants. Mol Cell Biol *22*, 6831-6841.

Morris, R. J., Liu, Y., Marles, L., Yang, Z., Trempus, C., Li, S., Lin, J. S., Sawicki, J. A., and Cotsarelis, G. (2004). Capturing and profiling adult hair follicle stem cells. Nat Biotechnol *22*, 411-417.

Muchardt, C., and Yaniv, M. (1993). A human homologue of Saccharomyces cerevisiae SNF2/SWI2 and Drosophila brm genes potentiates transcriptional activation by the glucocorticoid receptor. Embo J *12*, 4279-4290.

Muller-Rover, S., Handjiski, B., van der Veen, C., Eichmuller, S., Foitzik, K., McKay, I. A., Stenn, K. S., and Paus, R. (2001). A comprehensive guide for the accurate classification of murine hair follicles in distinct hair cycle stages. J Invest Dermatol *117*, 3-15.

Nakae, S., Komiyama, Y., Nambu, A., Sudo, K., Iwase, M., Homma, I., Sekikawa, K., Asano, M., and Iwakura, Y. (2002). Antigen-specific T cell sensitization is impaired in IL-17-deficient mice, causing suppression of allergic cellular and humoral responses. Immunity *17*, 375-387.

Nakamura, M., Sundberg, J. P., and Paus, R. (2001). Mutant laboratory mice with abnormalities in hair follicle morphogenesis, cycling, and/or structure: annotated tables. Exp Dermatol *10*, 369-390.

Nehls, M., Pfeifer, D., Schorpp, M., Hedrich, H., and Boehm, T. (1994). New member of the winged-helix protein family disrupted in mouse and rat nude mutations. Nature *372*, 103-107.

Nukaya, M., Takahashi, Y., Gonzalez, F. J., and Kamataki, T. (2004). Aryl hydrocarbon receptor-mediated suppression of GH receptor and Janus kinase 2 expression in mice. FEBS Lett *558*, 96-100.

O'Brien, K. B., O'Shea, J. J., and Carter-Su, C. (2002). SH2-B family members differentially regulate JAK family tyrosine kinases. J Biol Chem *277*, 8673-8681.

O'Shaughnessy, R. F., and Christiano, A. M. (2004). Inherited disorders of the skin in human and mouse: from development to differentiation. Int J Dev Biol *48*, 171-179.

Paller, A. S., Varigos, G., Metzker, A., Bauer, R. C., Opie, J., Martinez-Mir, A., Christiano, A. M., and Zlotogorski, A. (2003). Compound heterozygous mutations in the hairless gene in atrichia with papular lesions. J Invest Dermatol *121*, 430-432.

Panteleyev, A. A., Ahmad, W., Malashenko, A. M., Ignatieva, E. L., Paus, R., Sundberg, J. P., and Christiano, A. M. (1998a). Molecular basis for the rhino Yurlovo (hr(rhY)) phenotype: severe skin abnormalities and female reproductive defects associated with an insertion in the hairless gene. Exp Dermatol *7*, 281-288.

Panteleyev, A. A., Botchkareva, N. V., Sundberg, J. P., Christiano, A. M., and Paus, R. (1999). The role of the hairless (hr) gene in the regulation of hair follicle catagen transformation. Am J Pathol *155*, 159-171.

Panteleyev, A. A., Paus, R., Ahmad, W., Sundberg, J. P., and Christiano, A. M. (1998b). Molecular and functional aspects of the hairless (hr) gene in laboratory rodents and humans. Exp Dermatol *7*, 249-267.

Panteleyev, A. A., Paus, R., and Christiano, A. M. (2000). Patterns of hairless (hr) gene expression in mouse hair follicle morphogenesis and cycling. Am J Pathol *157*, 1071-1079.

Panteleyev, A. A., van der Veen, C., Rosenbach, T., Muller-Rover, S., Sokolov, V. E., and Paus, R. (1998c). Towards defining the pathogenesis of the hairless phenotype. J Invest Dermatol *110*, 902-907.

Pantelouris, E. M. (1968). Absence of thymus in a mouse mutant. Nature *217*, 370-371.

Pantelouris, E. M., and Hair, J. (1970). Thymus dysgenesis in nude (nu nu) mice. J Embryol Exp Morphol *24*, 615-623.

Paradisi, M., Chuang, G. S., Angelo, C., Pedicelli, C., Martinez-Mir, A., and Christiano, A. M. (2003). Atrichia with papular lesions resulting from a novel homozygous missense mutation in the hairless gene. Clin Exp Dermatol *28*, 535-538.

Paradisi, M., Masse, M., Martinez-Mir, A., Lam, H., Pedicelli, C., and Christiano, A. M. (2005). Identification of a novel splice site mutation in the human hairless gene underlying atrichia with papular lesions. Eur J Dermatol *15*, 332-338.

Park, H., Li, Z., Yang, X. O., Chang, S. H., Nurieva, R., Wang, Y. H., Wang, Y., Hood, L., Zhu, Z., Tian, Q., and Dong, C. (2005). A distinct lineage of CD4 T cells regulates tissue inflammation by producing interleukin 17. Nat Immunol *6*, 1133-1141.

Paus, R. (1998). Principles of hair cycle control. J Dermatol *25*, 793-802.

Paus, R., Botchkarev, V. A., Botchkareva, N. V., Mecklenburg, L., Luger, T., and Slominski, A. (1999a). The skin POMC system (SPS). Leads and lessons from the hair follicle. Ann N Y Acad Sci *885*, 350-363.

Paus, R., and Cotsarelis, G. (1999). The biology of hair follicles. N Engl J Med *341*, 491-497.

Paus, R., and Foitzik, K. (2004). In search of the "hair cycle clock": a guided tour. Differentiation *72*, 489-511.

Paus, R., Muller-Rover, S., and Botchkarev, V. A. (1999b). Chronobiology of the hair follicle: hunting the " hair cycle clock". J Investig Dermatol Symp Proc *4*, 338-345.

Pedone, P. V., Omichinski, J. G., Nony, P., Trainor, C., Gronenborn, A. M., Clore, G. M., and Felsenfeld, G. (1997). The N-terminal fingers of chicken GATA-2 and GATA-3 are independent sequence-specific DNA binding domains. Embo J *16*, 2874-2882.

Peters, E. M., Hansen, M. G., Overall, R. W., Nakamura, M., Pertile, P., Klapp, B. F., Arck, P. C., and Paus, R. (2005). Control of human hair growth by neurotrophins: brain-derived neurotrophic factor inhibits hair shaft elongation, induces catagen, and stimulates follicular transforming growth factor beta2 expression. J Invest Dermatol *124*, 675-685.

Pierard-Franchimont, C., and Pierard, G. E. (2004). [How I explore.Hair loss in cancer patients]. Rev Med Liege *59*, 525-529.

Porter, R. M. (2003). Mouse models for human hair loss disorders. J Anat *202*, 125-131.

Porter, R. M., Leitgeb, S., Melton, D. W., Swensson, O., Eady, R. A., and Magin, T. M. (1996). Gene targeting at the mouse cytokeratin 10 locus: severe skin fragility and changes of cytokeratin expression in the epidermis. J Cell Biol *132*, 925-936.

Potter, G. B., Beaudoin, G. M., 3rd, DeRenzo, C. L., Zarach, J. M., Chen, S. H., and Thompson, C. C. (2001). The hairless gene mutated in congenital hair loss disorders encodes a novel nuclear receptor corepressor. Genes Dev *15*, 2687-2701.

Potter, G. B., Zarach, J. M., Sisk, J. M., and Thompson, C. C. (2002). The thyroid hormone-regulated corepressor hairless associates with histone deacetylases in neonatal rat brain. Mol Endocrinol *16*, 2547-2560.

Prophet, E., Mills, B., Arrington, J., and Sobin, L. (1992). AFIP Laboratory Methods in Histotechnology (Washinton, DC: American Registry of Pathology).

Pruett, N. D., Tkatchenko, T. V., Jave-Suarez, L., Jacobs, D. F., Potter, C. S., Tkatchenko, A. V., Schweizer, J., and Awgulewitsch, A. (2004). Krtap16, characterization of a new hair keratin-associated protein (KAP) gene complex on mouse chromosome 16 and evidence for regulation by Hoxc13. J Biol Chem *279*, 51524-51533.

Rachez, C., and Freedman, L. P. (2000). Mechanisms of gene regulation by vitamin D(3) receptor: a network of coactivator interactions. Gene *246*, 9-21.

Raunio, H., and Pelkonen, O. (1983). Effect of polycyclic aromatic compounds and phorbol esters on ornithine decarboxylase and aryl hydrocarbon hydroxylase activities in mouse liver. Cancer Res *43*, 782-786.

Reichrath, J., Schilli, M., Kerber, A., Bahmer, F. A., Czarnetzki, B. M., and Paus, R. (1994). Hair follicle expression of 1,25-dihydroxyvitamin D3 receptors during the murine hair cycle. Br J Dermatol *131*, 477-482.

Ren, D., Li, M., Duan, C., and Rui, L. (2005). Identification of SH2-B as a key regulator of leptin sensitivity, energy balance, and body weight in mice. Cell Metab *2*, 95-104.

Rendl, M., Lewis, L., and Fuchs, E. (2005). Molecular Dissection of Mesenchymal-Epithelial Interactions in the Hair Follicle. PLoS Biol *3*, e331.

Reynolds, A. J., and Jahoda, C. A. (2004). Cultured human and rat tooth papilla cells induce hair follicle regeneration and fiber growth. Differentiation *72*, 566-575.

Roberts, J. L., Whiting, D. A., Henry, D., Basler, G., and Woolf, L. (1999). Marie Unna congenital hypotrichosis: clinical description, histopathology, scanning electron microscopy of a previously unreported large pedigree. J Investig Dermatol Symp Proc *4*, 261-267.

Rogers, G. E. (2004). Hair follicle differentiation and regulation. Int J Dev Biol *48*, 163-170.

Rosman, S. (2004). Cancer and stigma: experience of patients with chemotherapy-induced alopecia. Patient Educ Couns *52*, 333-339.

Rothnagel, J. A., Seki, T., Ogo, M., Longley, M. A., Wojcik, S. M., Bundman, D. S., Bickenbach, J. R., and Roop, D. R. (1999). The mouse keratin 6 isoforms are differentially expressed in the hair follicle, footpad, tongue and activated epidermis. Differentiation *65*, 119-130.

Rozen, S., and Skaletsky, H. (2000). Primer3 on the WWW for general users and for biologist programmers. Methods Mol Biol *132*, 365-386.

Sambrook, J., Fritsch, E., and Maniatis, T. (1989). Molecular Cloning: A Laboratory Manual. Cold Spring Harbor, NY: Cold Spring Harbor Laboratory Press.

San Jose, I., Garcia-Suarez, O., Hannestad, J., Cabo, R., Gauna, L., Represa, J., and Vega, J. A. (2001). The thymus of the hairless rhino-j (hr/rh-j) mice. J Anat *198*, 399-406.

Schlake, T., Schorpp, M., Maul-Pavicic, A., Malashenko, A. M., and Boehm, T. (2000). Forkhead/winged-helix transcription factor Whn regulates hair keratin gene expression: molecular analysis of the nude skin phenotype. Dev Dyn *217*, 368-376.

Schmidt-Ullrich, R., and Paus, R. (2005). Molecular principles of hair follicle induction and morphogenesis. Bioessays *27*, 247-261.

Schmidt, J. B. (1994). Hormonal basis of male and female androgenic alopecia: clinical relevance. Skin Pharmacol *7*, 61-66.

Schorpp, M., Schlake, T., Kreamalmeyer, D., Allen, P. M., and Boehm, T. (2000). Genetically separable determinants of hair keratin gene expression. Dev Dyn *218*, 537-543.

Shimizu, H., and Morgan, B. A. (2004). Wnt signaling through the beta-catenin pathway is sufficient to maintain, but not restore, anagen-phase characteristics of dermal papilla cells. J Invest Dermatol *122*, 239-245.

Soler, A. P., Gilliard, G., Megosh, L. C., and O'Brien, T. G. (1996). Modulation of murine hair follicle function by alterations in ornithine decarboxylase activity. J Invest Dermatol *106*, 1108-1113.

Spencer, L. V., and Callen, J. P. (1987). Hair loss in systemic disease. Dermatol Clin *5*, 565-570.

Sprecher, E., Bergman, R., Szargel, R., Friedman-Birnbaum, R., and Cohen, N. (1999a). Identification of a genetic defect in the hairless gene in atrichia with papular lesions: evidence for phenotypic heterogeneity among inherited atrichias. Am J Hum Genet *64*, 1323-1329.

Sprecher, E., Bergman, R., Szargel, R., Raz, T., Labay, V., Ramon, M., Baruch-Gershoni, R., Friedman-Birnbaum, R., and Cohen, N. (1998). Atrichia with papular lesions maps to 8p in the region containing the human hairless gene. Am J Med Genet *80*, 546-550.

Sprecher, E., Lestringant, G. G., Szargel, R., Bergman, R., Labay, V., Frossard, P. M., Friedman-Birnbaum, R., and Cohen, N. (1999b). Atrichia with papular lesions resulting from a nonsense mutation within the human hairless gene. J Invest Dermatol *113*, 687-690.

Sprecher, E., Shalata, A., Dabbah, K., Futerman, B., Lin, S., Szargel, R., Bergman, R., Friedman-Birnbaum, R., and Cohen, N. (2000). Androgenetic alopecia in heterozygous carriers of a mutation in the human hairless gene. J Am Acad Dermatol *42*, 978-982.

Staal, F. J., Meeldijk, J., Moerer, P., Jay, P., van de Weerdt, B. C., Vainio, S., Nolan, G. P., and Clevers, H. (2001). Wnt signaling is required for thymocyte development and activates Tcf-1 mediated transcription. Eur J Immunol *31*, 285-293.

Stelzner, K. F. (1983). Four dominant autosomal mutations affecting skin and hair development in the mouse. J Hered *74*, 193-196.

Stenn, K. S., and Paus, R. (1999). What controls hair follicle cycling? Exp Dermatol *8*, 229-233; discussion 233-226.

Stenn, K. S., and Paus, R. (2001). Controls of hair follicle cycling. Physiol Rev *81*, 449-494.

Stoler, A., Kopan, R., Duvic, M., and Fuchs, E. (1988). Use of monospecific antisera and cRNA probes to localize the major changes in keratin expression during normal and abnormal epidermal differentiation. J Cell Biol *107*, 427-446.

Stoye, J. P., Fenner, S., Greenoak, G. E., Moran, C., and Coffin, J. M. (1988). Role of endogenous retroviruses as mutagens: the hairless mutation of mice. Cell *54*, 383-391.

Strausberg, R. L., Feingold, E. A., Grouse, L. H., Derge, J. G., Klausner, R. D., Collins, F. S., Wagner, L., Shenmen, C. M., Schuler, G. D., Altschul, S. F.*, et al.* (2002). Generation and initial analysis of more than 15,000 full-length human and mouse cDNA sequences. Proc Natl Acad Sci U S A *99*, 16899-16903.

Sundberg, J. (1994). Handbook of mouse mutations with skin and hair abnormalities: animal models and biomedical tools: CRC Press, Inc.).

Sundberg, J. P., and Boggess, D. (1998). Rhino-9J (hr(rh9J)): a new allele at the hairless locus. Vet Pathol *35*, 297-299.

Sundberg, J. P., Roop, D. R., Dunstan, R., Lavker, R., and Sun, T. T. (1991). Interaction between dermal papilla and bulge: the rhino mouse mutation as a model system. Ann N Y Acad Sci *642*, 496-499.

Thompson, C. C. (1996). Thyroid hormone-responsive genes in developing cerebellum include a novel synaptotagmin and a hairless homolog. J Neurosci *16*, 7832-7840.

Thompson, C. C., and Bottcher, M. C. (1997). The product of a thyroid hormone-responsive gene interacts with thyroid hormone receptors. Proc Natl Acad Sci U S A *94*, 8527-8532.

Tkatchenko, A. V., Visconti, R. P., Shang, L., Papenbrock, T., Pruett, N. D., Ito, T., Ogawa, M., and Awgulewitsch, A. (2001). Overexpression of Hoxc13 in differentiating keratinocytes results in downregulation of a novel hair keratin gene cluster and alopecia. Development *128*, 1547-1558.

Trueb, R. M. (2003). Association between smoking and hair loss: another opportunity for health education against smoking? Dermatology *206*, 189-191.

Truett, G. E., Heeger, P., Mynatt, R. L., Truett, A. A., Walker, J. A., and Warman, M. L. (2000). Preparation of PCR-quality mouse genomic DNA with hot sodium hydroxide and tris (HotSHOT). Biotechniques *29*, 52, 54.

van der Neut, R., Cachaco, A. S., Thorsteinsdottir, S., Janssen, H., Prins, D., Bulthuis, J., van der Valk, M., Calafat, J., and Sonnenberg, A. (1999). Partial rescue of epithelial phenotype in integrin beta4 null mice by a keratin-5 promoter driven human integrin beta4 transgene. J Cell Sci *112 (Pt 22)*, 3911-3922.

van Steensel, M., Smith, F. J., Steijlen, P. M., Kluijt, I., Stevens, H. P., Messenger, A., Kremer, H., Dunnill, M. G., Kennedy, C., Munro, C. S.*, et al.* (1999). The gene for hypotrichosis of Marie Unna maps between D8S258 and D8S298: exclusion of the hr gene by cDNA and genomic sequencing. Am J Hum Genet *65*, 413-419.

Verbeek, S., Izon, D., Hofhuis, F., Robanus-Maandag, E., te Riele, H., van de Wetering, M., Oosterwegel, M., Wilson, A., MacDonald, H. R., and Clevers, H. (1995). An HMG-box-containing T-cell factor required for thymocyte differentiation. Nature *374*, 70-74.

Voegel, J. J., Heine, M. J., Tini, M., Vivat, V., Chambon, P., and Gronemeyer, H. (1998). The coactivator TIF2 contains three nuclear receptor-binding motifs and mediates transactivation through CBP binding-dependent and -independent pathways. Embo J *17*, 507-519.

Weeks, C. E., Herrmann, A. L., Nelson, F. R., and Slaga, T. J. (1982). alpha-Difluoromethylornithine, an irreversible inhibitor of ornithine decarboxylase, inhibits tumor promoter-induced polyamine accumulation and carcinogenesis in mouse skin. Proc Natl Acad Sci U S A *79*, 6028-6032.

Whiting, D. (1987). Structural abnormalities of the hair shaft. J Am Acad Dermatol *16*, 1-25.

Whitlock, J. P., Jr. (1990). Genetic and molecular aspects of 2,3,7,8-tetrachlorodibenzo-p-dioxin action. Annu Rev Pharmacol Toxicol *30*, 251-277.

Wojcik, S. M., Imakado, S., Seki, T., Longley, M. A., Petherbridge, L., Bundman, D. S., Bickenbach, J. R., Rothnagel, J. A., and Roop, D. R. (1999). Expression of MK6a dominant-negative and C-terminal mutant transgenes in mice has distinct phenotypic consequences in the epidermis and hair follicle. Differentiation *65*, 97-112.

Xie, Z., Chang, S., Oda, Y., and Bikle, D. D. (2006). Hairless suppresses vitamin D receptor transactivation in human keratinocytes. Endocrinology 147:314-23

Xiong, Y., and Harmon, C. S. (1997). Interleukin-1beta is differentially expressed by human dermal papilla cells in response to PKC activation and is a potent inhibitor of human hair follicle growth in organ culture. J Interferon Cytokine Res *17*, 151-157.

Yan, K. L., He, P. P., Yang, S., Li, M., Yang, Q., Ren, Y. Q., Cui, Y., Gao, M., Xiao, F. L., Huang, W., and Zhang, X. J. (2004). Marie Unna hereditary hypotrichosis: report of a Chinese family and evidence for genetic heterogeneity. Clin Exp Dermatol *29*, 460-463.

Yang, S., Gao, M., Cui, Y., Yan, K. L., Ren, Y. Q., Zhang, G. L., Wang, P. G., Xiao, F. L., Du, W. H., Liang, Y. H., *et al.* (2005). Identification of a novel locus for Marie Unna hereditary hypotrichosis to a 17.5 cM interval at 1p21.1-1q21.3. J Invest Dermatol *125*, 711-714.

Zarach, J. M., Beaudoin, G. M., 3rd, Coulombe, P. A., and Thompson, C. C. (2004). The co-repressor hairless has a role in epithelial cell differentiation in the skin. Development *131*, 4189-4200.

Zhang, J. T., Fang, S. G., and Wang, C. Y. (2005). A novel nonsense mutation and polymorphisms in the mouse hairless gene. J Invest Dermatol *124*, 1200-1205.

Zlotogorski, A., Ahmad, W., and Christiano, A. M. (1998). Congenital atrichia in five Arab Palestinian families resulting from a deletion mutation in the human hairless gene. Hum Genet *103*, 400-404.

Zlotogorski, A., Hochberg, Z., Mirmirani, P., Metzker, A., Ben-Amitai, D., Martinez-Mir, A., Panteleyev, A. A., and Christiano, A. M. (2003). Clinical and pathologic correlations in genetically distinct forms of atrichia. Arch Dermatol *139*, 1591-1596.

Zlotogorski, A., Martinez-Mir, A., Green, J., Lamdagger, H., Panteleyevdagger, A. A., Sinclair, R., and Christiano, A. M. (2002a). Evidence for pseudodominant inheritance of atrichia with papular lesions. J Invest Dermatol *118*, 881-886.

Zlotogorski, A., Panteleyev, A. A., Aita, V. M., and Christiano, A. M. (2002b). Clinical and molecular diagnostic criteria of congenital atrichia with papular lesions. J Invest Dermatol *118*, 887-890.

Appendix

1. Detailed protocols for aminoallyl labeling of RNA in microarray experiments

1. Purpose

This protocol describes the labeling of eukaryotic RNA with aminoallyl labeled nucleotides via first strand cDNA synthesis followed by a coupling of the aminoallyl groups to either Cyanine 3 or 5 (Cy3/Cy5) fluorescent molecules.

2. Materials

2.1 5-(3-aminoallyl)-2'deoxyuridine-5'-triphosphate (AA-dUTP) (Sigma; Cat # A0410)

2.2 100 mM dNTP Set PCR grade (Life Technologies; Cat # 10297-018)

2.3 Anchored T primer (2mg/mL)

2.4 SuperScript II RT (200U/µL) (Life Technologies; Cat # 18064-014)

2.5 Cy-3 ester (AmershamPharmacia; Cat # RPN5661)

2.6 Cy-5 ester (AmershamPharmacia; Cat # RPN5661)

2.7 QIAquick PCR Purification Kit (Qiagen; Cat # 28106)

2.8 RNeasy® Mini Kit (Qiagen; Cat # 74106)

3. Reagent preparation

3.1 Phosphate Buffers

3.1.1 Prepare 2 solutions: 1M K2HPO4 and 1M KH2PO4

3.1.2 To make a 1M Phosphate buffer (KPO4, pH 8.5-8.7) combine:

1M K2HPO4……..9.5 mL

1M KH2PO4……..0.5 mL

3.1.3 For 100 mL Phosphate wash buffer (5 mM KPO4, pH 8.0, 80% EtOH) mix:

1 M KPO4 pH 8.5…. 0.5 mL

MilliQ water……... 15.25 mL

95% ethanol……... 84.25 mL

Note: Wash buffer will be slightly cloudy.

3.1.4 Phosphate elution buffer is made by diluting 1 M KPO4, pH 8.5 to 4 mM with MilliQ water.

3.2 Aminoallyl dUTP

3.2.1 For a final concentration of 100mM add 19.1 µL of 0.1 M KPO4 buffer (pH 7.5) to a stock vial containing 1 mg of aa-dUTP. Gently vortex to mix and transfer the aa-dUTP solution into a new microtube. Store at –20ºC.

3.2.2 Measure the concentration of the aa-dUTP solution by diluting an aliquot 1:5000 in 0.1 M KPO4 (pH 7.5) and measuring the OD289. (Stock concentration in mM = OD289 x 704)

3.3 Labeling Mix (50X) with 2:3 aa-dUTP: dTTP ratio

3.3.1 Mix the following reagents:

Final concentration

dATP (100 mM)……5µL….. (25 mM)

dCTP (100 mM)……5µL….. (25 mM)

dGTP (100 mM)……5µL….. (25 mM)

dTTP (100 mM)……3µL……(15 mM)

aa-dUTP (100 mM)…...2µL……(10 mM)

Total: 20µL

3.3.1 Store unused solution at –20°C.

3.4 Sodium Carbonate Buffer (Na_2CO_3): 1M, pH 9.0

4.4.1 Dissolve 10.8 g Na_2CO_3 in 80 mL of MilliQ water and adjust pH to 9.0 with 12 N HCl; bring volume up to 100 mL with MilliQ water. Aliquot and store at -80°C.

4.4.2 To make a 0.1 M solution for the dye coupling reaction dilute 1:10 with water.

Note: Carbonate buffer changes composition over time; make it fresh every couple of weeks to a month.

3.5 Cy-dye esters

4. Procedure

4.1 Aminoallyl Labeling

4.1.1 To 10-15 µg of total RNA which has been DNase I-treated and Qiagen RNeasy purified, add 2.5 µL Anchored T primers (2 mg/mL) and bring the final volume up to 18.5 µL with RNase-free water.

4.1.2 Mix well and incubate at 65-70°C for 10 minutes.

4.1.3 Snap-freeze in ice for 2-3 minutes, centrifuge briefly at >10,000 rpm and continue at room temperature.

4.1.4 Add:

5X First Strand buffer…….. 6 µL

0.1 M DTT…….. 3 µL

50X aminoallyl-dNTP mix…….. 0.6 µL

SuperScript II RT (200U/µL)….. 2 µL

4.1.5 Mix and incubate at 42°C for 3 hours to overnight (usually overnight).

4.1.6 To hydrolyze RNA, add:

1 M NaOH 10 µL

0.5 M EDTA 10 µL

mix and incubate at 65°C for 15 minutes.

4.1.7 Add 10 µL of 1 M HCl to neutralize pH.

4.2 Reaction Purification I: Removal of unincorporated aa-dUTP and free amines (use the Qiagen method)

Note: This purification protocol is modified from the Qiagen QIAquick PCR purification kit protocol. The phosphate wash and elution buffers (prepared in 3.1.3 & 3.1.4) are substituted for the Qiagen supplied buffers because the Qiagen buffers contain free amines which compete with the Cy dye coupling reaction.

4.2.1 Mix cDNA reaction with 300 µL (5X reaction volume) buffer PB (Qiagen supplied) and transfer to QIAquick column.

4.2.2 Place the column in a 2 ml collection tube (Qiagen supplied) and centrifuge at ~13,000 rpm for 1 minute. Empty collection tube.

4.2.3 To wash, add 750 µL phosphate wash buffer to the column and centrifuge at ~13,000 rpm for 1 minute.

4.2.4 Empty the collection tube and repeat the wash and centrifugation step.

4.2.5 Empty the collection tube and centrifuge column an additional 1 minute at maximum speed.

4.2.6 Transfer column to a new 1.5 mL microtube and carefully add 40 µL phosphate elution buffer to the center of the column membrane.

4.2.7 Incubate for 5 minute at room temperature.

4.2.8 Elute by centrifugation at ~13,000 rpm for 1 minute.

4.2.9 Elute a second time into the same tube by repeating steps 4.2.6- 4.2.8. The final elution volume should be ~80 µL.

4.2.10 Measure the concentration of cDNA.

4.2.11 Dry sample in a speed-vac.

* Here the dried sample could be stored in –20 or –80 °C for a couple of weeks

4.3 Coupling aa-cDNA to Cy Dye Ester.

4.3.1 Resuspend aminoallyl-labeled cDNA in 10 µL 0.05 M sodium carbonate buffer (Na_2CO_3), pH 9.0; incubate at 37°C for 10-15 minutes.

Note: Carbonate buffer changes composition over time so make sure you make it fresh every couple of weeks to a month.

4.3.2 Add 10 ul of labeled cDNA to the appropriate tube of NHS-ester Cy dye (dry pellet)

Note: To prevent photobleaching of the Cy dyes wrap all reaction tubes in foil and keep them sequestered from light as much as possible.

4.3.3 Incubate the reaction for 1 hour in the dark at room temperature.

4.4 Reaction Purification II: Removal of uncoupled dye (Qiagen PCR Purification Kit)

4.4.1 To the reaction add 35 µL 100 mM NaOAc pH 5.2.

4.4.2 Add 250 µL (5X reaction volume) Buffer PB (Qiagen supplied).

4.4.3 Place a QIAquick spin column in a 2 mL collection tube (Qiagen supplied), apply the sample to the column, and centrifuge at ~13,000 for 1 minute. Empty the collection tube.

4.4.4 To wash, add 0.75 mL Buffer PE (Qiagen supplied) to the column and centrifuge at ~13,000 for 1 minute.

Note: Make sure Buffer PE has added ethanol before using (see label for correct volume).

4.4.5 Empty collection tube and centrifuge column for an additional 1 minute at maximum speed.

4.4.6 Place column in a clean 1.5 mL microtube and carefully add 40 µL Buffer EB (Qiagen supplied) to the center of the column membrane.

4.4.7 Incubate for 5 minutes at room temperature.

4.4.8 Elute by centrifugation at ~13,000 rpm for 1 minute.

4.4.9 Elute a second time into the same tube by repeating steps 4.4.6- 4.4.8. The final elution volume should be ~80 µL.

4.4.10 Measure the efficiency of dye coupling and dry the sample in the speed-vac for about 40-45 min.

2. Detailed protocols for microarray hybridizations

1. Purpose

This protocol describes how to perform microarray hybridization after the successful coupling of dyes with cDNA.

2. Materials and solutions

2.1 Formamide

2.2 20X SSC

2.3 10% BSA

2.4 10% SDS

2.5 Mouse cot1 DNA (1 mg/ml)

3. Reagents preparation

3.1 1X pre-hybridization buffer

Formamide	7.5 ml
20X SSC	7.5 ml
10% BSA	3.0 ml
10% SDS	300 ul
dH_2O	11.7 ml
Total	30 ml

It can be reused for a few times and store at 4°C. Preheat at 42°C before use.

3.2 1X hybridization buffer

Formamide	250 ul
20X SSC	250 ul
10% SDS	10 ul
Cot1 DNA(1ug/ul)	100 ul
dH_2O	390 ul
Total	1000 ul

Store at -20°C.

3.3 wash buffer 1

20X SSC	50 ml
10% SDS	10 ml
dH_2O	940 ml
Total	1000 ml

Microwave 1 min and 30 sec till the temperature is ~ 42°C. Stir to mix temperature.

3.4 wash buffer 2

20X SSC	10 ml
dH_2O	990 ml
Total	1000 ml

3.5 Wash buffer 3

20X SSC	10 ml
dH_2O	1990 ml
Total	2000 ml

4. Procedures

4.1 Prewarm the pre-hybridization buffer at 42 °C for 10 min.

4.2 Place printed slides in a slide container containing prehybridization buffer and incubate at 42°C water bath for 45 minutes.

4.3 Wash the prehybridized slides twice (using a forceps to hold the slides) in distilled water in two 50ml tubes.

4.4 Very carefully blow dry slides completely. Hold the slide near the bar code end with a forceps and blow-dry first at the barcode away from the array end towards the forceps. Then dry the array by blowing down the slides away from the forceps. Next dry the back of the slide. Do not wait too long following prehybridization to hybridize. Get the slides ready in the hybridization chamber (filled with 5X SSC to keep humidity).

4.5 Prewarm the 1X hyb buffer at 42 °C for 10-15 minutes. Add 35 ul 1X hyb buffer to each tube with dried down coupled pellet. Let it sit at room temperature for 5 minutes then pipet up and down to dissolve the pellet. The total hybridization volume is 70 ul for one mouse 22k slide. Mix for dye swap (Cy3+

Cy5) the appropriate samples, spin briefly and incubate at 95°Cfor 5 minutes and spin for 30 seconds.

Note: Never try to put the hyb buffer on ice due to SDS in the buffer!

4.6 Load the probes to the slides with M-series Lifterslips. The lifterslips should not be washed or cleaned by any means before hybridization. The hybridization buffer should be loaded from the end of slides without labeling to get samples loaded evenly.

4.7 Wrap the hybridization chamber in aluminum foil and incubate in a 42°C water bath overnight.

4.8 Take the slides out carefully and wash the slides in the rack with wash buffer 1 at 42°C for 5 minutes with strong stirring. Then the slides were washed with buffer 2 at room temperature for 3 minutes twice. The slides were finally washed with buffer 3 at room temperature for 1 minutes four times.

Notes: All the slides should face out of the stirring in the container. Try to keep the slides merged in the washing solutions all the time to reduce the chance of unwashed dyes to dry.

4.9 The slides were blowed dry and ready to scan.

Notes: The light should be turned off during the loading of samples to the slides and during the slide washing after hybridization.

3. Generation of the antiserum against murine *Hr*

The *Hr*-specific antiserum was generated based on the report from Thompson's group in John Hopkins University (Potter et al., 2001). Briefly, the amino acids 450-730 of mouse *Hr* were expressed as a GST (glutathione S-transferase) fusion protein and purified with GST beads. The fusion protein was used to immunize rabbits (Covance).

The region of *Hr* corresponding to amino acids 450-730 is 1728-2567 base pairs in NM_021877. A pair of primers was designed to amplify the segment: *Hr*-F5: 5'-CAACGGATCCATATAGGAAGCAAGGCGGAG-3'; *Hr*-R5: 5'-CGCCGAATTCCTC- TTCTTTGATGTCCTTGGTC-3'. PCR with *Hr*-F5/R5 was used to generate the fragments 1728-2567 bp in NM_021877. There are *BamH1* digestion site in *Hr*-F5 primer and *EcoRI* digestion site in *Hr*-R5 primer. The PCR products from *Hr*-F5/R5 were digested with *BamH1* and *EcoRI* at 37ºC. The pGEX-3X vector (a gift from Dr. Yisong Wang in Oak Ridge National Lab) was digested with *BamH1* and *EcoRI* at 37ºC at the same time. The digested PCR products and pGEX-3X vector were separated by agarose gel and purified by GFX column from Amersham. The PCR products were ligated with digested pGEX-3X vector, and transfected into JA226 cells by electroporation with 1700 Volts for 5 milli-seconds. The transfected clones were validated with digestion of *BamH1* and *EcoRI*. The expression of *Hr* peptide was induced by adding 1mM of IPTG (isopropyl-β-D-thiogalactopyranoside). GST-*Hr* protein was purified with GST agarose beads. The purification was validated by SDS-PAGE (sodium dodecyl sulfate polyacrylamide gel electrophoresis) with Comassie Blue staining. Totally one milligram of GST-*Hr* fusion protein was sent to Covance to immunize two rabbits to generate the *Hr* antiserum.

4. Regulation of human *HR* gene expression by thyroid hormone and vitamin D_3 in human keratinocyte HaCaT cell line

It has been reported that vitamin D receptor physically interacts with HR (Hsieh et al., 2003). *Hr* also acts as transcriptional co-repression of both thyroid hormone receptor (TR) and the orphan nuclear receptor, RORα (Moraitis et al., 2002; Potter et al., 2001). However, it is still unknown whether the expression of *Hr* inside the cells is ligand-dependent. Therefore, we used human keratinocyte HaCaT cell line (gift from Dr. G. Timothy Bowden in the University of Arizona, Tucson, Arizona) to study the effects of thyroid hormone (T3) and vitamin D3 (VD3) on the expression of *HR*. The final concentration of both TH and VD3 was 50 nM for the treatment according to the literatures. The cells were treated for 24 and 48 hours with TH or VD3. The cells from 0 hours of both treatments were used as time series control and the cells from either 24 or 48 hours group without either treatment were also used for treatment controls. Each group of treatment or the control contains at least 3 dishes of HaCaT cells for design. The total RNA was extracted from HaCaT cells after the proper treatments with RNeasy kit from Qiagen. The complimentary DNA (cDNA) was generated by RT-PCR with oligo(dT) primers and 1 ug of total RNA. A pair of primers for real time PCR was designed to amply the human hairless from the cell lines: HrQF5: 5'-CACCAGGTCTGGGTCAAGTT-3' and HrQR5: 5'-GGGCGTTTTCTGTGTTGATT-3'. It was found that the *HR* expression in HaCaT cells are not affected by either thyroid hormone or vitamin D3, suggesting the regulation of *HR* is ligand-independent of thyroid hormone and vitamin D3. Our results are consistent with the finding from Dr. Christiano's groups (Engelhard and Christiano, 2004), which is that the regulation of *Hr* expression in keratinocytes is T3 independent.

Vita

Yutao Liu was born in Shandong Province, China, on July 22, 1972. He graduated from Anqiu Sixth High School in 1990. He received his Bachelor of Medicine degree with major in basic medical science from Beijing Medical University (now called Health Science Center of Beijing University) in 1995 and degree of Master of Science majoring in Biology from Truman State University (formerly Northeastern Missouri State University) in 2001. In 2001, he was enrolled into the University of Tennessee-Oak Ridge National Laboratory Graduate School of Genome Science and Technology to pursue a doctoral degree with major in life science focusing on mouse functional genomics under the guidance of Dr. Brynn Voy.